POLITECNICO DI MILANO

School of Industrial and Information Engineering
Department of Aerospace Science and Technology
Master of Science in Aeronautical Engineering

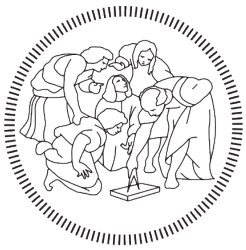

POLITECNICO
MILANO 1863

Thermodynamic analysis of a turboprop engine with regeneration and intercooling

Advisor: Prof. Roberto ANDRIANI

M.Sc. Dissertation of:
Rasheed Michael ISHOLA
Matr. 895396

April 2020
Academic Year 2019-2020

Contents

Introduction **1**

1 Turbopropeller engines overview **2**
1.1 Turbopropeller characteristics . . . 4
1.2 Comparison with turbojets and piston-powered engines . . . 4
1.3 Turbopropeller-powered aircrafts . . . 5
1.4 Turbopropeller manufacturers . . . 9
1.4.1 Pratt & Whitney Canada (PWC) [1] . . . 9
1.4.2 Rolls-Royce [2] . . . 17
1.4.3 General Electric Aviation [3] . . . 22
1.4.4 JSC Kuznetsov [4] . . . 26
1.4.5 JSC "UEC-Klimov" [5] . . . 27
1.4.6 Ivchenko-Progress ZMKB [6] . . . 28
1.4.7 Honeywell Aerospace [7] . . . 33
1.4.8 PBS Aerospace [8] . . . 34

2 Thermodynamics of a turbopropeller engine with heat exchange **36**
2.1 Intercooling and regeneration . . . 36
2.2 Thermodynamic cycle . . . 39
2.2.1 Assumptions . . . 39
2.2.2 The cycle . . . 42
2.3 Performances . . . 48

3 The code **53**
3.1 Assumptions and data used . . . 54
3.1.1 Efficiencies and pressure losses . . . 54
3.1.2 Fuel properties . . . 54
3.1.3 Specific heat values . . . 55
3.2 Code Structure . . . 57
3.2.1 Input file . . . 57
3.2.2 Output files . . . 58
3.2.3 Code details . . . 62

4 Numerical simulation **78**
4.1 Results . . . 78
4.1.1 Determination of the best β_n condition . . . 79
4.1.2 Performances vs β_c . . . 80
4.1.3 Performances vs E and R . . . 87
4.1.4 Performances vs ε_i and ε_r . . . 94

4.1.5 Heat exchanged in the intercooler and regenerator 95
4.1.6 $\lambda - \beta_n$ correspondence 98

5 Potential benefits of the application of regeneration and intercooling on current turbopropellers 99
5.1 Economical and environmental benefits 100
5.1.1 Results 100
5.2 Heat exchangers' weight estimation 102
5.2.1 Results 105
5.3 Conclusions 107

Acknowledgments 110

Bibliography 111

List of Figures

1.1 PW127M engine [1] . . . 10
1.2 PT6A-140 engine [1] . . . 12
1.3 PT6E series engine [1] . . . 16
1.4 T56 series engine [2] . . . 17
1.5 M250 series engine [2] . . . 19
1.6 T400-D6 engine [2] . . . 20
1.7 AE2100 engine [9] . . . 21
1.8 Catalyst engine [3] . . . 22
1.9 H-series engine [3] . . . 24
1.10 CT7-9 engine [3] . . . 25
1.11 Kuznetsov NK-12 engine . . . 26
1.12 TV7-117S engine [10] . . . 27
1.13 AI-20 engine [6] . . . 28
1.14 AI-24 engine [6] . . . 29
1.15 AI-450C engine [6] . . . 30
1.16 TV3-117VMA-SBM1 engine [6] . . . 32
1.17 TPE331 engine [7] . . . 33
1.18 TP100 engine [8] . . . 34

2.1 Sketch of a turboprop engine with intercooling and regeneration [11] . . . 36
2.2 Real gas factor for H_2O (T_{cr} = 647.3 K, P_{cr} = 22.12 MPa) [12] . . . 40
2.3 Real gas factor for CO_2 (T_{cr} = 304.4 K, P_{cr} = 7.38 MPa) [12] . . . 40
2.4 c_p variation with temperature, for various gases [12] . . . 41
2.5 Control volume adopted in the quasi-1D flow analysis [12] . . . 41
2.6 Thermodynamic cycle [11] . . . 42

3.1 Input file "Data.txt" . . . 58
3.2 Output file "Results 1.txt" - top part . . . 59
3.3 Output file "Results 1.txt" - bottom part . . . 60
3.4 Output file "Summary.txt" - top part . . . 61
3.5 Output file "Summary.txt" - bottom part . . . 62
3.6 Terminal view (Eclipse [13]) of the code running . . . 77

4.1 Optimal β_n - $R/E = 0.6$ . . . 79
4.2 Optimal β_n - $R/E = 0.8$ . . . 79
4.3 Optimal β_n - $R/E = 0$ . . . 80
4.4 $EBSFC - \beta_n$ . . . 80
4.5 Power$-\beta_n$ . . . 80
4.6 $EBSFC - \beta_c$, reference . . . 81
4.7 $EBSFC - \beta_c$, T_{max} (a) . . . 81

4.8 $EBSFC - \beta_c$, T_{max} (b) . . . 81
4.9 $EBSFC - \beta_c$, alt. (a) . . . 82
4.10 $EBSFC - \beta_c$, alt. (b) . . . 82
4.11 $EBSFC - \beta_c$, M (a) . . . 82
4.12 $EBSFC - \beta_c$, M (b) . . . 82
4.13 Power$-\beta_c$, reference . . . 83
4.14 Power$-\beta_c$, T_{max} (a) . . . 83
4.15 Power$-\beta_c$, T_{max} (b) . . . 83
4.16 Power$-\beta_c$, alt. (a) . . . 84
4.17 Power$-\beta_c$, alt. (b) . . . 84
4.18 Power$-\beta_c$, M (a) . . . 84
4.19 Power$-\beta_c$, M (b) . . . 84
4.20 $\eta_{th} - \beta_c$, reference . . . 85
4.21 $\eta_{th} - \beta_c$, T_{max} (a) . . . 85
4.22 $\eta_{th} - \beta_c$, T_{max} (b) . . . 85
4.23 $\eta_{th} - \beta_c$, alt. (a) . . . 86
4.24 $\eta_{th} - \beta_c$, alt. (b) . . . 86
4.25 $\eta_{th} - \beta_c$, M (a) . . . 86
4.26 $\eta_{th} - \beta_c$, M (b) . . . 86
4.27 $EBSFC - E$, T_{max} . . . 87
4.28 $EBSFC - R$, T_{max} . . . 87
4.29 $EBSFC - E/R$, T_{max} . . . 87
4.30 Power$-E$, T_{max} . . . 88
4.31 Power$-R$, T_{max} . . . 88
4.32 Power$-E/R$, T_{max} . . . 89
4.33 $\eta_{th} - E$, T_{max} . . . 90
4.34 $\eta_{th} - R$, T_{max} . . . 90
4.35 $\eta_{th} - E/R$, T_{max} . . . 90
4.36 $\eta_{th} - R$, M . . . 91
4.37 $\eta_{th} - E/R$, M . . . 91
4.38 $\eta_{th} - E$, M . . . 92
4.39 $EBSFC - \beta_c$, comparison . . . 92
4.40 Power$-\beta_c$, comparison . . . 92
4.41 $\eta_{th} - \beta_c$, comparison . . . 93
4.42 $EBSFC - \varepsilon_{i/r}$ . . . 94
4.43 Power$-\varepsilon_{i/r}$ . . . 94
4.44 $\eta_{th} - \varepsilon_{i/r}$ . . . 95
4.45 $Q_{int} - \beta_c$, alt. (a) . . . 96
4.46 $Q_{int} - \beta_c$, alt. (b) . . . 96
4.47 $Q_{int} - E$, alt. . . . 96
4.48 $Q_{reg} - \beta_c$, T_{max} (a) . . . 97
4.49 $Q_{reg} - \beta_c$, T_{max} (b) . . . 97
4.50 $Q_{reg} - R$, T_{max} . . . 97
4.51 $Q_{reg} - E/R$, T_{max} . . . 97
4.52 $Q_{reg} - \beta_n$ . . . 98
4.53 $\lambda - \beta_n$, M (a) . . . 98
4.54 $\lambda - \beta_n$, M (b) . . . 98

5.1 Regenerator specific weight as a function of its regeneration effectiveness [14] 104
5.2 Regenerator specific weight as a function of regeneration effectiveness: comparison between two exponential fitting curves 105
5.3 Saved fuel-time, $R = E = 0.5$ 106
5.4 Saved fuel-time, $R = E = 0.6$ 106
5.5 Saved fuel-time, $R = E = 0.7$ 107
5.6 Saved fuel-time, $R = E = 0.8$ 107

List of Tables

1.1 List of Airbus' turboprop aircrafts [15] . . . 5
1.2 List of Piaggio Aircraft's turboprop aircrafts [16] . . . 5
1.3 List of Daher-SOCATA's turboprop aircrafts [17] . . . 6
1.4 List of ATR Aircraft's turboprop aircrafts [18] . . . 6
1.5 List of Pilatus Aircraft's turboprop aircrafts [19] . . . 6
1.6 List of H3 Grob Aircraft's turboprop aircrafts [20] . . . 6
1.7 List of Diamond Aircraft Industries' turboprop aircrafts [21] . . . 6
1.8 List of Antonov Airlines' turboprop aircrafts [22] . . . 7
1.9 List of Ilyushin's turboprop aircrafts [23] . . . 7
1.10 List of Lockeed Martin's turboprop aircrafts [24] . . . 7
1.11 List of Beechcraft's turboprop aircrafts [25] . . . 7
1.12 List of Piper Aircraft's turboprop aircrafts [26] . . . 7
1.13 List of Evolution Aircraft's turboprop aircrafts [27] . . . 8
1.14 List of Epic Aircraft's turboprop aircrafts [28] . . . 8
1.15 List of Nextant Aerospace's turboprop aircrafts [29] . . . 8
1.16 List of Bombardier's turboprop aircrafts [30] . . . 8
1.17 List of Embraer's turboprop aircrafts [31] . . . 8
1.18 PW100/150 engines specs - part A. Data from [32] where not indicated . . . 10
1.19 PW100/150 engines specs - part B. Data from [32] where not indicated . . . 11
1.20 PW100/150 engines specs - part C. Data from [32] where not indicated . . . 11
1.21 PT6A engines specs - part A. Data from [32] where not indicated . . . 13
1.22 PT6A engines specs - part B. Data from [32] where not indicated . . . 13
1.23 PT6A engines specs - part C. Data from [32] where not indicated . . . 14
1.24 PT6A engines specs - part D. Data from [32] where not indicated . . . 14
1.25 PT6A engines specs - part E. Data from [32] where not indicated . . . 15
1.26 PT6A engines specs - part F . . . 15
1.27 PT6E engines specs . . . 16
1.28 T56 engines specs. Data from [32] where not indicated . . . 18
1.29 M250 engines specs. Data from [32] where not indicated . . . 19
1.30 TP400-D6 engine specs . . . 20
1.31 AE2100 engines specs . . . 21
1.32 Catalyst engines specs . . . 23
1.33 H-series engines specs . . . 24
1.34 T700/CT7 engines specs. Data from [32] where not indicated . . . 25
1.35 NK-12M engine specs. Data from [32] where not indicated . . . 26
1.36 TV7-117S engines specs . . . 27
1.37 AI-20 engines specs . . . 29
1.38 AI-24 engines specs . . . 30
1.39 AI-450C engines specs . . . 31

1.40 TV3-117VMA-SBM1 engine specs 32
1.41 TPE331 engine specs 34
1.42 TP100 engine specs 35

3.1 η and ε values used 54
3.2 Temperature ranges for the c_p evaluation 55
3.3 c_p and γ values 57
3.4 Definitions of the layers in the U.S. Standard Atmosphere Model 64

5.1 Performances: traditional engine 101
5.2 Performances: engine with heat exchange 101
5.3 Hourly savings 101
5.4 Heat exchangers' weight estimation 106

Nomenclature

β_{c1} Compression Ratio - Low Pressure Compressor

β_{c2} Compression Ratio - High Pressure Compressor

β_c Overall Compression Ratio

β_n Nozzle Expansion Ratio

Δh_{av} Total enthalpy drop available after the High Pressure Turbine, to be used for propulsive purposes

$\Delta h_{n,is}$ Isentropic enthalpy drop in the Nozzle

$\Delta h_{pt,is}$ Isentropic enthalpy drop in the Power Turbine

Δh_t Total Enthalpy Variation

$\dot{L}_{av}$ Total Power Available

$\dot{L}_{c1}$ Low Pressure Compressor Power

$\dot{L}_{c2}$ High Pressure Compressor Power

$\dot{L}_{diss,jet}$ Jet Dissipated Power

$\dot{L}_{diss,prop}$ Propeller Dissipated Power

$\dot{L}_{diss,tot}$ Total Dissipated Power

$\dot{L}_{eq}$ Equivalent Power

$\dot{L}_{j,jet}$ Jet Power "at the Shaft"

$\dot{L}_{j,prop}$ Propeller Power at the Shaft

$\dot{L}_{j,tot}$ Total "Jet" Power

$\dot{L}_{p,jet}$ Jet's Propulsive Power

$\dot{L}_{p,prop}$ Propeller's Propulsive Power

$\dot{L}_{p,tot}$ Total Propulsive Power

$\dot{L}_{t1}$ High Pressure Turbine Power

$\dot{L}_{t2}$ Power Turbine Power

$\dot{m}_{a,prop}$ Air Mass Flow Rate processed by the Propeller

$\dot{m}_a$ Air Mass Flow Rate

$\dot{m}_f$ Fuel Mass Flow Rate

$\dot{m}_g$ Combustion Gases Mass Flow Rate

$\dot{Q}_{comb}$ Power released by the Combustion

$\dot{Q}_{int}$ Power Exchanged in the Intercooler

$\dot{Q}_{reg}$ Power Exchanged in the Regenerator

η_b Combustion Efficiency

η_{c1} Low Pressure Compressor Adiabatic Efficiency

η_{c2} High Pressure Compressor Adiabatic Efficiency

η_{gb} Gear Box Efficiency

$\eta_{m,c1}$ Low Pressure Compressor Mechanical Efficiency

$\eta_{m,c2}$ High Pressure Compressor Mechanical Efficiency

$\eta_{m,t1}$ High Pressure Turbine Mechanical Efficiency

$\eta_{m,t2}$ Power Turbine Mechanical Efficiency

η_n Nozzle Efficiency

η_o Overall Efficiency

$\eta_{p,prop}$ Propeller's Propulsive Efficiency

η_p Propulsive Efficiency

η_{t1} High Pressure Turbine Adiabatic Efficiency

η_{t2} Power Turbine Adiabatic Efficiency

η_{th} thermal efficiency

γ_a Specific Heat Ratio of Air

γ_g Specific Heat Ratio of the Combustion Gases

λ Parameter for the enthalpy rop repartition between propeller and jet

λ_{opt} λ value that maximizes the Total Propulsive Power

$\mathcal{MM}$ Molar Mass

$\mathcal{R}$ Universal Gas Constant

$\prime$ Condition obtained through an Isentropic Process

ρ Density

ρ_a Air Density

ε_b Combustion Chamber Efficiency in terms of Pressure Losses

ε_d Air Intake Efficiency in terms of Pressure Losses

ε_i Intercooler Efficiency in terms of Pressure Losses

ε_r Regenerator Efficiency in terms of Pressure Losses

$C_{11}H_{21}$ Jet A-1 (approx. formula)

$c_{p_{a,cold}}$ Air Specific Heat Capacity at constant Pressure - low temperature

$c_{p_{a,hot}}$ Air Specific Heat Capacity at constant Pressure - high temperature

c_{p_a} Air Specific Heat Capacity at constant Pressure

c_{p_f} Specific Heat of the Fuel

$c_{p_{g,cold}}$ Combustion Gases Specific Heat Capacity at constant Pressure - low temperature

$c_{p_{g,hot}}$ Combustion Gases Specific Heat Capacity at constant Pressure - high temperature

c_{p_g} Combustion Gases Specific Heat Capacity at constant Pressure

c_p Specific Heat Capacity at constant Pressure

c_v Specific Heat at Constant Volume

CO_2 Carbon Dioxide

D_{prop} Propeller Diameter

E Intercooling Effectiveness

$EBSFC$ Equivalent Brake-Specific Fuel Consumption

ER Equivalence Ratio

f Fuel - Air Ratio

h Specific Enthalpy / Geopotential altitude

H/C Hydrogen - Carbon Ratio

H_2O Water

H_f Heat of Combustion of the Fuel

h_t Specific Total Enthalpy

HPC High Pressure Compressor

HPT High Pressure Turbine

IPT Intermediate Pressure Turbine

l Specific Work

l_{diss} Specific Work Dissipated

LPC Low Pressure Compressor

LPT Low Pressure Turbine

M Mach Number

NO_x Nitrogen Oxides

O_2 Oxygen

P Pressure

P_{cr} Critical Pressure

P_t Total Pressure

R Specific Gas Constant / Regeneration effectiveness

SO_x Sulphur Oxides

T Temperature

T_{cr} Critical Temperature

T_{jet} Thrust given by the Jet

$T_{max/min,hot/cold,air/gas}$ Maximum/minimum Temperature considered in the computation of the Air/Combustion Gases c_p value to be used in the "hot/cold" region of the engine

T_{max} Maximum temperature of the thermodynamic cycle

T_{prop} Thrust given by the Propeller

T_{tf} Fuel Total Temperature

T_{total} Total Thrust

T_t Total Temperature

TIT Turbine Inlet Temperature

V_∞ Flight Speed

v_{exit} Combustion Gases Speed at the Nozzle Exit

v_{wake} Air Speed donwstream the Propeller

w_{reg} Regenerator specific weight

Z Compressibility Factor

z Geometric altitude

Abstract

The scope of this thesis is to evaluate the performances of a turbopropeller engine with intercooling and regeneration, to assess qualitatively and quantitatively the improvements in the performances with respect to the traditional engine, and to determine the feasibility of the implementation of this kind of engines on commercial aircrafts. In order to do so, a thermodynamic analysis is carried out by means of a Fortran90 code, which computes the thermodynamic quantities at each point of the thermodynamic cycle along with the engine overall performances. The output data is then post-processed to obtain plots of the engine performances, showing their behavior at different operating conditions and engine configurations. The performances are then compared with those of a traditional engine, in order to assess the impact of regeneration and intercooling and their mutual interaction. Then, the projected benefits of the implementation of such engines are estimated by a comparison between a traditional engine currently in service and one simulated by the code. In addition, the weight of the additional heat exchangers is estimated. The data shows that intercooling and regeneration sensibly decrease the specific fuel consumption and increase the specific power of the engine, if used together and if high heat exchanger effectiveness can be achieved. Also, their mutual implementation yields optimal operating conditions, in terms of fuel consumption, at engine compression ratios commonly used in aeroengines. Overall, the implementation of recuperated engines can yield substantial reductions in fuel consumption and thus in emissions and related costs. On the other hand, the weight of the additional heat exchangers is high, especially for high heat exchanger effectiveness. Thus, in order to fully exploit the potential of this technology, it is imperative to be able to develop/implement heat exchangers that can achieve high effectiveness with low weight and pressure losses, otherwise the benefits deriving from their implementation might not be worth the additional weight, cost and complexity of the engine.

Estratto in lingua italiana

In questo periodo caratterizzato da un alto costo del combustibile e da una sempre maggiore attenzione alle emissioni ed all'impatto ambientale, si è riacceso l'interesse per motori che integrano tecniche di scambio termico per migliorare le proprie prestazioni, in quanto potrebbero fornire una valida risposta a diverse esigenze senza sconvolgere completamente la tecnologia attualmente in uso.

Questo elaborato si pone l'obiettivo di analizzare le prestazioni di motori turboelica con rigenerazione ed interrefrigerazione, valutare qualitativamente e quantitativamente i benefici dell'implementazione delle tecniche sopra citate e determinare la fattibilità di una possibile futura implementazione su velivoli commerciali. L'elaborato si apre con una pamoramica sui motori turboelica attualmente in servizio, in modo da identificare il contesto in cui i motori con rigenerazione ed interrefrigerazione andrebbero ad inserirsi. Viene poi effettuata la valutazione delle prestazioni per mezzo di un'analisi termodinamica, in cui le prestazioni del motore vengono calcolate per diverse condizioni di funzionamento, di volo e per diverse configurazioni del motore. Per effettuare l'analisi è stato sviluppato un programma in Fortran90, il quale è in grado di calcolare i vari punti del ciclo termodinamico e le prestazioni del motore a partire dai parametri di progetto e dalle condizioni operative indicate. Il risultato dell'analisi sono una serie di grafici per le varie prestazioni del motore, fra cui il consumo specifico equivalente, la potenza specifica equivalente, il rendimento e le potenze scambiate negli scambiatori di calore. Mediante confronti con le prestazioni di un motore tradizionale, ovvero senza interrefrigerazione e rigenerazione, è possibile valutare da questi grafici l'impatto che interrefrigerazione e rigenerazione hanno sulle prestazioni globali del motore e come queste due tecniche interagiscono fra di loro. Da questa analisi è stato quindi possibile determinare le configurazioni che ottimizzano il consumo specifico ed il comportamento delle prestazioni al variare di diversi parametri. Infine, è stato fatto un confronto fra un motore tradizionale attualmente in commercio, il Pratt & Whitney PW150A, ed un ipotetico motore con scambio termico con la stessa potenza nominale, simulato con il programma di cui sopra. Da questo confronto è stato possibile stimare i benefici che deriverebbero dall'uso di motori rigenerati, per diversi valori di efficacia degli scambiatori. Si è stimato il risparmio di combustibile e la conseguente riduzione di emissioni, costi e peso, ed inoltre si è stimato approssimativamente il peso degli scambiatori, basandosi su dati pregressi, in modo da poter avere un'idea dell'impatto che rigenerazione ed interrefrigerazione hanno sulla struttura del motore. Da questo lavoro si è determinato che motori con rigenerazione ed interrefrigerazione offrono un notevole incremento delle prestazioni del motore, sia in termini di consumi che di rendimento e di potenza. Essi lavorano al meglio, soprattutto in termini di consumo specifico, con rapporti di espansione nell'ugello intorno a 1.2 e con rapporti di compressione compresi fra 12 e 18. La combinazione di interrefrigerazione e rigenerazione da le migliori prestazioni, in particolare aumentando sensibilmente la potenza specifica fornita dal motore (rispetto

alla sola rigenerazione), che risulta superiore rispetto a quella del motore tradizionale per i rapporti di compressione di cui sopra. Inoltre, combinando le due tecniche le prestazioni migliori si ottengono per rapporti di compressione più alti, più vicini a quelli normalmente usati in ambito aeronautico. Inoltre si è determinato che l'efficacia degli scambiatori è fondamentale nell'ottenere alte prestazioni: per valori inferiori a 0.4 si ottengono prestazioni addirittura inferiori rispetto a quelle del motore tradizionale, e per ottenere miglioramenti significativi è fondamentale ottenere valori alti, intorno a 0.7-0.8. Dal confronto finale con il PW150A è emerso che l'implementazione di motori rigenerativi può portare ad un risparmio previsto intorno al 13% (efficacia scambiatori = 0.8), per quanto riguarda i consumi, con conseguente riduzione di costi ed emissioni. Ne consegue che l'implementazione di interrefrigerazione e rigenerazione è più vantaggiosa su motori dalle elevate potenze nominali, in quanto il risparmio interessa una quantità superiore di combustibile. Tuttavia, gli scambiatori aggiuntivi incrementano sensibilmente il peso del motore, con legge esponenziale rispetto all'efficacia dello scambiatore.

Si conclude quindi che questa tipologia di motori ha grandi potenzialità nel migliorare le prestazioni del motore e far fronte alle esigenze odierne, tuttavia la loro effettiva implementazione dipende molto dallo sviluppo tecnologico degli scambiatori di calore: è necessario sviluppare scambiatori con alta efficacia (~ 0.8) e con contenute perdite di pressione e peso, altrimenti il miglioramento nelle prestazioni potrebbe non giustificare il peso, costo e complessità addizionali del motore.

Introduction

The viability of propulsion gas turbines with heat exchange techniques in order to improve their performances was firstly investigated in the 1960's. In those years several turboshaft engines were tested. Of particular interest was the T63 engine, that alone powered the YOH-6A helicopter during flight in 1967 [14]. However, in the following years the interest in recuperated propulsion gas turbines has been intermittent. There were some design concepts and studies about other turboshaft engines, but none of them was actually manufactured. Also applications of heat exchange technology on other propulsion aeroengines were studied. The most noteworthy cases were [14]: the study about a small 187 kW turbopropeller with radial turbomachinery and a low compression ratio of 6, on which were integrated a ceramic rotary regenerator and a metallic rotary intercooler; a concept design for a propfan with intercooling and regeneration proposed by MTU Aero Engines, that later evolved in the IRA turbofan concept; and a study of a recuperated turbofan for a cruise missile, which contemplated a counterflow recuperator in order to achieve high recuperator effectiveness.

Anyhow, apart from few occasional studies, interest in this kind of engines has been very low. This was due to the fact that in that period fuel prices were very low and regenerators were very heavy. In addition, without intercooling the power provided by the engine was often too low. So, in the end, the reduced specific fuel consumption that characterizes recuperated engines was not appealing enough to justify the engine's increased cost and weight.

Nowadays, the scenario is quite different though. The price of aviation fuel is high, heat exchanger technology progressed and social factors, like emissions and noise, are now taken in serious consideration.

So, in a period in which legislation imposes increasingly stringent limits on noise levels and emissions and in which fuel price is on the rise, the interest in recuperated propulsion gas turbines has renewed.

In this thesis, after an overview on modern turbopropellers, it is of interest to study the performances of a generic turbopropeller with intercooling an regeneration, for different values of different parameters, and to compare those performances with those of an equivalent traditional engine (see chapter 4). This analysis is done by means of an ad-hoc Fortran 90 code, presented in chapter 3. It is then tackled the task to identify the optimal condition in terms of overall compression ratio and power distribution between power turbine and nozzle. Subsequently, it is studied how intercooling and regeneration interact with each other and which are the limits, in terms of intercooling and regeneration effectiveness, in order to have substantial benefits from their application.

In chapter 5 it is at last presented a comparison between a real modern traditional turbopropeller and a simulated turbopropeller with intercooling and regeneration. In this comparison are estimated the potential social and economical benefits deriving from the use of engines enhanced with heat exchangers.

Chapter 1

Turbopropeller engines overview

Turbopropellers are aero engines composed by a gas turbine core engine that drives a propeller, which provides the majority of the thrust.

The operational cycle of the engine consists of different phases:

- Intake
- Compression
- Combustion
- Expansion
- Exhaust

The air enters through the inlet duct, is compressed in the compressor stages and then enters in the combustion chamber, where atomized fuel is added and combustion occurs, generating hot combustion gases. The combustion gases are then expanded in a turbine, which provides the work needed by the compressor.

Up to this point, the engine operates just as a turbojet engine. But after the first turbine, turbopropeller and turbojet engines differ. Turbojet engines expand all the combustion gases through a nozzle, providing thrust. On the other hand, in turbopropellers the combustion gases pass through an additional turbine (called power turbine), which extracts almost all the energy contained in the gas flow and uses it to drive the propeller. After the power turbine, the gases are expanded in a nozzle and discharged in the atmosphere, providing additional thrust.

As most of the energy is absorbed by the power turbine, the thrust generated by the gases expanding in the nozzle is very limited. The majority of the thrust, usually around 90%, is provided by the propeller. The propeller develop thrust by moving a large mass of air through a small increment of velocity. Propellers are very efficient, expecially at low-medium speeds. In fact, as the speed at the blade tips approaches sonic conditions, the efficiency of the propeller sharply decreases, due to the insurgence of shockwaves and other non-uniformities in the flow.

The propeller can be connected to the core engine in two different ways:

- Fixed Shaft-constant speed: the propeller is hosted on the same shaft of the core engine, through a reduction gear that converts the high RPM-low torque of the main shaft to the low RPM-high torque needed by the propeller in order to operate efficiently.

This type of engine works at almost constant speed. In fact, in flight the engine RPM can be varied within only a narrow range, usually from 96% to 100%, while during ground operation the RPM can be lowered up to 70%.

Since during flight the rotational speed is constant, power changes are obtained through fuel flow and propeller blade angle variations: an increased fuel flow yields an higher gas temperature in the engine and therefore more energy available for the turbine. The turbine then absorbs more energy and therefore provides more torque to the propeller shaft. The increased torque then forces the increment of the propeller blade angle in order to maintain a constant rotational speed.

Failures in this kind of engine can be particularly problematic. In fact a failure leads to a severe drag condition due to the large power requirements of the compressor being provided by the propeller that works as a turbine in this case. In order to avoid this, usually fixed-shaft engines are equipped with a Negative Torque Sensing (NTS) system. The NTS system activates only in case of engine failure, where the propeller now drives the engine and generates drag. The NTS system reduces the drag by moving the propeller blades to their feathered condition [33].

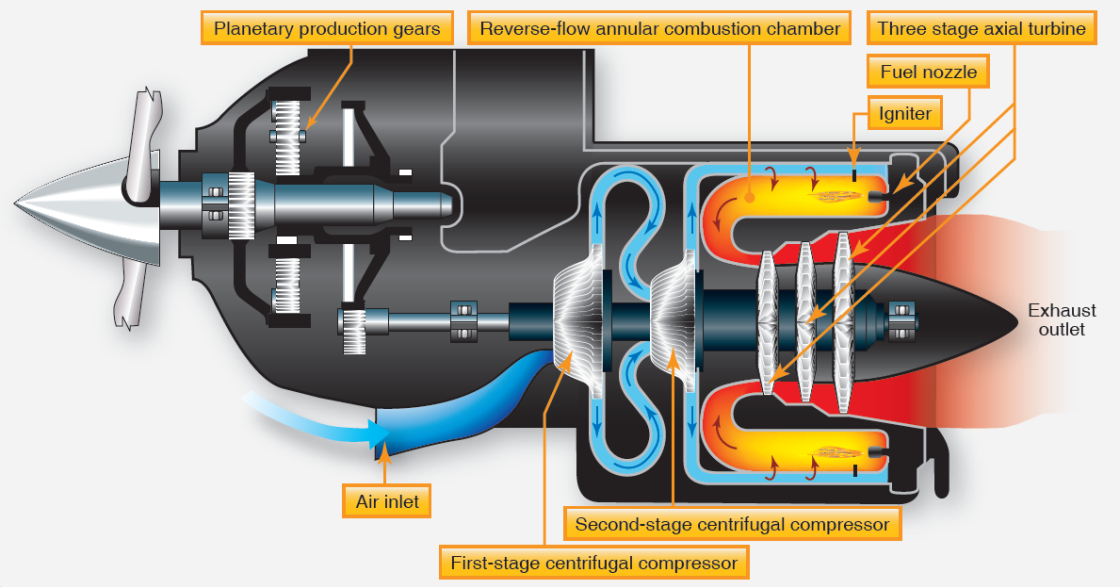

Garrett TPE331 fixed shaft engine [33]

- Free Turbine: the propeller is not hosted on a the same shaft of the main engine. The power turbine in fact is on a different shaft than the rest of the engine and drives the propeller through a reduction gear, in order to have turbine and propeller working at their optimal RPM regimes.

  Differently from the fixed shaft configuration, it is now possible for the pilot to choose the desired propeller rotational speed, independently from the engine RPM (which determines the power output). The propeller RPM range is usually between 1500 and 1900 [33].

  Typically, this kind of engines has two independent counter-rotating turbines: the one that drives the compressor, hosted on the main shaft, and the one that drives the propeller, on a different shaft. The air intake usually in in the rear part of the engine. The air enters, flows forward through the compressor stages and then enters

in a reverse-flow combustion chamber. After combustion, the hot gases expand in both turbines and are discharged through exhaust ports near the front of the engine [33].

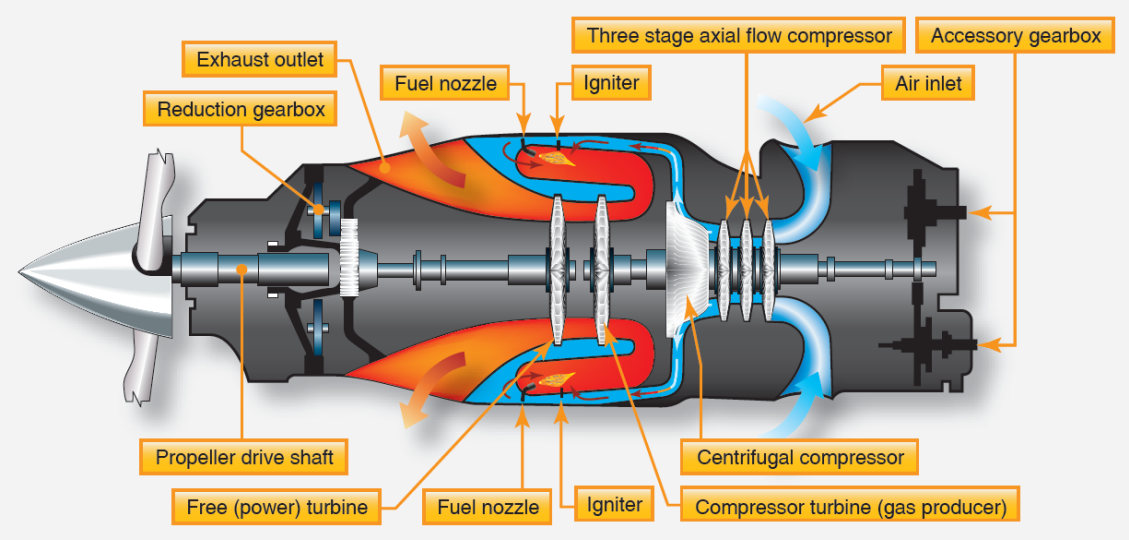

Pratt & Whitney PT-6 free turbine engine [33]

1.1 Turbopropeller characteristics

Turbopropellers are most efficient at low to medium speeds, usually between 400 km/h and 650 km/h [33], due to the propeller sharp loss of efficiency when its blades approach the sonic condition. For this reason, turbopropellers usually operate at Mach numbers not higher than 0.6 [34]. For this reason, turbopropellers are the engines of choice for most commuter and cargo aircrafts, which operate at relatively low speeds and often over relatively short distances [34] [35]. In fact, in these conditions the high performances and low specific fuel consumption offset the low flight speed.

In terms of altitude, turbopropellers are most efficient between 5500 m and 9000 m, but can fly up to 10500 m without problems [33] [36]. The minimum specific fuel consumption is usually attained in the altitude range between 7500 m and the tropopause [33].

Turbopropeller also perform well during the take-off, climb and landing, requiring less runaway. This is due to the fact that the propeller is able to accelerate a large mass of air even when the aircraft is moving at a relatively low speed.

1.2 Comparison with turbojets and piston-powered engines

Turbopropellers vs piston-powered engines

The principal difference between piston-powered engines and turbopropellers is that in the first the propeller is driven by a reciprocating engine, while in the latter the propeller is driven by a gas turbine engine.

Turbopropellers usually are larger, lighter, can flight higher and faster, yield more power at sea level and can carry more payload and passengers than piston-powered engines.

They also can easily operate the propeller in beta and reverse conditions, differently from piston-powered engines in which thrust reversal, if possible at all, is more problematic to implement.

On the other hand, piston-powered engines have lower specific fuel consumption, but turbopropeller specific fuel consumption decreases faster with the altitude and can fly higher, thus they can be as efficient as their piston counterparts if they fly sufficiently high and long.

Turbopropellers vs turbojets

The principal difference between turbojets and turbopropellers is that in the first the propeller is absent and the thrust is obtained entirely by expanding the hot combustion gases in the nozzle, while in the latter the majority of the thrust is given by the propeller, which is driven by an additional turbine in the gas turbine core engine.

Turbopropellers usually are more complicated, heavier (due to the presence of the gearbox and additional turbine) and slower than turbojets of comparable size and power.

On the other hand they have lower specific fuel consumption, require less runaway for take-off and landing and yield more thrust at low speeds [33] [34] [36].

1.3 Turbopropeller-powered aircrafts

It is now presented and overview on the turbopropeller engines that are currently in service throughout the world.

First of all are presented the major producers of turbopropeller-powered aircrafts. For each company are reported the aircraft models that are currently being produced and the engine model that they use:

Airbus (Europe)	
Aircraft	**Engine**
A400M	EuroProp TP400-D6
C295	Pratt & Whitney Canada PW127G
European MALE RPAS (UAV) (in development)	Twin Turboprops
Atlante (UAV)	Single Turboprop

Table 1.1: List of Airbus' turboprop aircrafts [15]

Piaggio Aerospace (Italy)	
Aircraft	**Engine**
P180 Avanti EVO	Pratt & Whitney Canada PT6A–66B
P1HH HammerHead (UAV)	Pratt & Whitney Canada PT6A–66B
Piaggio Aerospace MPA	Pratt & Whitney Canada PT6A–66B

Table 1.2: List of Piaggio Aircraft's turboprop aircrafts [16]

Daher-SOCATA TBM (France)	
Aircraft	**Engine**
TBM 910	Pratt & Whitney Canada PT6A-66D
TBM 940	Pratt & Whitney Canada PT6A-66D
Kodiak 100	Pratt & Whitney Canada PT6A-34

Table 1.3: List of Daher-SOCATA's turboprop aircrafts [17]

ATR Aircraft (France)	
Aircraft	**Engine**
600 Series	Pratt & Whitney Canada PW127 series

Table 1.4: List of ATR Aircraft's turboprop aircrafts [18]

Pilatus Aircraft (Switzerland)	
Aircraft	**Engine**
PC-6	Pratt & Whitney Canada PT6A-27
PC-7 Mk II	Pratt & Whitney Canada PT6A-25C
PC-9 M	Pratt & Whitney Canada PT6A-62
PC-12 NGX	Pratt & Whitney Canada PT6E-67XP
PC-21	Pratt & Whitney Canada PT6A-68B

Table 1.5: List of Pilatus Aircraft's turboprop aircrafts [19]

H3 Grob Aircraft (Germany)	
Aircraft	**Engine**
G 120TP	Rolls-Royce M250-B17F
G 520NG	Pratt & Whitney Canada PT6A-67

Table 1.6: List of H3 Grob Aircraft's turboprop aircrafts [20]

Diamond Aircraft Industries (Austria/Canada)	
Aircraft	**Engine**
Diamond DART-550	GE H75-100
Diamond DART-450	Ivchenko AI-450S

Table 1.7: List of Diamond Aircraft Industries' turboprop aircrafts [21]

Antonov Airlines (Ucraine)	
Aircraft	**Engine**
AN-26-100	Ivchenko AI-24T
AN-22A	Kuznetsov NK-12

Table 1.8: List of Antonov Airlines' turboprop aircrafts [22]

Ilyushin (Russia)	
Aircraft	**Engine**
Il-112 Series	Klimov TV7-117ST / Klimov TV7-117SM
Il-114 Series	Klimov TV7-117ST / Klimov TV7-117SM Pratt & Whitney Canada PW127
Il-38	Ivchenko AI-20M series 6I

Table 1.9: List of Ilyushin's turboprop aircrafts [23]

Lockeed Martin (USA)	
Aircraft	**Engine**
C-130J Super Hercules and variants	Rolls-Royce T56-A-15
P-3 Orion	Rolls-Royce T56-A-14
LM-100J	Rolls-Royce AE2100-D3

Table 1.10: List of Lockeed Martin's turboprop aircrafts [24]

Beechcraft (USA)	
Aircraft	**Engine**
T-6A	Pratt & Whitney Canada PT6A-68/D
AT-6	Pratt & Whitney Canada PT6A-68/D
King Air 250	Pratt & Whitney Canada PT6A-52
King Air 350i	Pratt & Whitney Canada PT6A-60A
King Air C90GTx	Pratt & Whitney Canada PT6A-135A

Table 1.11: List of Beechcraft's turboprop aircrafts [25]

Piper Aircraft (USA)	
Aircraft	**Engine**
M660/SLS	Pratt & Whitney Canada PT6A-42A
M500	Pratt & Whitney Canada PT6A-42A

Table 1.12: List of Piper Aircraft's turboprop aircrafts [26]

Evolution Aircraft (USA)	
Aircraft	**Engine**
EVOT-850	Pratt & Whitney Canada PT6A-140A
EVOT-750	Pratt & Whitney Canada PT6A-135A
EVOT-550	Pratt & Whitney Canada PT6A-21

Table 1.13: List of Evolution Aircraft's turboprop aircrafts [27]

Epic Aircraft (USA)	
Aircraft	**Engine**
E1000	Pratt & Whitney Canada PT6A-67A

Table 1.14: List of Epic Aircraft's turboprop aircrafts [28]

Nextant Aerospace (USA)	
Aircraft	**Engine**
Nextant G90XT	GE H75

Table 1.15: List of Nextant Aerospace's turboprop aircrafts [29]

Bombardier (Canada)	
Aircraft	**Engine**
Bombardier 415	Pratt & Whitney Canada PW123 series
Bombardier Q200	Pratt & Whitney Canada PW123 series
Bombardier Q300	Pratt & Whitney Canada PW123 series
Bombardier Q400	Pratt & Whitney Canada PW150A

Table 1.16: List of Bombardier's turboprop aircrafts [30]

Embraer (Brazil)	
Aircraft	**Engine**
Super Tucano	Pratt & Whitney Canada PT6A-68C

Table 1.17: List of Embraer's turboprop aircrafts [31]

As anticipated before, turbopropellers are employed mainly in civil/military cargo aircrafts, regional airliners, private/business light aircrafts and military light aircrafts for training and surveillance.

An new emerging field of application for turbopropeller engines is that of UAVs (Unmanned Aerial Vehicle), in particular in those for surveillance and reconnaissance. In fact, the low fuel consumption of turbopropellers grants high autonomy to these light aircrafts, which is of fundamental importance for the success of those kind of missions.

1.4 Turbopropeller manufacturers

Now follows an overview of the leading global turbopropeller engine manufacturers. For each manufacturer are reported the specifications of the engine models in use on aircrafts currently in service.

1.4.1 Pratt & Whitney Canada (PWC) [1]

Pratt & Whitney Canada is probably the most renowned turbopropeller engine manufacturer. It is a division of Pratt & Whitney US and is specialized in small and medium aircraft engines. Although a division of the US-based company, PWC is responsible for the manufacturing, research, development and marketing of its engines.

Currently, PWC offers three different families of turbopropeller engines: the PW100/150 family, the PT6A family and the PT6E family.

PW100/150 engines

This family of engines is focused on low fuel consumption on routes of 350 miles or less.

They consume 25% to 40% less fuel than comparable jets, thus reducing CO_2 emissions up to 50%.

The PW100 family is a two-spool, three-shaft engine with cooled turbine blades. The third shaft couples the power turbine to the propeller through a reduction gearbox.

The PW100 series comprises 38 engine models, ranging from 1800 to 5000 shaft horsepower (shp).

General characteristics:

- Engine models from PW118 to PW127: two-spool, two-stage centrifugal compressors with integrally bladed rotors, independently driven by LP and HP turbines. No variable geometry is present and no APU required, since the engine features an electric start
- Engine model PW150: two-spool, four stage - three axial plus single centrifugal - compressors with integrally bladed rotors, independently driven by LP and HP turbines. No variable geometry is present and no APU required, since the engine features an electric start
- Reverse flow combustion chamber
- Single-stage HPT and IPT
- Two-stage power turbine with shrouded blades, in free turbine configuration
- Electronic engine control (EEC)
- Full Authority Digital Engine Control (FADEC)

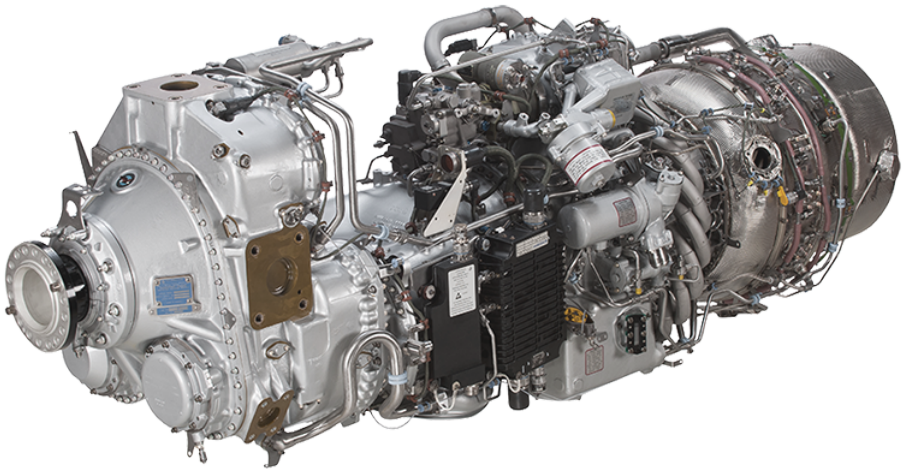

Figure 1.1: PW127M engine [1]

Here below the specifications for the PW100/150 engines in use on aircrafts currently in service. Power and specific fuel consumption values are referred to the propeller's shaft and at take off unless otherwise indicated:

	PW118	**PW121**	**PW123AF**	**PW123B**
Application	Embraer EMB 120 Brasilia	ATR42	Bombardier 415	Bombardier Q300
Power	1342 kW	1600 kW	1775 kW	1864 kW
Sp. fuel cons.	0.303 kg/kWh	0.289 kg/kWh	0.286 kg/kWh	0.282 kg/kWh
Overall PR	-	-	-	-
Compr. stages	1C+1C	1C+1C	1C+1C	1C+1C
HPT stages	1A	1A	1A	1A
IPT stages	1A	1A	1A	1A
LPT stages	2A	2A	2A	2A
Length	2057 mm	2134 mm	2134 mm	2134 mm
Width/diameter	787 mm	787 mm	838 mm	838 mm
Weight	390 kg	425 kg	450 kg	450 kg

A = axial, C = centrifugal

Table 1.18: PW100/150 engines specs - part A. Data from [32] where not indicated

	PW123C/D	**PW127A**	**PW127E**	**PW127F/M**
Application	Bombardier Q200	Antonov An-140	ATR 42-500	ATR 72-500, ATR 72-600, ATR 42-600
Power	1600 kW	1775 kW	1790 kW	2050 kW
Sp. fuel cons.	0.294 kg/kWh	0.279 kg/eq-kWh*	0.279 kg/eq-kWh*	0.279 kg/kWh
Overall PR	-	-	-	-
Compr. stages	1C+1C	1C+1C	1C+1C	1C+1C
HPT stages	1A	1A	1A	1A
IPT stages	1A	1A	1A	1A
LPT stages	2A	2A	2A	2A
Length	2134 mm	2134 mm	2134 mm	2134 mm
Width/diameter	838 mm	838 mm	838 mm	838 mm
Weight	481 kg	481 kg	481 kg	481 kg

** source: PW127 Turboprop Sales Specification No 1009 Datasheet*

Table 1.19: PW100/150 engines specs - part B. Data from [32] where not indicated

	PW127G*	**PW150A**
Application	Airbus C295	Bombardier Q400
Power	2178 kW	3784 kW
Sp. fuel cons.	-	0.263 kg/kWh**
Overall PR	-	18**
Compr. stages	1C+1C	3A+1C
HPT stages	1A	1A
IPT stages	1A	1A
LPT stages	2A	2A
Length	2130 mm	2420 mm***
Width/diameter	679 mm	790 mm***
Weight	484 kg	717 kg***

** source: https://www.easa.europa.eu/sites/default/files/dfu/EASA%20IM.E.041%20TCDS%20Issue%204.pdf*

*** source: https://engineering.purdue.edu/~propulsi/propulsion/jets/tprops/pw100.html*

**** source:*

https://www.easa.europa.eu/sites/default/files/dfu/TCDS%20PW150%20series%20issue%2001_20141119_1.0.pdf

Table 1.20: PW100/150 engines specs - part C. Data from [32] where not indicated

PT6A engine

The PT6A engine family is the most popular in turbopropeller aircrafts. Over 70 different engine models belong to this family, ranging from 500 shp to 1900 shp, providing flexibility, versatility and high capability in a variety of applications.

The PT6A series is also the only engine to achieve the Single Engine Instrument Flight Rules (IFR) status for passengers revenue activity in USA, Europe, Australia and New Zealand.

General characteristics:

- Two shafts
- Multistage compressor driven by a single-stage HPT
- Independent power turbine with shrouded blades, in free turbine configuration
- Epicyclic concentric reduction gearbox
- Reverse flow combustion chamber
- Reverse flow radial inlet with Foreign Object Damage (FOD) protection
- Electronic engine control (EEC)

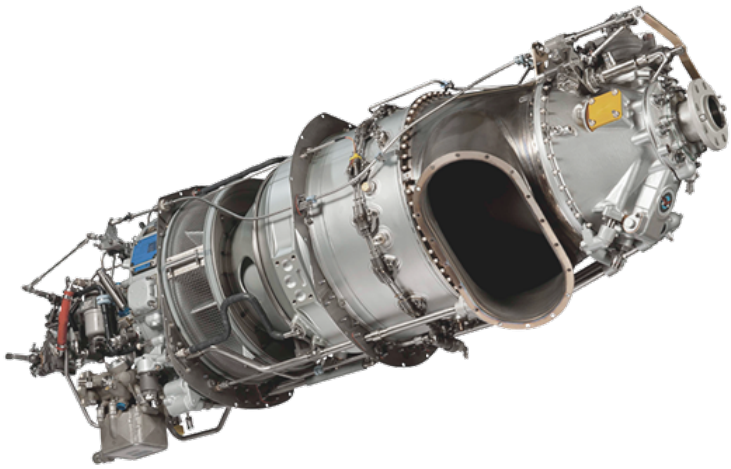

Figure 1.2: PT6A-140 engine [1]

Here below the specifications for the PT6A engines in use on aircrafts currently in service. Power and specific fuel consumption values are referred to the propeller's shaft and at take off unless otherwise indicated:

	PT6A-21*	**PT6A-25C**	**PT6A-27**	**PT6A-34**
Application	EVOT-550	Pilatus PC-7 Mk II	Pilatus PC-6 Turbo Porter	Kodiak 100
Power	410 kW	560 kW	462 kW	418 kW
Sp. fuel cons.	0.383 kg/eq-kWh	0.362 kg/kWh	0.366 kg/kWh	0.362 kg/eq-kWh
Overall PR	-	-	6.7	-
Compr. stages	3A+1C	3A+1C	3A+1C	3A+1C
HPT stages	1A	2A	2A	2A
IPT stages	no	no	no	no
LPT stages	1A	1A	1A	1A
Length	1574 mm	1574 mm	1574 mm	1574 mm
Width/diameter	463 mm	463 mm	463 mm	463 mm
Weight	148 kg	152 kg	149 kg	150 kg

** source: https://www.evolutionaircraft.com/wp-content/uploads/PT6A21-1158-GENERIC.pdf*

Table 1.21: PT6A engines specs - part A. Data from [32] where not indicated

	PT6A-42	**PT6A-52***	**PT6A-60A**	**PT6A-62**
Application	Piper Meridian	Beechcraft King Air B200gt, King Air 250	Beechcraft King Air 350	Pilatus PC-9 M
Power	634 kW	634 kW	783 kW	858 kW
Sp. fuel cons.	0.366 kg/kWh	0.549 kg/kWh (at max cruise, FL230)**	0.333 kg/kWh	0.345 kg/kWh
Overall PR	-	-	-	-
Compr. stages	3A+1C	multistage	3A+1C	3A+1C
HPT stages	2A	1A	2A	2A
IPT stages	no	no	no	no
LPT stages	2A	2A	2A	2A
Length	1700 mm	1696 mm	1829 mm	1778 mm
Width/diameter	463 mm	464 mm	463 mm	463 mm
Weight	183 kg	204 kg	215 kg	206 kg

** source: https://www.easa.europa.eu/sites/default/files/dfu/EASA-TCDS-E.078_%28IM%29_Pratt_and_Whitney_Canada_PT6A--41_series_engines-01-31082007.pdf*

*** source: Brochure - Blackhawk Super XR52 Engine Upgrade - English, downloaded from https://air-alliance.de/*

Table 1.22: PT6A engines specs - part B. Data from [32] where not indicated

	PT6A-64	**PT6A-65SC**	**PT6A-66B**	**PT6A-66D****
Application	EADS Socata TBM 700 C2	Cessna 408 SkyCourier	Piaggio P180 Avanti Evo, Piaggio P1HH HammerHead, Piaggio Aerospace MPA	EADS Socata TBM 850, TBM 910, TBM 940
Power	522 kW	820 kW	634 kW	634 kW
Sp. fuel cons.	0.428 kg/kWh	-	0.377 kg/kWh	0.259 kg/kWh (at normal cruise)***
Overall PR	-	-	-	-
Compr. stages	3A+1C	4A+1C*	4A+1C	4A+1C
HPT stages	2A	1A*	2A	1A
IPT stages	no	no*	no	no
LPT stages	2A	2A*	2A	2A
Length	-	approx 1490 mm*	1778 mm	1777 mm
Width/diameter	463 mm	approx 464 mm*	463 mm	466 mm
Weight	207 kg	approx 227 kg*	213 kg	207 kg

** source: https://www.easa.europa.eu/sites/default/files/dfu/EASA-TCDS-E.078_(IM)_Pratt_and_Whitney_Canada_PT6A--41_series_engines-01-31082007.pdf*

*** source: https://www.easa.europa.eu/sites/default/files/dfu/PT6A_67%20Series%20Issue%2005_20191011.pdf*

**** source: "TBM 910 pilot's operating handbook" (PDF). Daher - 15 January 2017*

Table 1.23: PT6A engines specs - part C. Data from [32] where not indicated

	PT6A-67A	**PT6A-67B**	**PT6A-67R**	**PT6A-68**
Application	Epic LT, Epic Dynasty, Epic E1000	Pilatus PC-12 NG	Basler BT-67	Beechcraft T-6C
Power	895 kW	895 kW	1062 kW	932 kW
Sp. fuel cons.	0.334 kg/kWh	0.336 kg/kWh	0.316 kg/kWh	0.328 kg/kWh
Overall PR	-	-	-	-
Compr. stages	4A+1C	4A+1C	4A+1C	4A+1C
HPT stages	2A	2A	2A	1A
IPT stages	no	no	no	no
LPT stages	2A	2A	2A	2A
Length	-	-	1930 mm	1778 mm
Width/diameter	463 mm	463 mm	463 mm	463 mm
Weight	230 kg	234 kg	234 kg	250 kg

Table 1.24: PT6A engines specs - part D. Data from [32] where not indicated

	PT6A-68B*	**PT6A-68C***	**PT6A-114A**	**PT6A-135A**
Application	Pilatus PC-21	Embraer EMB 314 Super Tucano	Cessna Caravan, Gran Caravan, Caravan Amphibian	Beechcraft King Air C90gti, EVOT-750
Power	1194 kW	1194 kW	503 kW	560 kW
Sp. fuel cons.	0.328 kg/kWh**	0.328 kg/kWh**	0.389 kg/kWh**	0.356 kg/kWh
Overall PR	-	-	-	-
Compr. stages	4A+1C	4A+1C	3A+1C	3A+1C
HPT stages	1A	1A	2A	2A
IPT stages	no	no	no	no
LPT stages	2A	2A	1A	1A
Length	1813 mm	1823 mm	1574 mm	1574 mm
Width/diameter	565 mm	570 mm	463 mm	463 mm
Weight	269 kg	272 kg	159 kg	156 kg

** source: https://www.easa.europa.eu/sites/default/files/dfu/EASA_TCDS_IM.E.038_PT6A-68_issue%2001_20161904_1.0.pdf*

*** source: "Gas Turbine Engines" (PDF). Aviation Week. 28 January 2008. pp. 137–138*

Table 1.25: PT6A engines specs - part E. Data from [32] where not indicated

	PT6A-140*
Application	Cessna Grand Caravan EX, EVOT-850
Power	646 kW
Sp. fuel cons.	0.344 kg/eq-kWh
Overall PR	-
Compr. stages	multistage
HPT stages	multistage
IPT stages	no
LPT stages	1A
Length	1625 mm
Width/diameter	533 mm
Weight	175 kg

** source: https://www.evolutionaircraft.com/wp-content/uploads/PT6A140A-1196.pdf*

Table 1.26: PT6A engines specs - part F

PT6E engines

The PT6E family is General Aviation's first dual-channel integrated electronic propeller and engine control system. This reduces the workload on the pilot, leaving him free to focus on other aspects.

The PT6E two independent control systems process all the engine's data and makes the necessary adjustments to optimize the engine performance throughout the flight.

Furthermore, the engine parameters are continuously monitored, optimizing the maintenance planning and reducing its related costs.

General characteristics:

- Single-crystal HPT blades
- Optimized turbine cooling
- Longer maintenance and TBO intervals

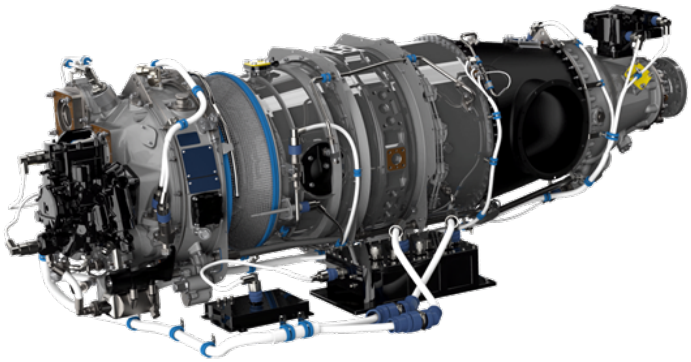

Figure 1.3: PT6E series engine [1]

Here below the specifications for the PT6E engines in use on aircrafts currently in service. Power and specific fuel consumption values are referred to the propeller's shaft and at take off unless otherwise indicated:

	PT6E-67XP*
Application	Pilatus PC-12 NGX
Power	895 kW
Sp. fuel cons.	-
Overall PR	-
Compr. stages	4A+1C
HPT stages	1A
IPT stages	no
LPT stages	2A
Length	1871 mm
Width/diameter	482 mm
Weight	270 kg

* source: https://www.easa.europa.eu/sites/default/files/dfu/PT6A_67%20Series%20Issue%2005_20191011.pdf

Table 1.27: PT6E engines specs

1.4.2 Rolls-Royce [2]

Rolls-Royce is a British company that designs and manufactures power system for aviation, naval and other applications.

It is one of the world's largest producers of aircraft engines and is also predominant in the marine and energy sectors.

Here below the main turbopropeller engines curently produced by Rolls-Royce.

T56 engines

The T56 family provides large, robust and reliable turboprop engines operating in civil and military aircrafts, mainly for maritime patrols and transport.

General characteristics:

- Single-shaft
- Modular design
- 14 stages axial flow compressor
- 4 stages turbine
- Gearbox with two stages of gear reduction, propeller brake and connected to the power section by a torquemeter assembly

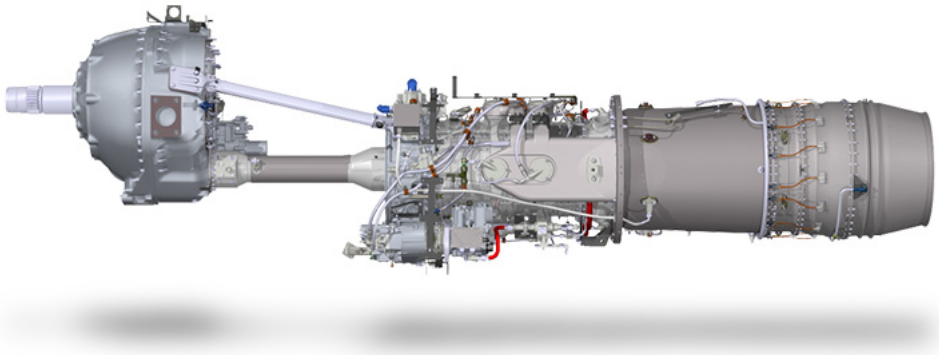

Figure 1.4: T56 series engine [2]

Here below the specifications for the T56 engines in use on aircrafts currently in service. Power and specific fuel consumption values are referred to the propeller's shaft and at take off unless otherwise indicated:

	T56-A-14	**T56-A-15**	**T56-A-427**
Application	Lockheed Martin P-3 Orion	Lockheed Martin C-130J Super Hercules	Northrop Grumman E 2C Hawkeye 2000
Power	3423 kW	3423 kW	3915 kW
Sp. fuel cons.	0.328 kg/kWh	0.328 kg/kWh	0.286 kg/kWh
Overall PR	9.6	9.6	12
Compr. stages	14A	14A	14A
HPT stages	4A	4A	4A
IPT stages	no	no	no
LPT stages	no	no	no
Length	3716 mm	3716 mm	3711 mm
Width/diameter	1245 mm	1132 mm	1227 mm
Weight	855 kg	838 kg	880 kg

Table 1.28: T56 engines specs. Data from [32] where not indicated

M250 turboprop engines

The M250 series provides small, lightweight, high power engines for light fixed-wing aircrafts and helicopters (turboshaft version).

They are characterized by low vibration and noise levels, providing a more comfortable flight experience.

General characteristics:

- Power ratings between 420-450 shp
- 4 or 6 stages axial plus single-stage centrifugal compressors
- Two-stage HPT with hydro-mechanical fuel control system
- Two-stage power turbine
- Compact design

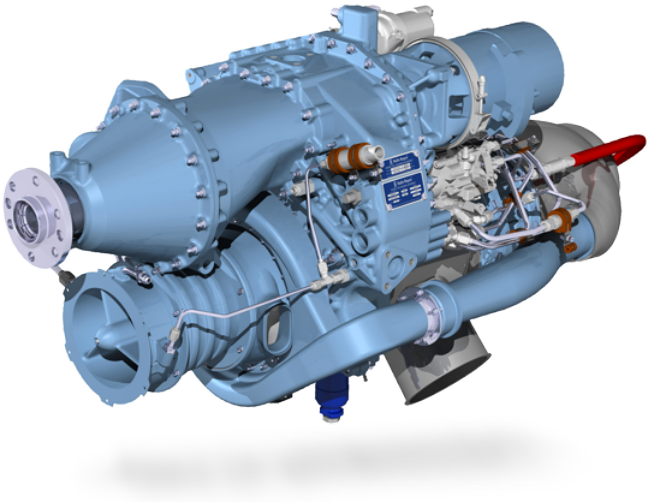

Figure 1.5: M250 series engine [2]

Here below the specifications for the M250 engines in use on aircrafts currently in service. Power and specific fuel consumption values are referred to the propeller's shaft and at take off unless otherwise indicated:

	M250-B17F/2
Application	Grob G-140TP, Extra EA 500, BAE Systems Mantis
Power	336 kW
Sp. fuel cons.	0.371 kg/kWh
Overall PR	7.9
Compr. stages	4A+1C
HPT stages	2A
IPT stages	no
LPT stages	2A
Length	1140 mm
Width/diameter	571 mm
Weight	96 kg

Table 1.29: M250 engines specs. Data from [32] where not indicated

TP400-D6 engine

The TP400-D6 engine was designed for the Airbus A400M aircraft in collaboration with MTU, Safran Aircraft Engines and IPT. Rolls-Royce was responsible for the 6-stage high pressure compressor, air and oil systems, intermediate casing, low pressure shaft, and overall engine performance.

General characteristics:

- Three-shafts counter-rotating engine

- 11600 shp of power
- Low susceptibility to FODs and erosion
- Designed to operate in harsh environments

Figure 1.6: T400-D6 engine [2]

Here below the specifications for the TP400-D6 engine. Power and specific fuel consumption values are referred to the propeller's shaft and at take off unless otherwise indicated:

	TP400-D6*
Application	Airbus A400M
Power	8203 kW
Sp. fuel cons.	0.225 kg/kWh**
Overall PR	25
Compr. stages	5A+6A
HPT stages	1A
IPT stages	1A
LPT stages	3A
Length	3500 mm
Width/diameter	924 mm
Weight	1826 kg

** source: "TP400-D6" - Rolls-Royce*

*** source: Coniglio, Sergio (July 2003). "A400M, An-70, C-130J, C-17: How Do They Stand?". Military Technology (MILTECH). Vol. 27 no. 7. Mönch Publishing Group. pp. 51–60*

Table 1.30: TP400-D6 engine specs

AE2100 engines

The AE2100 is a turbopropeller engine designed for military transport and long-range maritime patrol aircrafts.

It is characterized by low maintenance costs due to its modular design and its easily accessible components.

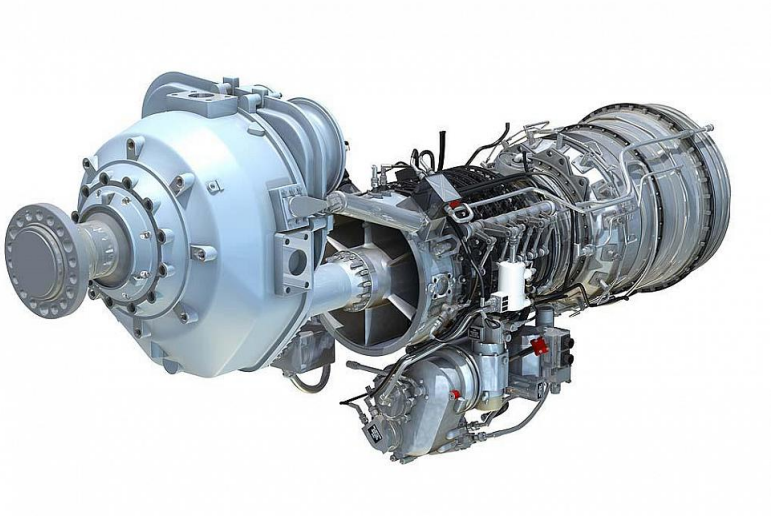

Figure 1.7: AE2100 engine [9]

Here below the specifications for the AE2100 engines in use on aircrafts currently in service. Power and specific fuel consumption values are referred to the propeller's shaft and at take off unless otherwise indicated:

	AE2100-D3*
Application	Alenia C-27J Spartan
Power	3458 kW
Sp. fuel cons.	0.249 kg/kWh**
Overall PR	16.6
Compr. stages	14A
HPT stages	2A
IPT stages	no
LPT stages	2A
Length	3150 mm
Width/diameter	729 mm
Weight	873 kg

** source: http://www.fi-powerweb.com/Engine/Rolls-Royce-AE-2100.html*

*** source: [32]*

Table 1.31: AE2100 engines specs

1.4.3 General Electric Aviation [3]

GE Aviation, a subsidiary of General Electric, is a US-based company leader in the development, production and supply of aircraft engines.

Concerning turbopropeller engines, GE currently offers three different series of engines: the Catalyst, the H-series and the T700/CT7 family.

Catalyst engines

The Catalyst engine is the first all-new turbopropeller engine developed by GE in the last 50 years.

The driving parameter in its design was simplicity. To that end, the engine is equipped with a FADEC, that automatically manages the engine operating conditions, reducing the pilot's workload. It also collects engine data during its operation, allowing for optimized maintenance scheduling and thus increasing the engine availability.

The Catalyst engine is also the first turbopropeller engine with 3D-printed parts. This allows for a reduced number of engine parts, reducing complexity, weight, fuel consumption, durability (due to fewer seams), leakage (due to tighter tolerances) and manufacturing time.

General characteristics:

- Compressors with variable stator vanes
- Two-stage, single-crystal HPT with internal air cooling
- Three-stage power turbine
- Propeller gearbox with planetary gears
- Reverse flow combustor
- Digital controls
- Compact design

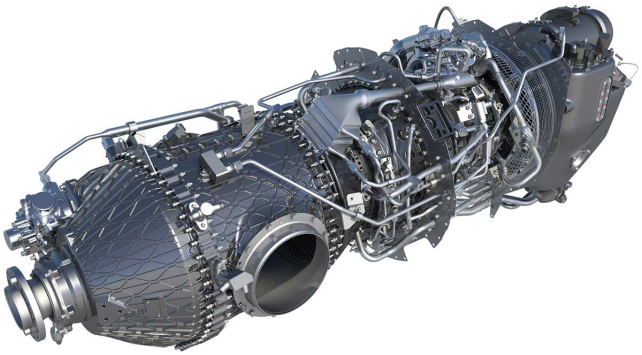

Figure 1.8: Catalyst engine [3]

Here below the specifications for the Catalyst engines in use on aircrafts currently in service. Power and specific fuel consumption values are referred to the propeller's shaft and at take off unless otherwise indicated:

	GE Catalyst*
Application	Cessna Denali
Power	969 kW
Sp. fuel cons.	0.293 kg/kWh (15% less than PT6A-140)**
Overall PR	16
Compr. stages	4A+1C
HPT stages	2A
IPT stages	no
LPT stages	3A
Length	-
Width/diameter	-
Weight	272 kg

** source: "GE Aviation launches new turboprop engine" (Press release), GE Aviation. November 16, 2015. // Guy Norris (November 17, 2015). "GE Takes On PT6 Engine With Advanced Turboprop". Aviation Week. // Guy Norris (November 17, 2015). "GE Takes On PT6 Engine With Advanced Turboprop". Aviation Week.*

*** source: https://m.aviationweek.com/ge-catalyst-makes-first-full-power-tests*

Table 1.32: Catalyst engines specs

H-series engines

The H-series are designed for a variety of utility missions, such as cargo transport, medical support and skydiving. They are designed to be able to operate in rugged conditions and with mission readiness in mind.

The H-series comprises three engine models: the H75, the H80 and the H85.

General characteristics:

- Power in the range of 750-850 shp
- No need for fuel nozzles and hot section inspections, allowing for easier maintenance
- Annular flow combustor

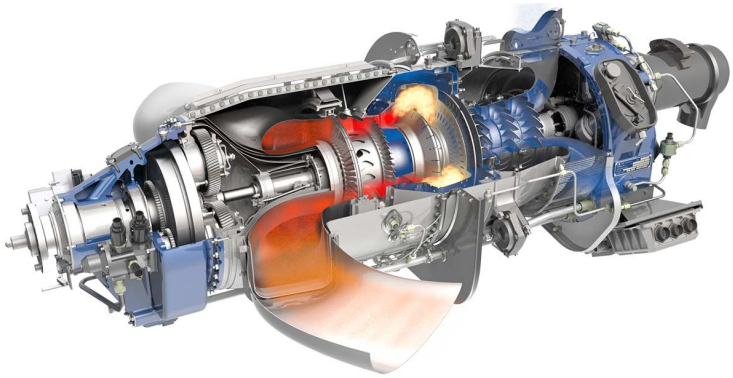

Figure 1.9: H-series engine [3]

Here below the specifications for the H-series engines in use on aircrafts currently in service. Power and specific fuel consumption values are referred to the propeller's shaft and at take off unless otherwise indicated:

	GE H75/H80/H85*
Application	CAIGA Primus 150, Diamond DART 550, L-410 Turbolet, Nextant G90XT
Power	559 (H75), 597(H80), 634(H85) kW
Sp. fuel cons.	0.356 kg/kWh**
Overall PR	6.7***
Compr. stages	2A+1C
HPT stages	1A
IPT stages	no
LPT stages	1A
Length	1670 mm
Width/diameter	560 mm
Weight	177 kg

** source: "GE H Series Turboprop Engine" (PDF). GE Aviation. Nov 2017.*

*** source: https://www.ainonline.com/aviation-news/business-aviation/2012-10-31/smyrna-air-center-h80-engine-conversions-now-available*

**** source: Daly, Mark (2015). Jane's Aero-Engines 2016-2017. London: Ihs Jane's.*

Table 1.33: H-series engines specs

T700/CT7 engines

The T700/CT7 is a family of turbopropeller and turboshaft engines. The turbopropeller variants use the same core as the turboshaft engines with the addition of a turbopropeller gearbox.

General characteristics:

- Six-stage compressor
- Two-stage HPT
- Two-stage power turbine

Figure 1.10: CT7-9 engine [3]

Here below the specifications for the T700/CT7 engines in use on aircrafts currently in service. Power and specific fuel consumption values are referred to the propeller's shaft and at take off unless otherwise indicated:

	GE CT7-9B
Application	Sukhoi Su-80
Power	1305 kW
Sp. fuel cons.	0.277 kg/kWh*
Overall PR	17**
Compr. stages	5A+1C
HPT stages	2A
IPT stages	no
LPT stages	2A
Length	2438 mm
Width/diameter	737 mm
Weight	365 kg

** source: https://www.geaviation.com/commercial/engines/ct7-engine*

*** source: https://www.wikiwand.com/en/General_Electric_T700*

Table 1.34: T700/CT7 engines specs. Data from [32] where not indicated

1.4.4 JSC Kuznetsov [4]

JSC Kuznetsov is one of the leading Russian manufacturers of aeroengines and rocket engines. It is a joint-stock company born from the consolidation of several aerospace companies.

Kuznetsov NK-12

The Kuznetsov NK-12 engine (and its variants) is the most noteworthy turbopropeller engine developed by the Kuznetsov design bureau. Designed in the 1950's, is characterized by two four-blade counter-rotating propellers and is the most powerful turbopropeller to enter service. Among other aircrafts, it powers the Antonov An-22 and the Tupolev Tu-95 bomber.

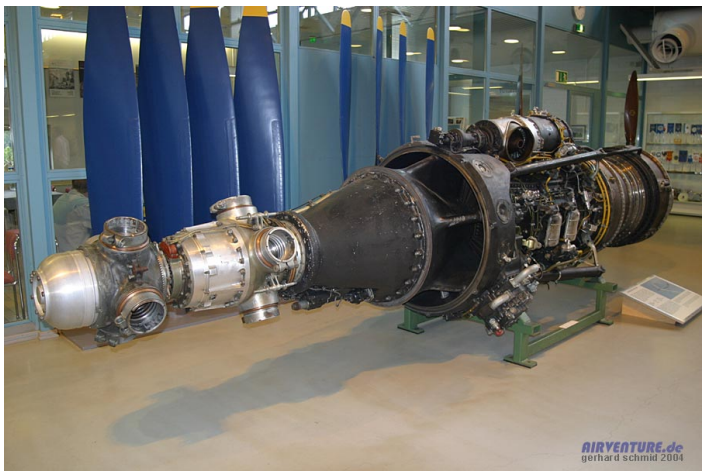

Figure 1.11: Kuznetsov NK-12 engine

source: `http://culturaaeronautica.blogspot.com/2011/10/kuznetsov-nk-12-o-mais-poderoso-motor.html`

Here below the specifications for the Kuznetsov NK-12 engines in use on aircrafts currently in service. Power and specific fuel consumption values are referred to the propeller's shaft and at take off unless otherwise indicated:

	NK-12M
Application	Tupolev TU-95M, Antonov An-22
Power	11032 kW
Sp. fuel cons.	0.219 kg/kWh
Overall PR	13
Compr. stages	14A
HPT stages	5A
IPT stages	no
LPT stages	no
Length	6000 mm
Width/diameter	1150 mm
Weight	2350 kg

Table 1.35: NK-12M engine specs. Data from [32] where not indicated

1.4.5 JSC "UEC-Klimov" [5]

The JSC "UEC-Klimov" is a Russian company leader in the design and production of gas turbine engines for both military and civil aircrafts.

TV7-117S engines

The TV7-117S is the company's turbopropeller family of engines. They range in power from 2500 shp to 300 shp and have a modular design, which allows for in-field replacements and thus dramatically reduce costs and maintenance time.

Figure 1.12: TV7-117S engine [10]

Here below the specifications for the TV7-117S engines in use on aircrafts currently in service. Power and specific fuel consumption values are referred to the propeller's shaft and at take off unless otherwise indicated:

	TV7-117ST*	**TV7-117SM***
Application	Ilyushin Il-114, Ilyushin Il-112	Ilyushin Il-114, Ilyushin Il-112
Power	2088 kW	1864 kW
Sp. fuel cons.	0.255 kg/kWh	0.268 kg/kWh
Overall PR	-	-
Compr. stages	-	-
HPT stages	-	-
IPT stages	-	-
LPT stages	-	-
Length	2136 mm	2136 mm
Width/diameter	940 mm	940 mm
Weight	450kg	530kg

* *source: http://klimov.ru/en/production/aircraft/TV7-117S-family/*

Table 1.36: TV7-117S engines specs

1.4.6 Ivchenko-Progress ZMKB [6]

The Zaporozhye Machine-Building Design Bureau Progress State Enterprise (named after Academician A.G. Ivchenko) is an Ukrainian company involved in the design of aircraft and helicopter engines and other special industrial equipment.

Currently, it offers several families of turbopropeller engines, as reported below.

AI-20 engines

AI-20 engines are designed for two- or four-engine passenger and transport aircrafts on up to 6500 km routes.

General characteristics [37]:

- High reliability
- Long service life
- Simple maintenance

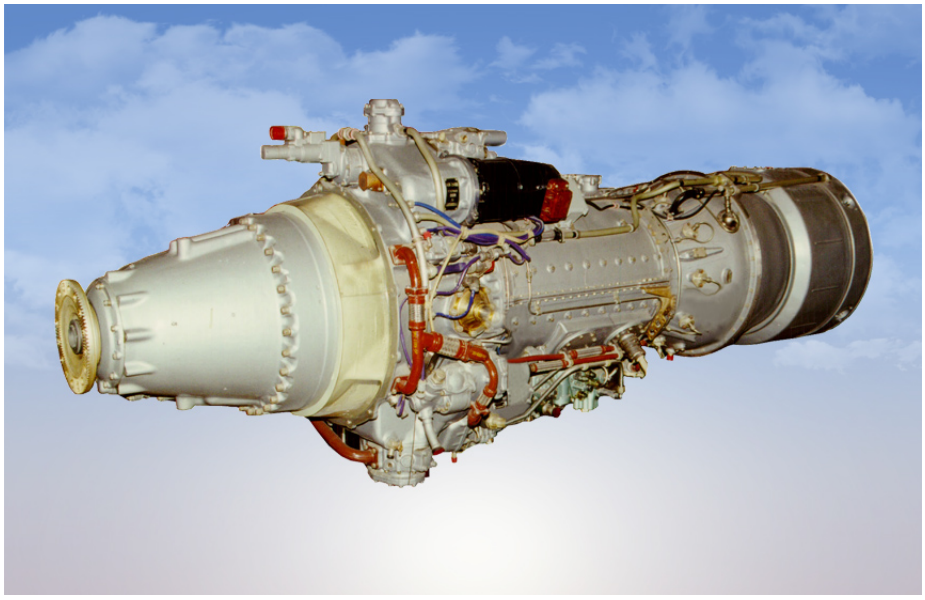

Figure 1.13: AI-20 engine [6]

Here below the specifications for the AI-20 engines in use on aircrafts currently in service. Power and specific fuel consumption values are referred to the propeller's shaft and at take off unless otherwise indicated:

	AI-20D series 5*
Application	Antonov An-32
Power	3169 kW
Sp. fuel cons.	0.432 kg/kWh
Overall PR	7.6
Compr. stages	10A
HPT stages	3A
IPT stages	no
LPT stages	no
Length	3096 mm
Width/diameter	450 mm
Weight	1040 kg

** source: Lambert, Mark "Jane's All The World's Aircraft 1993–94" // Motor Sich website* `http://www.motorsich.com/eng/` *// Wilkinson, Paul H. "Aircraft engines of the World 1970"*

Table 1.37: AI-20 engines specs

AI-24 engines

AI-24 engines are designed for passenger and transport aircrafts on up to 2500 km routes.

General characteristics [37]:

- High reliability
- Long service life
- Simple maintenance
- Simple design
- Engine protection system against limit power overloads

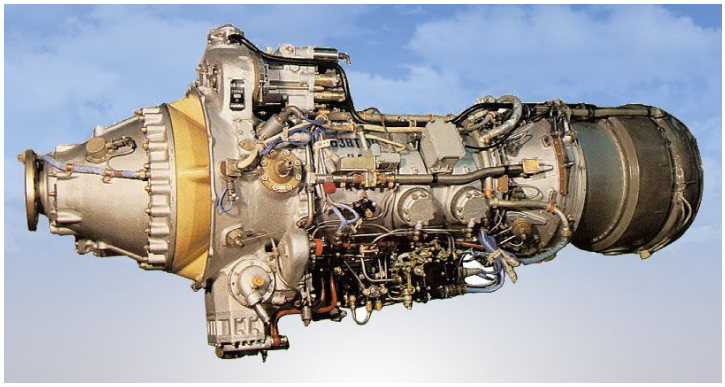

Figure 1.14: AI-24 engine [6]

Here below the specifications for the AI-24 engines in use on aircrafts currently in service. Power and specific fuel consumption values are referred to the propeller's shaft and at take off unless otherwise indicated:

	AI-24T*
Application	Antonov An-30, Antonov An-26, Antonov An-24
Power	2088 kW
Sp. fuel cons.	0.324 kg/kWh
Overall PR	7.05
Compr. stages	10A
HPT stages	3A
IPT stages	no
LPT stages	no
Length	2436 mm
Width/diameter	360 mm
Weight	600 kg

** source: Wilkinson, Paul H. "Aircraft engines of the World 1970"*

Table 1.38: AI-24 engines specs

AI-450C engines

The AI-450C/CD/CP/CM engines are designed for multipurpose general aviation aircrafts and UAVs.

Figure 1.15: AI-450C engine [6]

Here below the specifications for the AI-450C engines in use on aircrafts currently in service. Power and specific fuel consumption values are referred to the propeller's shaft and at take off unless otherwise indicated:

	AI-450C /CD/CP/CM*
Application	DART-450, DA50-JP7
Power	336 kW
Sp. fuel cons.	0.371 kg/kWh
Overall PR	-
Compr. stages	-
HPT stages	-
IPT stages	-
LPT stages	-
Length	1097 mm
Width/diameter	587 mm
Weight	130 kg

* *source:* `http://ivchenko-progress.com/?portfolio=%d0%b0%d0%b8-450%d1%81&lang=en#prettyPhoto`

Table 1.39: AI-450C engines specs

TV3-117VMA-SBM1 engine

The TV3-117VMA-SBM1 engine is designed for regional/local aircrafts of 6000 kg / 52 passengers capacity class.

General characteristics [37]:

- High efficiency
- Long service life
- Simple reliability
- Engine Electronic Control system
- Low emissions
- Low noise level
- Low operating costs
- Emergency power condition in order to allow take-off and level flight even with one engine inoperative

Figure 1.16: TV3-117VMA-SBM1 engine [6]

Here below the specifications for the TV3-117VMA-SBM1 engines in use on aircrafts currently in service. Power and specific fuel consumption values are referred to the propeller's shaft and at take off unless otherwise indicated:

	TV3-117VMA-SBM1*
Application	Antonov An-140
Power	1864 kW
Sp. fuel cons.	0.276 kg/eq-kWh
Overall PR	-
Compr. stages	-
HPT stages	-
IPT stages	-
LPT stages	-
Length	2953 mm
Width/diameter	988 mm
Weight	570 kg

* *source:* `http://ivchenko-progress.com/?portfolio=sbm1&lang=en#prettyPhoto`

Table 1.40: TV3-117VMA-SBM1 engine specs

1.4.7 Honeywell Aerospace [7]

Honeywell Aerospace, a division of the Honeywell International conglomerate, is a US-based company that manufactures aircraft engines, avionics, APUs, space equipment, brakes, wheels and other avionic equipment.

TPE331 engines

The TPE331 is Honeywell's family of turbopropeller engines. They are designed for multiple applications, both military and civil, such as regional airliners and general aviation aircrafts. Nowadays, the series includes 18 engine models and 106 engine configurations.

General characteristics:

- High fuel efficiency
- High reliability
- Long maintenance intervals
- Quick throttle response
- High power-to-weight ratio

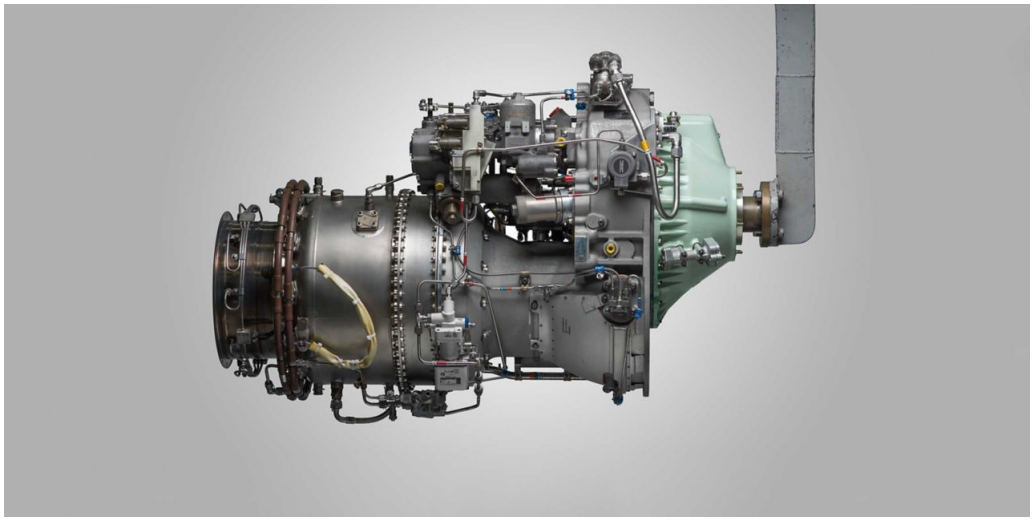

Figure 1.17: TPE331 engine [7]

Here below the specifications for the TPE331 engines in use on aircrafts currently in service. Power and specific fuel consumption values are referred to the propeller's shaft and at take off unless otherwise indicated:

	TPE331-10*
Application	Epic Escape, MQ-9 Reaper
Power	700 kW
Sp. fuel cons.	0.325 kg/kWh
Overall PR	10.55
Compr. stages	2C
HPT stages	3A
IPT stages	no
LPT stages	no
Length	1088 mm
Width/diameter	533 mm
Weight	175 kg

** source: "TPE331-10 Turboprop Engine" (PDF). Honeywell Aerospace. April 2006*

Table 1.41: TPE331 engine specs

1.4.8 PBS Aerospace [8]

PBS Velká Bíteš is a Czech company involved in the design and manufacturing of gas turbines (both for aerospace applications and power generation), turbomachinery and other aircraft and industrial components.

Concerning aerospace engines, the company is specialized in tubojets and turbopropellers/turboshafts for light/ultralight aircrafts and UAVs.

TP100 engine

The TP100 engine is PBS's turboprop engine. It is a small engine that finds its application on UAVs and experimental planes. It is equipped with a FADEC and can be operated in pusher or tractor mode.

Figure 1.18: TP100 engine [8]

Here below the specifications for the TP100 engines in use on aircrafts currently in service. Power and specific fuel consumption values are referred to the propeller's shaft and at take off unless otherwise indicated:

	TP100*
Application	experimental and unmanned aircrafts
Power	180 kW
Sp. fuel cons.	0.515 kg/kWh
Overall PR	-
Compr. stages	-
HPT stages	-
IPT stages	-
LPT stages	-
Length	891 mm
Width/diameter	398 mm
Weight	62 kg

** source: TP100 Turboprop Engine data sheet*

https://www.pbs.cz/en/our-business/aerospace/aircraftgines/turbopropgine-pbs-tp100

Table 1.42: TP100 engine specs

Chapter 2

Thermodynamics of a turbopropeller engine with heat exchange

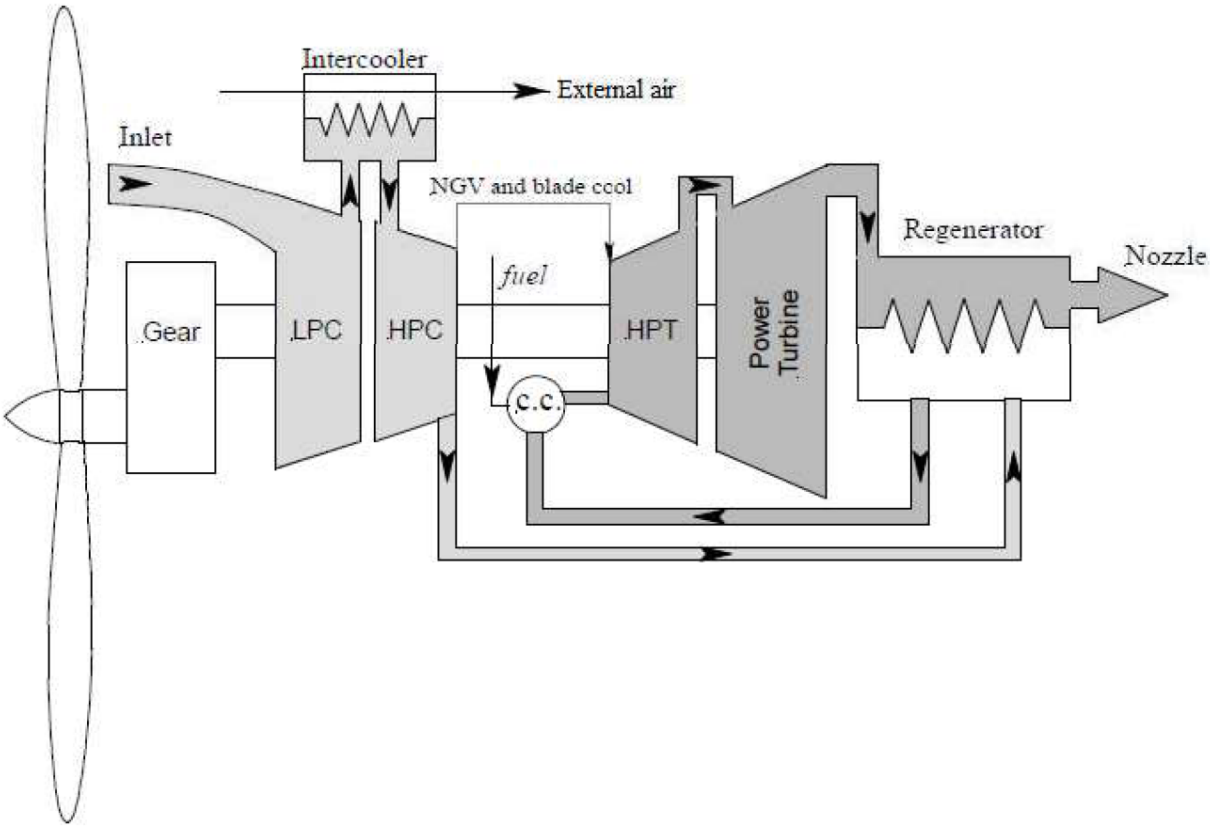

Figure 2.1: Sketch of a turboprop engine with intercooling and regeneration [11]

2.1 Intercooling and regeneration

This treatment is focused on the study of the impact that intercooling and regeneration have on the performances of gas turbine aero-engines, in particular turbopropellers.

Intercooling and regeneration are techniques bases on heat exchange that modify the traditional Joule-Brayton thermodynamic cycle that characterizes gas turbine engines.

Their implementation requires the addition of (additional) heat exchangers to the engine, adding complexity and weight to the system. However, the benefits granted by their implementation could justify these drawbacks.

Regeneration

The scope of regeneration is to partially substitute the heat addition in the combustor by an heat exchange internal to the thermodynamic cycle. The air flow exiting the compressor is pre-heated before entering the combustion chamber by means of heat exchange with the exhaust gases. This requires a gas-gas heat exchanger, which introduces pressure losses and usually requires wide exchange surfaces, due to the small gas/gas heat exchange coefficient.

The primary benefit of regeneration lies in the reduced heat that needs to be added to the system by combustion, lowering the specific fuel consumption and increasing the thermodynamic cycle efficiency.

However, regeneration is not always possible. In fact, necessary condition in order to have regeneration is that the air temperature after compression must be lower than the gas temperature after expansion in the turbine. This imposes a limit to the maximum heat that can be recovered with regeneration.

The regeneration effectiveness, also known as degree of regeneration, is defined as the ratio between the heat actually recovered and the maximum heat recoverable:

$$R = \frac{h_{turbine,exit} - h_{regenerator(gas),exit}}{h_{turbine,exit} - h_{compressor,exit}} \tag{2.1}$$

Usually R assumes values between 0.6 and 0.8.

The efficiency of an ideal Joule-Brayton cycle with complete regeneration ($R = 1$) is given by the following expression:

$$\eta_{id,R=1} = 1 - \left(\frac{\beta^{\frac{\gamma-1}{\gamma}}}{\tau} \right) \tag{2.2}$$

where $\tau = \frac{T_{max}}{T_{in,air}}$ and $\beta =$ compression ratio.

From this expression it is clear that regeneration is most beneficial for engines with:

- low compression ratios
- high maximum temperatures

It is also clear that:

- the cycle's efficiency decreases as the compression ratio increases
- the cycle's specific power is not affected by the regeneration, but the jet's propulsive power decreases, as the exhaust gases are at lower temperature

Considering the real thermodynamic cycle, some other considerations can be made:

- as the compressor efficiency decreases the heat recoverable decreases, since losses rise the fluid discharge temperature

- as the turbine efficiency decreases the heat recoverable increases, since losses rise the fluid discharge temperature
- the presence of an heat exchanger introduces additional pressure losses, both air and gas side, which per se decrease the cycle's efficiency

Intercooling

The scope of intercooling is to reduce the power required by the overall compression process, increasing the useful power provided by the engine.

This is achieved by the introduction of one (or multiple) air cooling during the compression process, by using multiple compressors. In this way the second compressor works with a fluid that is cooler and denser, requiring less work in order to achieve a certain compression ratio.

The air cooling is obtained by the introduction of a gas/gas heat exchanger. Usually on one side is present the compressed air and on the other side is present the external air.

As it was done for the regenerator, it is possible to define the intercooling effectiveness as the ratio between the heat actually removed and the maximum heat removable:

$$E = \frac{h_{compr1,exit} - h_{intercooler,exit}}{h_{compr1,exit} - h_{in,air}} \tag{2.3}$$

The introduction of intercooling has several effects on the performances of the thermodynamic cycle:

- the specific power increments, even in the real case when pressure losses due to the presence of the heat exchanger are accounted for
- the fuel consumption increases, since the air enters the combustion chamber at a lower temperature
- the cycle efficiency in the ideal case decreases. In fact the intercooled cycle can be viewed as the sum of two Joule-Brayon cycles: the base one and an additional, smaller one (green cycle in fig. 2.1). Since the efficiency of the ideal Joule-Brayton cycle depends on the compression ratio (see eqn. 2.4), the efficiency of the intercooled cycle will be lower than that of the base cycle, since the additional smaller cycle has a lower compression ratio (see fig. 2.1)

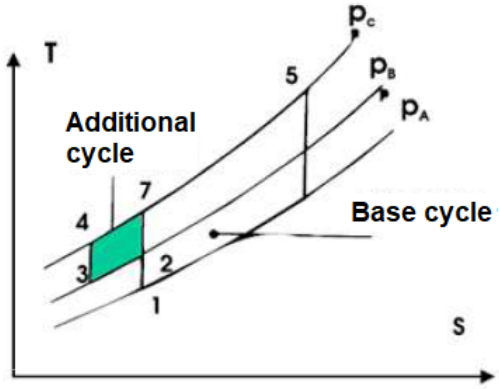

Figure 2.1: Ideal Joule-Brayton thermodynamic cycle with intercooling [11]

$$\eta_{id} = 1 - \frac{1}{\beta^{\frac{\gamma-1}{\gamma}}} \tag{2.4}$$

- the cycle efficiency in the real case could increase, but usually decreases as in the ideal case
- the possibility of regeneration is incremented, since intercooling decreases the air temperature at the exit of the compression process

Therefore, although intercooling generally does not give benefits in terms of cycle efficiency, it expands the limits of regeneration, and thus when the two techniques are combined the resulting thermodynamic cycle typically is characterized by higher useful specific power and efficiency.

2.2 Thermodynamic cycle

2.2.1 Assumptions

It is now described the thermodynamic cycle of interest in this analysis, the one for a turboprop with intercooling and regeneration. It consist in a modified Joule-Brayton cycle, in which the compression is divided in two steps, separated by a cooling process in order to reduce the work needed to increment the fluid pressure to the target one. Now the heating process is obtained in part by the combustor, as usual, and in part in the regenerator, which exploits the high temperature gases at the exit ofthe power turbine to pre-heat the compressed air before entering the combustor, reducing the amount of heat needed from the combustion process itself and thus reducing the fuel consumption.

The entire analysis has been conducted under several assumptions in order to simplify the computations, but without an excessive loss of accuracy.

First of all, the working fluid is assumed to behave like ad ideal gas, so thermally and calorically perfect. Therefore its equation of state assumes the following form:

$$\frac{P}{\rho} = RT \tag{2.5}$$

where:

$$R = \frac{\mathcal{R}}{\mathcal{MM}} \tag{2.6}$$

being $\mathcal{R}$ the universal gas constant and $\mathcal{MM}$ the molar mass of the gas.

Usually, the assumption of thermally perfect gas is valid for the temperature and pressure values typical of combustors and nozzles. In fact, for those values the compressibility/real gas factor Z, defined as:

$$Z = \frac{P}{\rho RT} \tag{2.7}$$

is very close to one, as shown in figure 2.2 and figure 2.3, thus justifying the assumption.

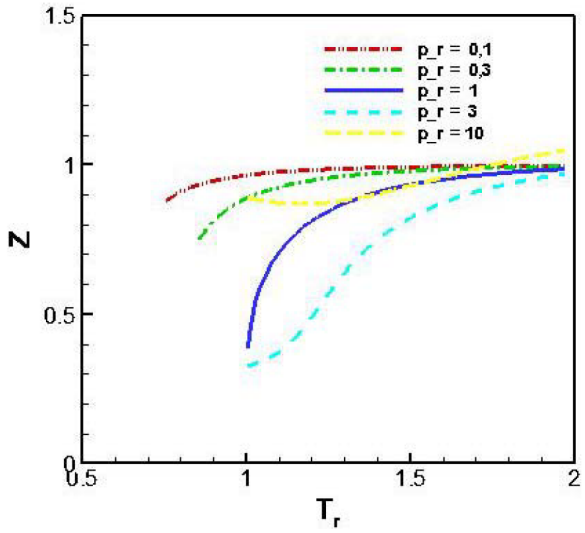

Figure 2.2: Real gas factor for H_2O (T_{cr} = 647.3 K, P_{cr} = 22.12 MPa) [12]

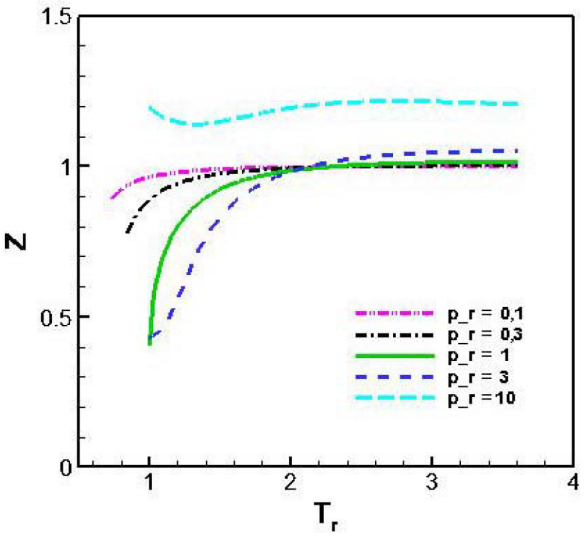

Figure 2.3: Real gas factor for CO_2 (T_{cr} = 304.4 K, P_{cr} = 7.38 MPa) [12]

On the other hand, the assumption of calorically perfect gas, that is of specific heat constant with respect to temperature, is not so readily verified. In fact, for the substances usually used in propulsion the specific heat is quite sensible with respect to the temperature, and since the gas is subjected to big temperature changes, its specific heat can change consistently, as shown in figure 2.4.

In order to account for its variation with temperature, different values will be used throughout the description of the thermodynamic cycle. A "cold" and a "hot" c_p will be employed, both for air and the combustion gases. For air, the "cold" c_p will be used in the computations in the diffuser, intercooler and compressors. For the combustion gases it will be used for the computations in the nozzle. The "hot" c_p will be used in the computations in the regenerator (air side) for air, while for the combustion gases it will be used in the computations in the combustor, turbines and regenerator (gas side).

Their values are evaluated as a mean between the c_p values at the extremes of the temperature interval to which they refer. For instance, regarding air' s cold temperature

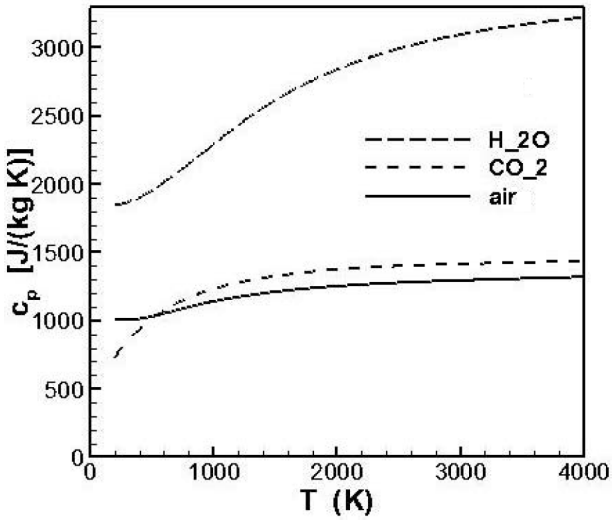

Figure 2.4: c_p variation with temperature, for various gases [12]

range:

$$c_{p_{a,cold}} = \frac{c_{p_a}\left(T_{max,cold}\right) + c_{p_a}\left(T_{min,cold}\right)}{2} \tag{2.8}$$

and the same for the "hot" temperature range and for the hot gases.

The c_p values at each temperature are computed by means of correlations. Refer to section 3.1.3 for further information.

The second assumption is that of steady, quasi-monodimensional flow. This implies constant flow properties on every section of the duct normal to its axis and those properties are function of only one spatial variable: the abscissa along the duct's axis. This assumption strongly simplifies the equations and the computations and gives very good results when considering the mean values of the physical quantities and the errors introduced are consistent with the level of detail requested by this analysis.

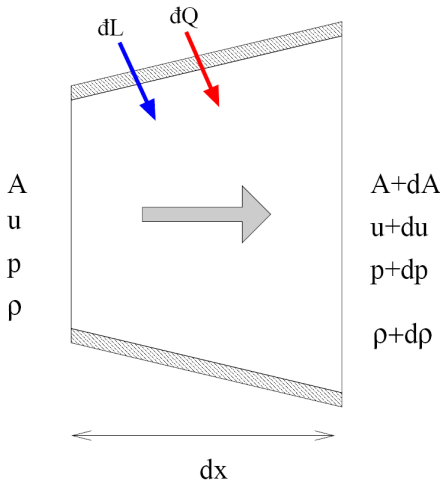

Figure 2.5: Control volume adopted in the quasi-1D flow analysis [12]

Lastly, the real thermodynamic cycle is obtained from the ideal one (no losses and heat dissipation, adiabatic and isentropic compressions and expansions) considering the

efficiencies of the various engine's components: compressors, heat exchangers, combustion chamber, turbines, diffuser and nozzle.

2.2.2 The cycle

As shown in figure 2.6 the thermodynamic cycle can be divided into several steps:

- 0 - 2: Air inlet (diffuser)
- 2 - 25: Low pressure compressor
- 25 - 27: Intercooler
- 27 - 3: High pressure compressor
- 3 - 35: Regenerator, air side
- 35 - 4: Combustor
- 4 - 45: High pressure turbine
- 45 - 5: Power turbine
- 5 - 7: Regenerator, gas side
- 7 - 9: Nozzle

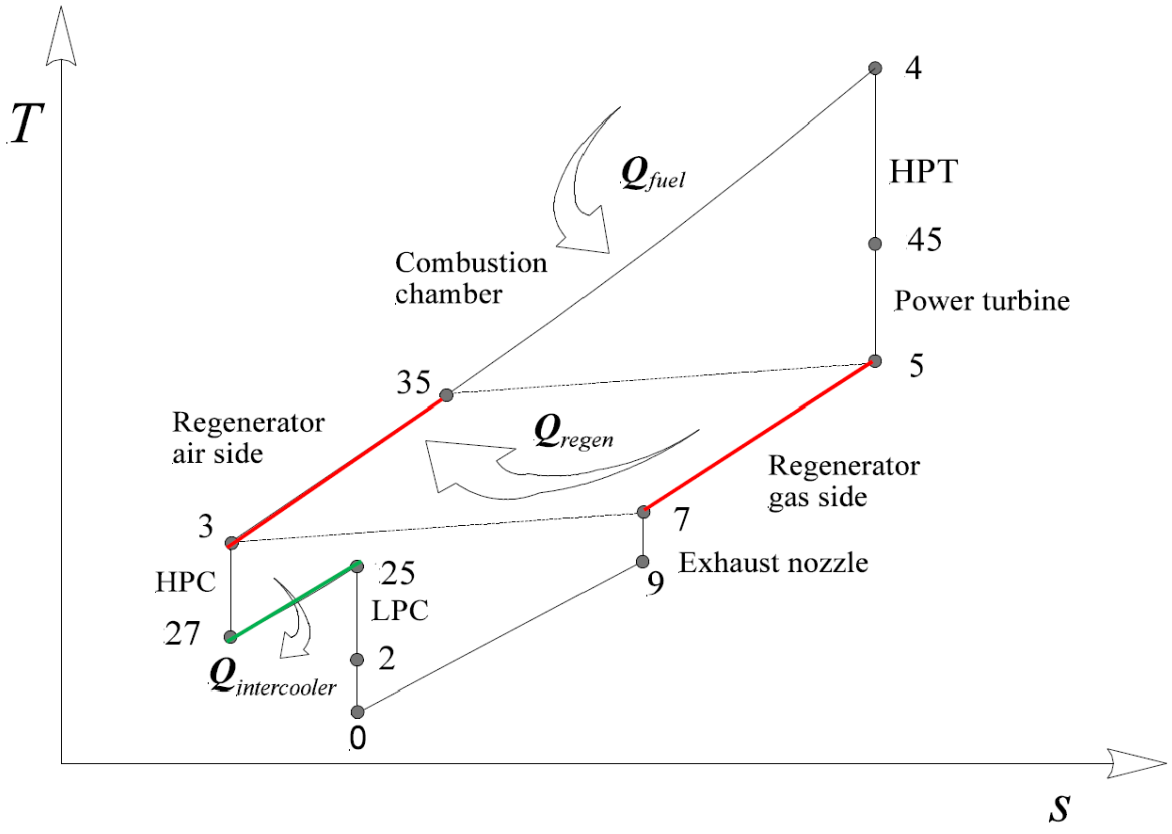

Figure 2.6: Thermodynamic cycle [11]

It is of interest now to fully describe the cycle, computing the values of the physical properties of the gas in each of its points and any useful performance parameter.

Air inlet (diffuser)

The scope of the diffuser is to reduce the air velocity and to increase its pressure, in order to have suitable conditions at the inlet of the compressor even at high flight speeds (M > 0.6).

Point 0 is characterized by the external ambient conditions: T_0, P_0 and M_0. Since no work nor heat are added/subtracted in the diffuser, the total enthalpy is conserved.

Therefore:

$$h_{t0} = h_{t2} \quad \Rightarrow \quad c_{p_a} T_{t0} = c_{p_a} T_{t2} \quad \Rightarrow \quad T_{t0} = T_{t2} \tag{2.9}$$

Since the static properties and the Mach number are known at the inlet of the diffuser, it is possibile to compute the total quantities in point 0:

$$T_{t0} = T_0 \left(1 + \frac{\gamma_a - 1}{2} M_0^2 \right) = T_{t2} \tag{2.10}$$

$$P_{t0} = P_0 \left(1 + \frac{\gamma_a - 1}{2} M_0^2 \right)^{\frac{\gamma_a}{\gamma_a - 1}} \tag{2.11}$$

where γ_a is the specific heat ratio of air.

In the ideal case, the flow would be isentropic and therefore also the total pressure would be conserved in the diffuser. It is introduced the parameter ε_d = efficiency of the diffuser, which accounts for the deviation from the ideal case.

Therefore it is possible to determine the total pressure at the outlet of the diffuser as:

$$\varepsilon_d = \frac{P_{t2}}{P_{t0}} \quad \Rightarrow \quad P_{t2} = \varepsilon_d P_{t0} \tag{2.12}$$

Low pressure compressor

Here starts the real compression process, with the work addition to the fluid and its total pressure increment, in order to be able to expand it in the turbine and in the nozzle later on.

The conditions at the compressor's inlet are those of point 2, at the outlet of the diffuser. The pressure at the compressor outlet, that is point 3, is readily obtained applying the definition of the compression ratio β_{c1}:

$$\beta_{c1} = \frac{P_{t25}}{P_{t2}} \quad \Rightarrow \quad P_{t25} = \beta_{c1} P_{t2} \tag{2.13}$$

The ideal temperature at the compressor's outlet can be computed applying the relationship valid for an isentropic and adiabatic process:

$$\frac{T_{t25'}}{T_{t2}} = \left(\frac{P_{t25}}{P_{t2}} \right)^{\frac{\gamma_a - 1}{\gamma_a}} \quad \Rightarrow \quad T_{t25'} = T_{t2} \left(\beta_{c1} \right)^{\frac{\gamma_a - 1}{\gamma_a}} \tag{2.14}$$

The real temperature can then be computed from the definition of adiabatic efficiency:

$$\eta_{c1} = \frac{\Delta h_{t2-t25'}}{\Delta h_{t2-t25}} = \frac{T_{t25'} - T_{t2}}{T_{t25} - T_{t2}} \quad \Rightarrow \quad T_{t25} = T_{t2} \left(1 + \frac{\left(\beta_{c1} \right)^{\frac{\gamma_a - 1}{\gamma_a}}}{\eta_{c1}} \right) \tag{2.15}$$

Intercooler

The intercooler is an heat exchanger, usually counter-current, with the scope to cool down the air coming from the LPC before entering the HPC. In this way the HPC will work with a denser fluid, thus requiring less work in order to be brought to the required pressure:

$$l - l_{diss} = \int \frac{dP}{\rho} \tag{2.16}$$

where $l - l_{diss}$ is the useful work done by the compressor.

The conditions at the exit of the intercooler can be computed once its parameters ε_i and E are known. In fact:

$$\varepsilon_i = \frac{P_{t27}}{P_{t25}} \quad \Rightarrow \quad P_{t27} = \varepsilon_i P_{t25} \tag{2.17}$$

and

$$E = \frac{T_{t25} - T_{t27}}{T_{t25} - T_{t2}} \quad \Rightarrow \quad T_{t27} = T_{t25} - E\big(T_{t25} - T_{t2}\big) \tag{2.18}$$

The parameter E is the ratio between the heat actually exchanged and the maximum heat exchangeable and is a sort of intercooler efficiency in terms of heat exchange. The parameter ε_i is the intercooler efficiency in terms of pressure and accounts for the deviation from the ideal case, in which the heat exchange is done with constant pressure, without losses.

High pressure compressor

The high pressure compressor brings the fluid to the final desired pressure level. Recalling what has been already said for the LPC, it is straightforward to compute the conditions at the end of the compression:

$$P_{t3} = \beta_{c2} P_{t27} \tag{2.19}$$

$$T_{t3'} = T_{t27}\Big(\beta_{c2}\Big)^{\frac{\gamma_a - 1}{\gamma_a}} \tag{2.20}$$

$$\eta_{c2} = \frac{\Delta h_{t27-t3'}}{\Delta h_{t27-t3}} = \frac{T_{t3'} - T_{t27}}{T_{t3} - T_{t27}} \quad \Rightarrow \quad T_{t3} = T_{t27}\left(1 + \frac{\Big(\beta_{c2}\Big)^{\frac{\gamma_a - 1}{\gamma_a}}}{\eta_{c2}}\right) \tag{2.21}$$

Regenerator - air side

In this side of the regenerator the air coming from the HPC is heated at the expense of the hot gases exiting from the power turbine. Again, the regenerator is an heat exchanger, usually counter-current or cross-flow.

In order to determine the fluid temperature at the exit of the regenerator, the temperature of the fluid at the power turbine discharge must be known. Therefore its computation will be done later on.

For now it is possible to determine the pressure at the regenerator (air side) exit, in the same way as it was done for the intercooler:

$$\varepsilon_r = \frac{P_{t35}}{P_{t3}} \quad \Rightarrow \quad P_{t35} = \varepsilon_r P_{t3} \tag{2.22}$$

where ε_r accounts for the pressure losses in the regenerator.

Combustor

In the combustor fuel is added to the air flow and exothermic combustion reactions occur. In this way, the working fluid heating is completed and the final desired total temperature T_{t4} is reached. Subsequently, the now highly energetic flow will be expanded in the turbines to extract the power needed by the compressor and by the propeller.

The desired temperature T_{t4} is assumed known by design, usually a trade-off between the cycle's efficiency (that grows with its maximum temperature) and the turbine blade's mechanical resistance.

The combustion process is at constant pressure only in the ideal case, while in the reality some pressure losses are inevitable. They are taken into account by the parameter ε_b:

$$\varepsilon_b = \frac{P_{t4}}{P_{t35}} \quad \Rightarrow \quad P_{t4} = \varepsilon_b P_{t35} \tag{2.23}$$

From an energy balance it possible to determine the f parameter, which is the ratio between the mass flow rate of fuel and air:

$$f = \frac{\dot{m}_f}{\dot{m}_a} \tag{2.24}$$

Energy balance:

$$\dot{m}_a c_{p_a} T_{t35} + \dot{m}_f c_{p_f} T_{tf} + \dot{m}_f H_f \eta_b = \left(\dot{m}_a + \dot{m}_f\right) c_{p_g} T_{t4} \tag{2.25}$$

Therefore:

$$f = \frac{c_{p_g} T_{t4} - c_{p_a} T_{t35}}{c_{p_f} T_{tf} + H_f \eta_b - c_{p_g} T_{t4}} \tag{2.26}$$

where η_b indicates the combustion efficiency, c_{p_f} and T_{tf} the fuel's specific heat and total temperature at the injection in the combustor, c_{p_g} the specific heat of the combustion gases and H_f the heat of combustion of the fuel.

It is important to note that the temperature of point 35 is still unknown, since it depends of the heat recovered from the combustion gases at the power turbine exit, which depends on parameter f itself. Therefore, it will be adopted an iterative method in order to determine f, imposing a starting value equal to 0.

High pressure turbine

The scope of the high pressure turbine is to provide the power required by the high and low pressure compressors.

Therefore, it is possible to determine the flow properties at the end of the expansion by equating the power given by the turbine and the power required by the compressors:

$$\dot{L}_{t1} = \dot{L}_{c1} + \dot{L}_{c2} = \dot{m}_a c_{p_a} \left[\left(\frac{T_{t3} - T_{t2\gamma}}{\eta_{m,c2}} \right) + \left(\frac{T_{t25} - T_{t2}}{\eta_{m,c1}} \right) \right] \tag{2.27}$$

$$\dot{L}_{t1} = \left(\dot{m}_a + \dot{m}_f\right) c_{p_g} \left(T_{t4} - T_{t45}\right) \eta_{m,t1} \tag{2.28}$$

where $\eta_{m,c1}$, $\eta_{m,c2}$ and $\eta_{m,t1}$ represent the mechanical efficiencies of the compressors (low and high pressure) and turbine, respectively. These efficiencies are taken into account in order to evaluate the real power available/needed at the shaft.

By equating the two expression for $\dot{L}_t$ it is possible to compute the gas temperature at the exit of the turbine:

$$T_{t45} = T_{t4} - \frac{\left(\frac{T_{t3}-T_{t2\gamma}}{\eta_{m,c2}}\right) + \left(\frac{T_{t25}-T_{t2}}{\eta_{m,c1}}\right)}{\eta_{m,t1}\left(1+f\right)} \cdot \frac{c_{p_a}}{c_{p_g}} \tag{2.29}$$

Exploiting the definition of the adiabatic efficiency of the turbine it is possible to compute the ideal temperature $T_{t45'}$:

$$\eta_{t1} = \frac{\Delta h_{t4-t45}}{\Delta h_{t4-t45'}} = \frac{T_{t4} - T_{t45}}{T_{t4} - T_{t45'}} \quad \Rightarrow \quad T_{t45'} = T_{t4} - \frac{T_{t4} - T_{t45}}{\eta_{t1}} \tag{2.30}$$

and by applying the relationship valid for an adiabatic isentropic process it is now possible to compute the total pressure at the turbine discharge (since $P_{t45} = P_{t45'}$):

$$\frac{P_{t4}}{P_{t45}} = \left(\frac{T_{t4}}{T_{t45'}}\right)^{\frac{\gamma_g}{\gamma_g - 1}} \quad \Rightarrow \quad P_{t45} = P_{t4}\left(1 - \frac{1 - \frac{T_{t45}}{T_{t4}}}{\eta_{t1}}\right)^{\frac{\gamma_g}{\gamma_g - 1}} \tag{2.31}$$

where γ_g is the specific heat ratio of the combustion gases.

Power Turbine

The scope of the power turbine is to provide the power required by the propeller, which provides the majority of the thrust.

In order to compute the gas properties at the turbine's exit and the air mass flow rate, the total propulsive power value is imposed. The total propulsive power is defined as the sum of the jet and propeller propulsive powers:

$$\dot{L}_{p,tot} = \dot{L}_{p,prop} + \dot{L}_{p,jet} \tag{2.32}$$

with:

$$\dot{L}_{p,prop} = \eta_{p,prop}\eta_{t2}\eta_{m,t2}\eta_{gb}\dot{m}_a\left(1+f\right)\lambda\Delta h_{av} \tag{2.33}$$

$$\dot{L}_{p,jet} = \eta_n \dot{m}_a\left(1+f\right)\left(1-\lambda\right)\Delta h_{av} = \dot{m}_a V_\infty\left[\left(1+f\right)v_{exit} - V_\infty\right] \tag{2.34}$$

and:

$$v_{exit} \approx \sqrt{2\left(1-\lambda\right)\Delta h_{av}\eta_n} \tag{2.35}$$

where v_{exit} and V_∞ are the gas velocity at the exit of the nozzle and the flight velocity respectively, and Δh_{av} is the enthaply drop available for propulsive purposes (propeller and nozzle). As a first approximation, Δh_{av} can be defined as the enthalpy drop obtained with an isentropic adiabatic expansion from the total pressure P_{t45} at the exit of the HPT to the static ambient pressure $P_9 = P_0$:

$$\Delta h_{av} \approx c_{p_g}\left(T_{t45} - T_{9''}\right) \tag{2.36}$$

with

$$T_{9''} = T_{t45}\left(\frac{P_9}{P_{t45}}\right)^{\frac{\gamma_g - 1}{\gamma_g}} \tag{2.37}$$

The various efficiencies η used in eq 2.33 are needed in order to consider only the power available at the propeller shaft. In particular:

- $\eta_{prop,p}$ is the propulsive efficiency of the propeller, defined as the ratio between the power used for propulsion purposes $\dot{L}_{p,prop}$ and the entire power $\dot{L}_{j,prop}$ available at the propeller's shaft: $\eta_{prop,p} = \frac{\dot{L}_{p,prop}}{\dot{L}_{j,prop}}$ (refer to section 2.3 for further details);
- η_{t2} is the adiabatic efficiency of the power turbine
- $\eta_{m,t2}$ is the mechanical efficiency of the power turbine
- η_{gb} is the efficiency of the gear box (between the propeller shaft and the power turbine shaft)

The parameter $\lambda \in \big[0, 1\big]$ represents how much of the Δh_{av} is allocated to the power turbine, and therefore to the propeller. It is a design parameter and its value must be chosen in order to be able to compute the gas properties at the exit of the power turbine. Usually, its value is determined such that the total propulsive power is maximized:

$$\frac{\partial \dot{L}_{p,tot}}{\partial \lambda} = 0 \quad \Rightarrow \quad \lambda_{opt} = 1 - \frac{\eta_n V_\infty^2}{2\big(\eta_{p,prop}\eta_{t2}\eta_{m,t2}\eta_{gb}\big)^2\big(1+f\big)\Delta h_{av}} \tag{2.38}$$

Once λ is known, it is finally possible to determine the gas properties at the end of the expansion in the power turbine:

$$T_{t5'} = T_{t45} - \frac{\lambda \Delta h_{av}}{c_{p_g}} \quad \Rightarrow \quad T_{t5} = T_{t45} - \eta_{t2}\big(T_{t45} - T_{t5'}\big) \tag{2.39}$$

$$\frac{P_{t45}}{P_{t5}} = \left(\frac{T_{t45}}{T_{t5'}}\right)^{\frac{\gamma_g}{\gamma_g - 1}} \quad \Rightarrow \quad P_{t5} = P_{t45}\left(\frac{T_{t45}}{T_{t5'}}\right)^{-\left(\frac{\gamma_g}{\gamma_g - 1}\right)} \tag{2.40}$$

However, the λ value obtained with eqn. 2.38 only maximizes the total propulsive power, without taking into account the power-specific fuel consumption (e.g. $EBSFC$). In a traditional engine, to maximize the specific power is to minimize the $EBSFC$, since the fuel mass flow rate is set once the properties up to the turbine inlet temperature are known.

On the other hand, in a regenerative engine the fuel mass flow rate depends on the amount of heat recuperated from the exhaust gases and therefore on the properties at the exit of the power turbine, hence on the λ parameter. For this reason, the λ that maximizes the propulsive power generated and the λ that minimizes the specific fuel consumption may not coincide, and since in a regenerative engine the fuel consumption is one of most important performance parameters, eqn. 2.38 is not reliable anymore.

Thus, that expression will not be used and the performances will be computed for different nozzle expansion ratio values (which correspond to different λ values), to assess which of them gives the best performances, prioritizing the specific fuel consumption.

Refer to section 3.2 for further details.

Regenerator - gas side

In this side of the regenerator, the hot gases coming from the power turbine are cooled down in order to heat the air coming from the HPC.

Employing the definition of the degree of regeneration R, it is now possible to determine temperature T_{t35}. In fact:

$$R = \frac{T_{t35} - T_{t3}}{T_{t5} - T_{t3}} \quad \Rightarrow \quad T_{t35} = T_{t3} + R\big(T_{t5} - T_{t3}\big) \tag{2.41}$$

It is now possible to compute the temperature at the exit of the regenerator, gas side, by equating the heat exchanged between the air and gas sides:

$$\dot{Q}_{reg} = \dot{m}_a\, c_{p_a}\big(T_{t35} - T_{t3}\big) = \big(\dot{m}_a + \dot{m}_f\big)\, c_{p_g}\big(T_{t5} - T_{t7}\big) \tag{2.42}$$

therefore:

$$T_{t7} = T_{t5} - \frac{T_{t35} - T_{t3}}{\big(1+f\big)} \cdot \frac{c_{p_a}}{c_{p_g}} \tag{2.43}$$

Finally, the total pressure losses that occur in the regenerator are taken into account by the parameter ε_r, as seen before:

$$P_{t7} = \varepsilon_r P_{t5} \tag{2.44}$$

Nozzle

In the nozzle the gas coming from the regenerator is expanded and accelerated in order to provide an additional contribution to the thrust.

Since no work nor heat is exchanged in the nozzle, the total enthalpy of the flow is conserved during the expansion process:

$$h_{t7} = h_{t9} \quad \Rightarrow \quad c_{p_g} T_{t7} = c_{p_g} T_{t9} \quad \Rightarrow \quad T_{t7} = T_{t9} \tag{2.45}$$

Under the hypothesis of adapted nozzle ($P_9 = P_0$), it is possible to compute the static temperature at the end of the expansion and then the gas velocity at the nozzle exit:

$$T_{9'} = T_{t7}\left(\frac{P_9}{P_{t7}}\right)^{\frac{\gamma_g - 1}{\gamma_g}} \tag{2.46}$$

(adiabatic and isentropic process)

$$\eta_n = \frac{\Delta h_{t7-9}}{\Delta h_{t7-9'}} = \frac{T_{t7} - T_9}{T_{t7} - T_{9'}} \quad \Rightarrow \quad T_9 = T_{t7} - \eta_n\big(T_{t7} - T_{9'}\big) \tag{2.47}$$

$$h_{t7} = h_{t9} \quad \Rightarrow \quad c_{p_g} T_{t7} = c_{p_g} T_9 + \frac{v_9^2}{2} \quad \Rightarrow \quad v_9 = v_{exit} = \sqrt{2 c_{p_g}\big(T_{t7} - T_9\big)} \tag{2.48}$$

where η_n is the nozzle efficiency and accounts for the losses in the nozzle.

Note that the hypothesis of adapted nozzle is very likely to be true: in fact the flow in it will likely be subsonic, since λ usually is close to 1 and therefore the Δh available for the expansion in the nozzle is very small.

2.3 Performances

It is of interest now to compute some performance parameters in order to be able to assess the performance of the engine and to be able to make comparisons between different configurations/operative conditions.

Mass flow rate

In section 2.2.2 it was said that the total propulsive power is assumed known by design/requirements. At this point, it is possible to determine the air mass flow rate processed by the engine by exploiting its definition:

$$\dot{L}_{p,tot} = \dot{L}_{p,prop} + \dot{L}_{p,jet} \tag{2.49}$$

$$\dot{L}_{p,prop} = \eta_{p,prop}\eta_{t2}\eta_{m,t2}\eta_{gb}\dot{m}_a\big(1+f\big)\lambda\Delta h_{av} \tag{2.50}$$

$$\dot{L}_{p,jet} = \dot{m}_a V_\infty\big[\big(1+f\big)v_{exit} - V_\infty\big] \tag{2.51}$$

therefore:

$$\dot{m}_a = \frac{\dot{L}_{p,tot}}{\eta_{p,prop}\eta_{t2}\eta_{m,t2}\eta_{gb}\big(1+f\big)\lambda\Delta h_{av} + V_\infty\big[\big(1+f\big)v_{exit} - V_\infty\big]} \tag{2.52}$$

and:

$$\dot{m}_f = f\cdot\dot{m}_a \quad \Rightarrow \quad \dot{m}_g = \dot{m}_a + \dot{m}_f \tag{2.53}$$

where $\dot{m}_g$ indicates the mass flow rate of the combustion gases.

Propeller properties

In order to compute the thrust given by the engine and the propeller it is necessary to know the mass flow rate processed by the propeller and the air velocity downstream.

As a first approximation:

$$\dot{m}_{a,prop} = \rho_a V_\infty \pi \frac{D_{prop}^2}{4} \tag{2.54}$$

where D_{prop} is the propeller diameter and ρ_a the density of the external air.

At this point the air velocity downstream of the propeller can be computed by equating the following two expression for the propeller power at the shaft:

$$\dot{L}_{j,prop} = \eta_{t2}\eta_{m,t2}\eta_{gb}\dot{m}_a\big(1+f\big)\lambda\Delta h_{av} \tag{2.55}$$

$$\dot{L}_{j,prop} = \frac{1}{2}\dot{m}_{a,prop}\big(v_{wake}^2 - V_\infty^2\big) \tag{2.56}$$

where v_{wake} is the air velocity downstream the propeller.

Therefore:

$$v_{wake} = \sqrt{\frac{2\eta_{t2}\eta_{m,t2}\eta_{gb}\dot{m}_a\big(1+f\big)\lambda\Delta h_{av}}{\dot{m}_{a,prop}} + V_\infty^2} \tag{2.57}$$

Thrust

For a turbopropeller the thrust can be expressed as the sum of the contributions of the propeller and of the jet of hot gases expelled by the nozzle:

$$T_{total} = T_{prop} + T_{jet} \tag{2.58}$$

$$T_{prop} = \dot{m}_{a,prop}\big(v_{wake} - V_\infty\big) \tag{2.59}$$

$$T_{jet} = \dot{m}_a\big[\big(1+f\big)v_{exit} - V_\infty\big] \tag{2.60}$$

Note that the jet propulsive power can be expressed as the jet thrust times the flight speed:

$$\dot{L}_{p,jet} = T_{jet}\, V_\infty \tag{2.61}$$

and the same is true for the propeller propulsive power:

$$\dot{L}_{p,prop} = T_{prop}\, V_\infty \tag{2.62}$$

Specific fuel consumption

The specific fuel consumption is the most important and interesting performance parameter for a regenerated engine, since it can be used to asses how much fuel can be saved with respect to a conventional engine.

For a turbopropeller, the particular parameter to be considered is the equivalent brake-specific fuel consumption. It is defined as:

$$EBSFC = \frac{\dot{m}_f}{\dot{L}_{eq}} \tag{2.63}$$

$\dot{L}_{eq}$ is the Equivalent Power and is the sum of the power available at the propeller shaft, $\dot{L}_{j,prop}$, plus a term that takes into account the contribution of the jet as an equivalent additional power available at the propeller shaft. This is obtained by adding the jet's propulsive power divided by the propeller's propulsive efficiency:

$$\dot{L}_{eq} = \dot{L}_{j,prop} + \frac{\dot{L}_{p,jet}}{\eta_{p,prop}} \tag{2.64}$$

Efficiencies

At this point, it is of interest to evaluate how well the engine and the propulsion system convert the primary energy (chemical in this case) in the final propulsive energy.

Three different efficiencies are considered:

- η_{th} = thermal efficiency. It represents the engine efficiency in converting the primary chemical energy in a form suitable for propulsion purposes. It is defined as:

$$\eta_{th} = \frac{\dot{L}_{j,prop} + \dot{L}_{j,jet}}{\dot{L}_{av}} \tag{2.65}$$

  where $\dot{L}_{av}$ is the total power available (combustion of a fuel at V_∞, characterized by heat of combustion H_f) :

$$\dot{L}_{av} = \dot{m}_f\left(H_f + \frac{V_\infty^2}{2}\right) \tag{2.66}$$

and $L_{j,jet}$ is the jet power available at an hypothetical shaft and is the sum of the jet's propulsive power $L_{p,jet}$, which represents the power used to propel the aircraft, and the jet's dissipated power $L_{diss,jet}$, which represents the power used to accelerate the jet and not used for the propulsion (it is the jet's residual kinetic energy):

$$\dot{L}_{j,jet} = \dot{L}_{p,jet} + \dot{L}_{diss,jet} = \dot{m}_a V_\infty \big[\big(1+f\big) v_{exit} - V_\infty \big] + \frac{1}{2} \dot{m}_a \big(1+f\big) \big(v_{exit} - V_\infty\big)^2 \tag{2.67}$$

which can be written in the following form, after manipulation:

$$\dot{L}_{j,jet} = \frac{1}{2} \dot{m}_a \big[\big(1+f\big) v_{exit}^2 - \big(1-f\big) V_\infty^2 \big] \tag{2.68}$$

- η_p = propulsive efficiency. It accounts for the fact that part of the energy given to the propulsive fluid is not used for propulsion: part of it is used to accelerate the flow and remains as residual kinetic energy:

$$\dot{L}_{j,tot} = \dot{L}_{p,tot} + \dot{L}_{diss,tot} \tag{2.69}$$

and:

$$\eta_p = \frac{\dot{L}_{p,tot}}{\dot{L}_{j,tot}} \tag{2.70}$$

with:

$$\dot{L}_{p,tot} = \dot{L}_{p,prop} + \dot{L}_{p,jet} = T_{prop} V_\infty + T_{jet} V_\infty \tag{2.71}$$

$$\dot{L}_{j,tot} = \dot{L}_{j,prop} + \dot{L}_{j,jet} \tag{2.72}$$

where $\dot{L}_{j,tot}$ is the total "jet" power and $\dot{L}_{diss,tot}$ is the total dissipated power:

$$\dot{L}_{diss,tot} = \dot{L}_{diss,prop} + \dot{L}_{diss,jet} = \frac{1}{2} \dot{m}_{a,prop} \big(v_{wake} - V_\infty\big)^2 + \frac{1}{2} \dot{m}_a \big(1+f\big) \big(v_{exit} - V_\infty\big)^2 \tag{2.73}$$

- η_o = overall efficiency. It represents the system's global efficiency and it is a measure of the efficiency with which the available power is converted into effective propulsive power:

$$\eta_o = \frac{\dot{L}_{p,tot}}{\dot{L}_{av}} = \eta_p \eta_{th} \tag{2.74}$$

Turbomachinery and heat exchangers

Finally, is is possible to compute the power required/provided by each component of the engine:

- Power required by the LPC:

$$\dot{L}_{c1} = \frac{\dot{m}_a \, c_{p_a} \big(T_{t25} - T_{t2} \big)}{\eta_{m,c1}} \tag{2.75}$$

- Power required by the HPC:

$$\dot{L}_{c2} = \frac{\dot{m}_a \, c_{p_a} \big(T_{t3} - T_{t27} \big)}{\eta_{m,c2}} \tag{2.76}$$

- Power provided by the HPT:

$$\dot{L}_{t1} = \dot{m}_a \big(1 + f \big) \, c_{p_g} \big(T_{t4} - T_{t45} \big) \eta_{m,t1} \tag{2.77}$$

- Power provided by the power turbine:

$$\dot{L}_{t2} = \dot{m}_a \big(1 + f \big) \, c_{p_g} \big(T_{t45} - T_{t5} \big) \eta_{m,t2} \tag{2.78}$$

- Heat exchanged in the intercooler:

$$\dot{Q}_{int} = \dot{m}_a \, c_{p_a} \big(T_{t25} - T_{t27} \big) \tag{2.79}$$

- Heat exchanged in the regenerator:

$$\dot{Q}_{reg} = \dot{m}_a \, c_{p_a} \big(T_{t35} - T_{t3} \big) \tag{2.80}$$

- Heat generated by the combustion process:

$$\dot{Q}_{comb} = \dot{m}_f \, H_f \, \eta_b \tag{2.81}$$

Chapter 3

The code

The next step in the analysis is to develop a code to compute the thermodynamic and performance quantities presented in sections 2.2.2 and 2.3 for different operating conditions.

This is achieved by means of a custom Fortran 90 code, which essentially follows the steps reported in section 2.2.2 during the description of the thermodynamic cycle, but with some differences.

The first difference consist in the fact that instead of fixing the λ parameter it was decided to fix the nozzle expansion ratio, β_n. In fact, in the case of a regenerative turbopropeller engine it is not straightforward to estimate the Δh_{av}, since the heat exchanged in the regenerator is unknown at the beginning.

Once β_n is known, the conditions at the exit of the power turbine are too.

In fact:

$$P_{t7} = \beta_n P_9 \tag{3.1}$$

$$P_{t5} = \frac{P_{t7}}{\varepsilon_r} \tag{3.2}$$

$$T_{t5'} = T_{t45}\left(\frac{P_{t5}}{P_{t45}}\right)^{\frac{\gamma_g - 1}{\gamma_g}} \tag{3.3}$$

$$T_{t5} = T_{t45} - \eta_{t2}\left(T_{t45} - T_{t5'}\right) \tag{3.4}$$

At this point it is necessary to define Δh_{av} in a slightly different way than usual.

As mentioned in section 2.2.2, usually it is defined as the enthalpy drop obtained with an isentropic adiabatic expansion from the total pressure P_{t45} at the exit of the HPT to the static ambient pressure P_9:

$$\Delta h_{av} = c_{p_g}\left(T_{t45} - T_{9''}\right) \tag{3.5}$$

with:

$$T_{9''} = T_{t45}\left(\frac{P_9}{P_{t45}}\right)^{\frac{\gamma_g - 1}{\gamma_g}} \tag{3.6}$$

In this analysis it was instead defined as the sum of the isentropic enthalpy drop in the power turbine and the isentropic enthalpy drop in the nozzle:

$$\Delta h_{pt,is} = c_{p_g}\left(T_{t45} - T_{5'}\right) \tag{3.7}$$

$$\Delta h_{n,is} = c_{p_g}\left(T_{t7} - T_{9'}\right) \tag{3.8}$$

$$\Delta h_{av} = \Delta h_{pt,is} + \Delta h_{n,is} \tag{3.9}$$

Then, the λ parameter corresponding to the chosen β_n can be computed as:

$$\lambda = \frac{\Delta h_{pt,is}}{\Delta h_{av}} \tag{3.10}$$

3.1 Assumptions and data used

The code relies on the assumptions presented in section 2.2.1, plus others that will be presented below.

In order to work, the code needed information about the efficiencies of the components, properties of the fuel, pressure losses and c_p values.

3.1.1 Efficiencies and pressure losses

Values for the efficiencies of the various components and for the pressure losses in the heat exchangers are chosen after a research in the available literature. Here below the values used:

η_{c1}	0.85 [38]	η_b	0.98 [39]
η_{c2}	0.85 [38]	η_n	0.98 [40]
$\eta_{m,c1}$	0.98 [41]	η_{gb}	0.99 [42]
$\eta_{m,c2}$	0.98 [41]	$\eta_{p,prop}$	0.85 [43]
η_{t1}	0.88 [38]	ε_d	0.95 [44]
η_{t2}	0.92 [38]	ε_i	0.95 [44]
$\eta_{m,t1}$	0.98 [41]	ε_r	0.95 [44]
$\eta_{m,t2}$	0.98 [41]	ε_b	0.95 [39]

Table 3.1: η and ε values used

For each value is reported the corresponding literature reference.

The compressors are assumed to be centrifugal, at least for some of their stages if not completely, since they are often used in turbopropeller engines due to their compactness and minor weight [33]. Furthermore, as suggested by [38], the value used can be representative also for axial compressors, although they usually tend to have slightly higher efficiencies.

Concerning the turbines, the HPT is assumed less efficient with respect to the power turbine since usually high pressure stages are impulse (or close to) stages (reaction degree ~ 0), characterized by lower efficiencies (due to higher flow velocity), since the losses can be partially recovered in the following stages. The values have been selected using the Smith Chart, using typical flow and loading coefficient values for impulse and reaction stages, as reported in [38].

3.1.2 Fuel properties

Turboprop engines usually operate with Jet A or Jet A-1, which are kerosene based fuels. The major difference between Jet A and Jet A-1 resides in the freezing point: -40°C for

Jet A and $-47°$C for Jet A-1.

The fuel properties of interest are assumed as suggested by [45], [46] and [47]:

- Heat of combustion, $H_f = 43.200$ [MJ/kg]
- c_{p_f} (at $15°C$) $= 1.92$ [kJ/kgK]
- Hydrogen - Carbon ratio, $H/C = 1.91$

The H/C ratio is needed in order to determine the c_p values of the combustion gases later on.

3.1.3 Specific heat values

The c_p values for air and combustion gases are computed with the approach already mentioned in section 2.2.1.

Here below are presented the temperatures used in the computation of the $c_p s$:

	$T_{max,cold}[K]$	$T_{min,cold}[K]$	$T_{max,hot}[K]$	$T_{min,hot}[K]$
Air	450	236.15	800	450
Gas	450	450	1500	450

Table 3.2: Temperature ranges for the c_p evaluation

In particular, it is assumed that $T_{max,cold} = T_{min,hot}$ and $T_{max,cold,gas} \simeq T_{min,cold,gas}$, since the enthalpy drop in the nozzle usually is small.

In order to estimate reasonable values for the air and gas temperature at the various points in the engine, it was used a very simplified thermodynamic cycle, with a constant specific heat ratio $\gamma = 1.4$, constant fluid composition, $f = 0$ and no losses. Ideal flight conditions for a turbopropeller were chosen, as suggested by [33]: 7000m altitude and Mach number equal to 0.7.

From this analysis it was possible to estimate $T_{min,cold,air}$ and $T_{max,cold,air}$. The value of $T_{max,cold,air}$ that was initially used ($550K$) was subsequently corrected after the completion of the code: in fact the simplified model did not account for the intercooling and therefore yielded an higher temperature value after the compression process.

Then, assuming a perfect regenerator, it was possible to estimate $T_{max,hot,air}$ and $T_{max,cold,gas}$, since in these conditions $T_{t35} = T_{t5}$ and $T_{t3} = T_{t7}$.

Concerning $T_{max,hot,gas}$, it was chosen a typical TIT (turbine inlet temperature) value for turbopropellers, as suggested by [48].

These values have the only scope to provide a reasonable temperature interval for a reasonable estimation of mean c_p values in the hot and cold part of the engine and therefore their accuracy is not crucial.

Finally, the c_p and the specific heat ratio $\gamma = \frac{c_p}{c_v}$ values can be determined (since $c_v = c_p - R$ for an ideal gas).

As already said before, the c_p evaluation at different temperatures is achieved by means of correlations.

Concerning air, its c_p values are computed using the NASA Glenn Coefficients, the same method by which the NASA CEA code computes the thermodynamic properties of species [49]. The correlation consist in a seven term functional form for the adimensional quantity $\frac{c_p}{R}$:

$$\frac{c_p(T)}{R} = a_1 T^{-2} + a_2 T^{-1} + a_3 + a_4 T + a_5 T^2 + a_6 T^3 + a_7 T^4 \tag{3.11}$$

and is valid for temperatures ranging from $200K$ to $6000K$. The coefficients a_i are reported in the appendix of [49] and for air are given in two sets: one valid for $200K \leq T < 1000K$ and one for $1000K \leq T \leq 6000K$.

The combustion gases c_p values are instead determined by means of tables, in particular the ones reported in the NASA technical paper reported here: [50]. In these tables, various transport and thermodynamic properties are reported, for different kinds of combustion gases deriving from combustion processes between hydrocarbons and air.

To identify the table to be used for a specific application it is necessary to know the following quantities:

- H/C ratio, which defines the type of fuel of interest. Tables are provided for H/C values of 1.7, 2 and 2.1, which cover the range of common aviation fuels.
- Equivalence ratio ER, defined as:

$$ER = \frac{\left(\frac{fuel}{air}\right)}{\left(\frac{fuel}{air}\right)_{stoich}} \tag{3.12}$$

  Tables are provided for ER values of 0, 0.25, 0.5, 0.75, 1 and 1.25.
- Wet-dry air mass ratio: tables are provided for values of 0 and 0.03.
- Pressure, which is relevant only in the case of non-constant gas composition. Tables are provided for values of 0.01, 0.1, 1, 10, 50 atm.
- Constant gas composition or shifting gas composition, determined by chemical equilibrium.

In this analysis the gas properties are taken from table 7A, which is valid for dry air (composition derived from a simplified version of the U.S. Standard Atmosphere Model [51]), $ER = 0.25$, $H/C = 2$ and constant gas composition.

In fact, the H/C ratio of Jet A and Jet A-1 is 1.91, so 2 is the closest value considered in the technical paper. Usually, ER values for turbojets are around 0.45, as reported by [52], but in this analysis a regenerator is present, which reduces the amount of fuel to be burnt to reach the target TIT. Therefore a lower ER value is expected, and this assumption was then confirmed by the numerical results. It was also assumed a constant composition for the combustion gases, as suggested by [50], since the maximum temperature in the engine is expected to be around $1500K$ (with the only exception of the primary combustion zone), due to limitations imposed by the maximum stresses allowed in HPT blades.

Here below are reported the c_p and γ values used in the code:

	Air, "hot"	Air, "cold"	Gas, "hot"	Gas, "cold"
c_p $[\frac{J}{Kg \cdot K}]$	1059.69	1011.73	1145.65	1043.50
γ	1.37	1.40	1.33	1.38

Table 3.3: c_p and γ values

3.2 Code Structure

The code was written with Eclipse [13] and compiled with GFortran.

It is structured in the following way:

1. it reads the data/parameters provided in an input file
2. for each case provided in the input file it computes the engine performances
3. for each case provided in the input files, the performances are computed for each β_n value provided in the input file. This is useful in order to determine which β_n value gives the lowest $EBSFC$, for example
4. output files are generated: one for each case plus a file with a summary of the results of most interest

3.2.1 Input file

The code needs an input file, "Data.txt", in which the following information must be present:

- the total number of cases, identified by a set of parameters as shown below, that will be analyzed
- the total number of β_n values for which the performances are to be computed (in each of the cases)
- the engine's components efficiencies, as reported in table 3.1
- the list of β_n values for which the performances are to be computed
- the list of cases for which the performances are to be computed. Each case is identified by the following set of properties:

  Flight altitude, flight Mach number, maximum total temperature of the cycle, LPC and HPC compression ratios, E and R parameters, propeller diameter and total propulsive power required. A maximum of 999 cases can be specified at once

It is possible to simulate a traditional engine (without intercooler and regenerator) by setting E and R to 0 and ε_i and ε_r to 1.

The information about the propeller diameter and total propulsive power required are not needed if interested only in air mass flow rate-specific quantities, and those parameters can be set to 0.

Here below an example of the input file:

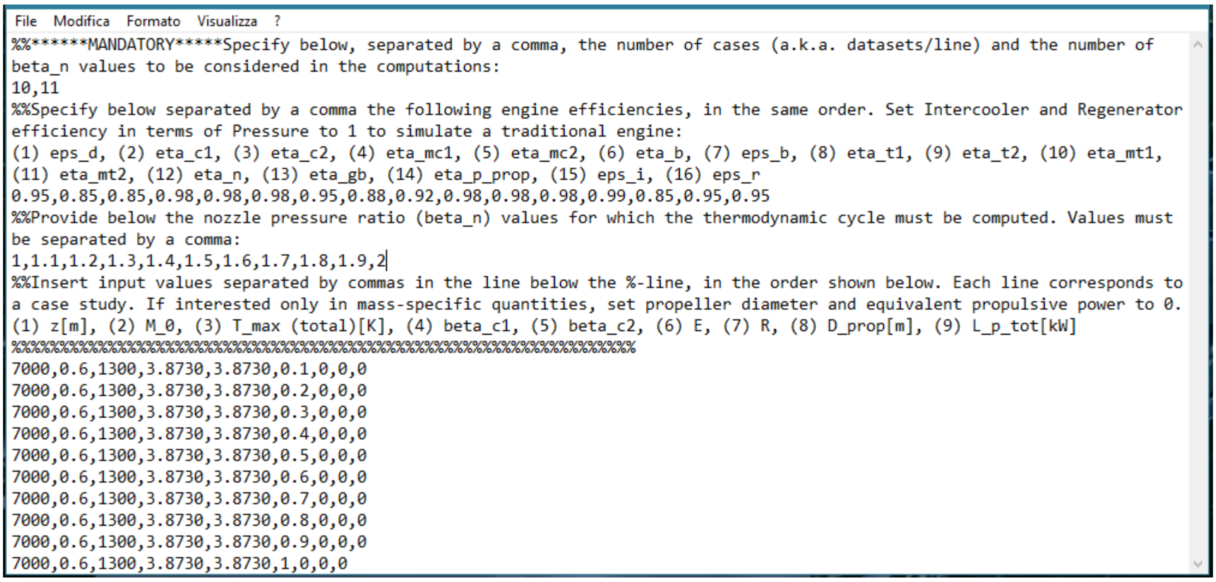

```
File   Modifica   Formato   Visualizza   ?
%%******MANDATORY*****Specify below, separated by a comma, the number of cases (a.k.a. datasets/line) and the number of
beta_n values to be considered in the computations:
10,11
%%Specify below separated by a comma the following engine efficiencies, in the same order. Set Intercooler and Regenerator
efficiency in terms of Pressure to 1 to simulate a traditional engine:
(1) eps_d, (2) eta_c1, (3) eta_c2, (4) eta_mc1, (5) eta_mc2, (6) eta_b, (7) eps_b, (8) eta_t1, (9) eta_t2, (10) eta_mt1,
(11) eta_mt2, (12) eta_n, (13) eta_gb, (14) eta_p_prop, (15) eps_i, (16) eps_r
0.95,0.85,0.85,0.98,0.98,0.98,0.95,0.88,0.92,0.98,0.98,0.98,0.99,0.85,0.95,0.95
%%Provide below the nozzle pressure ratio (beta_n) values for which the thermodynamic cycle must be computed. Values must
be separated by a comma:
1,1.1,1.2,1.3,1.4,1.5,1.6,1.7,1.8,1.9,2
%%Insert input values separated by commas in the line below the %-line, in the order shown below. Each line corresponds to
a case study. If interested only in mass-specific quantities, set propeller diameter and equivalent propulsive power to 0.
(1) z[m], (2) M_0, (3) T_max (total)[K], (4) beta_c1, (5) beta_c2, (6) E, (7) R, (8) D_prop[m], (9) L_p_tot[kW]
%%%%%%%%%%%%%%%%%%%%%%%%%%%%%%%%%%%%%%%%%%%%%%%%%%%%%%%%%%%%%%%%%
7000,0.6,1300,3.8730,3.8730,0.1,0,0,0
7000,0.6,1300,3.8730,3.8730,0.2,0,0,0
7000,0.6,1300,3.8730,3.8730,0.3,0,0,0
7000,0.6,1300,3.8730,3.8730,0.4,0,0,0
7000,0.6,1300,3.8730,3.8730,0.5,0,0,0
7000,0.6,1300,3.8730,3.8730,0.6,0,0,0
7000,0.6,1300,3.8730,3.8730,0.7,0,0,0
7000,0.6,1300,3.8730,3.8730,0.8,0,0,0
7000,0.6,1300,3.8730,3.8730,0.9,0,0,0
7000,0.6,1300,3.8730,3.8730,1,0,0,0
```

Figure 3.1: Input file "Data.txt"

3.2.2 Output files

The code generates two types of output files:

- "Results X.txt", where X is a number between 1 and 999. One "Results" file is generated for each case indicated in the input file. In each "Results" file are reported the values of the thermodynamic quantities in each point of the thermodynamic cycle along with each performance parameter, for each β_n value indicated in the input file

- "Summary.txt". In this file are reported the values of the most important performances for each case and for each β_n value, organized in matrix/vector form. This file is generated to provide the data in a form more suitable for post-processing

At the beginning of each "Results" file are reported the case input parameters and engine efficiencies. After that, for each β_n are reported the quantities and performances values. Non-specific quantities are present only if in the input file the total propulsive power requested was set different from zero.

At the bottom of each "Results" file, $EBSFC$, λ and equivalent specific power values for each β_n are reported in vector form, along with the indication of the β_n of minimum $EBSFC$ and of maximum equivalent specific power and their corresponding λ, $EBSFC$, equivalent specific power, thermal efficiency and heat exchanged values.

Here below an example of "Results" file:

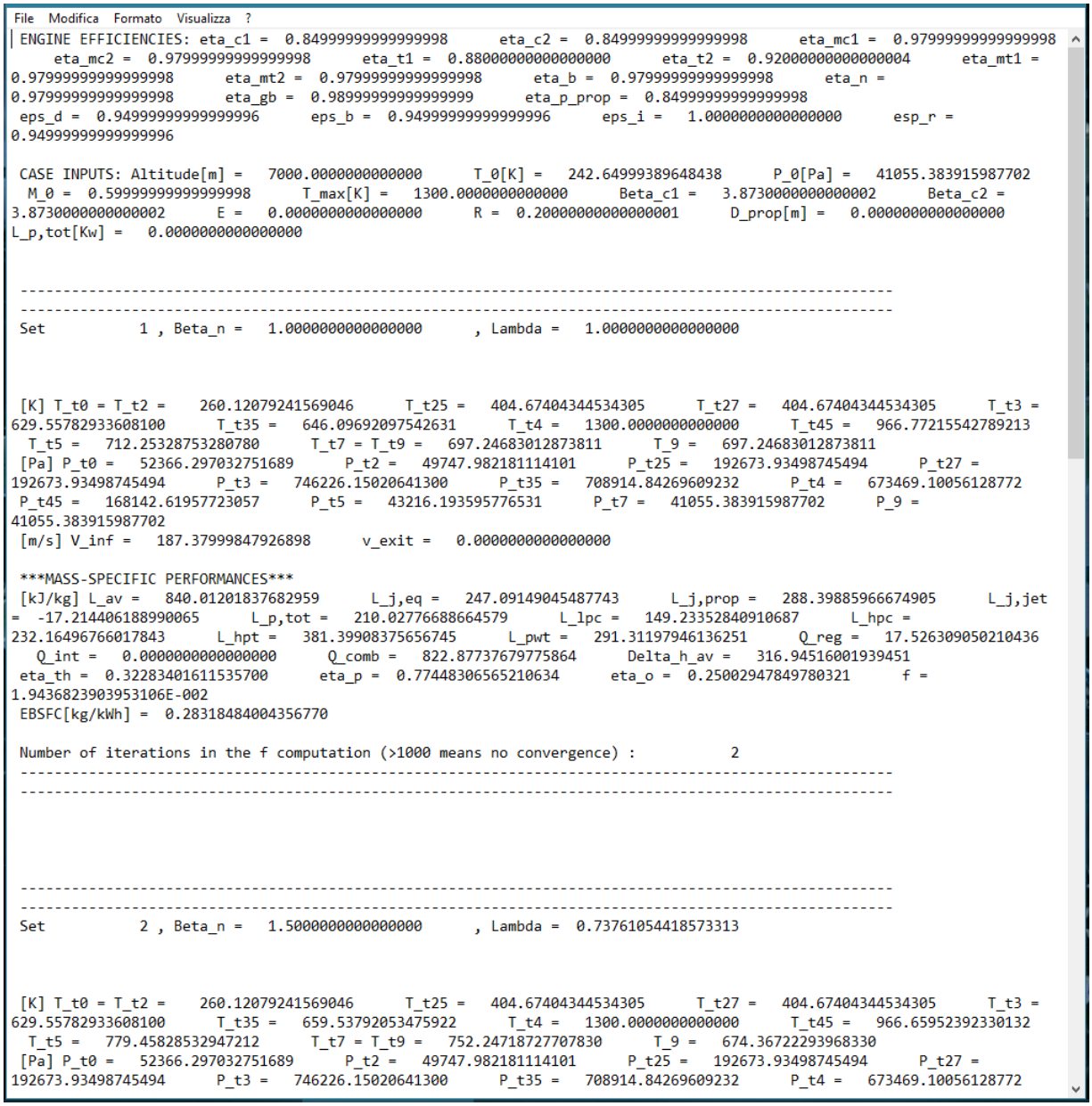

```
File  Modifica  Formato  Visualizza  ?
 ENGINE EFFICIENCIES: eta_c1 =  0.84999999999999998      eta_c2 =  0.84999999999999998      eta_mc1 =  0.97999999999999998
     eta_mc2 =  0.97999999999999998      eta_t1 =  0.88000000000000000      eta_t2 =  0.92000000000000004      eta_mt1 =
0.97999999999999998      eta_mt2 =  0.97999999999999998      eta_b =  0.97999999999999998      eta_n =
0.97999999999999998      eta_gb =  0.98999999999999999      eta_p_prop =  0.84999999999999998
 eps_d =  0.94999999999999996      eps_b =  0.94999999999999996      eps_i =   1.0000000000000000      esp_r =
0.94999999999999996

 CASE INPUTS: Altitude[m] =   7000.0000000000000      T_0[K] =   242.64999389648438      P_0[Pa] =   41055.383915987702
  M_0 =  0.59999999999999998      T_max[K] =   1300.0000000000000      Beta_c1 =   3.8730000000000002      Beta_c2 =
3.8730000000000002      E =   0.0000000000000000      R =  0.20000000000000001      D_prop[m] =   0.0000000000000000
L_p,tot[Kw] =   0.0000000000000000


 ----------------------------------------------------------------------------------------------------
 ----------------------------------------------------------------------------------------------------
 Set           1 , Beta_n =   1.0000000000000000      , Lambda =   1.0000000000000000



 [K] T_t0 = T_t2 =    260.12079241569046      T_t25 =   404.67404344534305      T_t27 =   404.67404344534305      T_t3 =
629.55782933608100      T_t35 =   646.09692097542631      T_t4 =   1300.0000000000000      T_t45 =   966.77215542789213
  T_t5 =   712.25328753280780      T_t7 = T_t9 =   697.24683012873811      T_9 =   697.24683012873811
 [Pa] P_t0 =   52366.297032751689      P_t2 =   49747.982181114101      P_t25 =   192673.93498745494      P_t27 =
192673.93498745494      P_t3 =   746226.15020641300      P_t35 =   708914.84269609232      P_t4 =   673469.10056128772
 P_t45 =   168142.61957723057      P_t5 =   43216.193595776531      P_t7 =   41055.383915987702      P_9 =
41055.383915987702
 [m/s] V_inf =   187.37999847926898      v_exit =   0.0000000000000000

 ***MASS-SPECIFIC PERFORMANCES***
 [kJ/kg] L_av =   840.01201837682959      L_j,eq =   247.09149045487743      L_j,prop =   288.39885966674905      L_j,jet
=  -17.214406188990065      L_p,tot =   210.02776688664579      L_lpc =   149.23352840910687      L_hpc =
232.16496766017843      L_hpt =   381.39908375656745      L_pwt =   291.31197946136251      Q_reg =   17.526309050210436
   Q_int =   0.0000000000000000      Q_comb =   822.87737679775864      Delta_h_av =   316.94516001939451
 eta_th =  0.32283401611535700      eta_p =  0.77448306565210634      eta_o =  0.25002947849780321      f =
1.9436823903953106E-002
 EBSFC[kg/kWh] =  0.28318484004356770

 Number of iterations in the f computation (>1000 means no convergence) :           2
 ----------------------------------------------------------------------------------------------------
 ----------------------------------------------------------------------------------------------------




 ----------------------------------------------------------------------------------------------------
 ----------------------------------------------------------------------------------------------------
 Set           2 , Beta_n =   1.5000000000000000      , Lambda =  0.73761054418573313



 [K] T_t0 = T_t2 =    260.12079241569046      T_t25 =   404.67404344534305      T_t27 =   404.67404344534305      T_t3 =
629.55782933608100      T_t35 =   659.53792053475922      T_t4 =   1300.0000000000000      T_t45 =   966.65952392330132
  T_t5 =   779.45828532947212      T_t7 = T_t9 =   752.24718727707830      T_9 =   674.36722293968330
 [Pa] P_t0 =   52366.297032751689      P_t2 =   49747.982181114101      P_t25 =   192673.93498745494      P_t27 =
192673.93498745494      P_t3 =   746226.15020641300      P_t35 =   708914.84269609232      P_t4 =   673469.10056128772
```

Figure 3.2: Output file "Results 1.txt" - top part

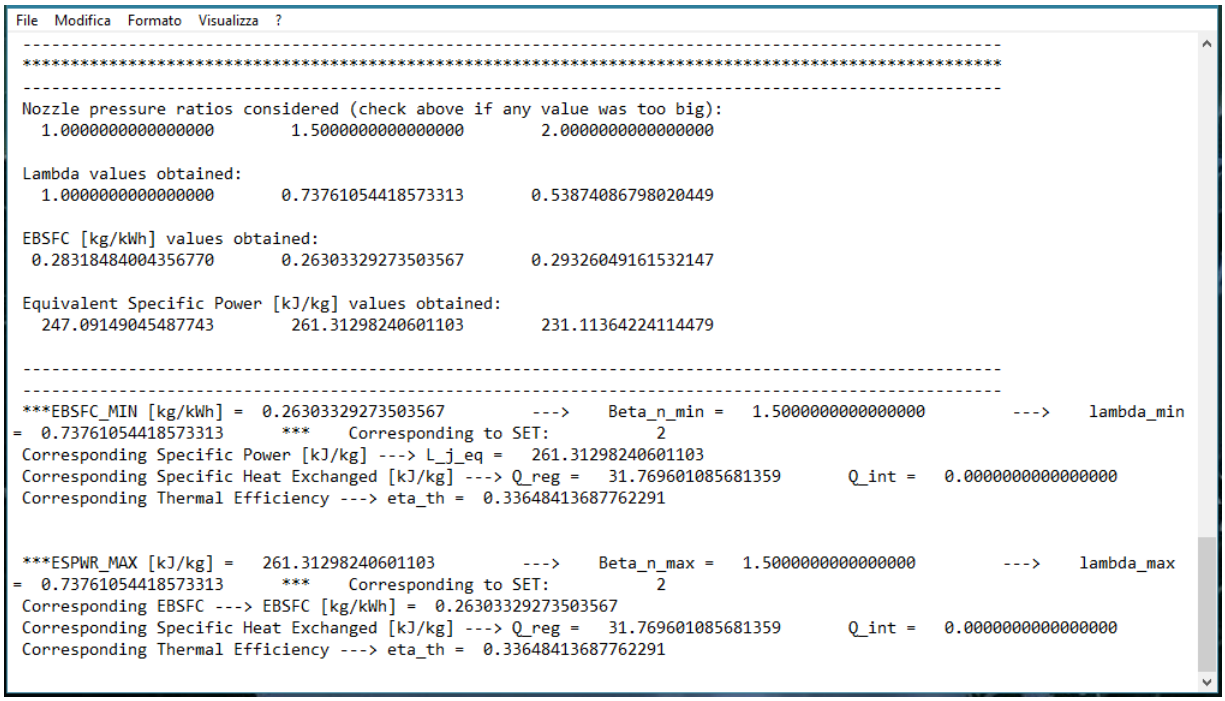

Figure 3.3: Output file "Results 1.txt" - bottom part

At the beginning of the "Summary" file are reported the engine efficiencies and β_n values used in the computations. After that, the values of the following quantities are reported, for each case and β_n value: $EBSFC$, equivalent specific power, λ, specific heat exchanged in the regenerator, specific heat exchanged in the intercooler and thermal efficiency.

At the bottom of the "Summary" file, for each case are reported the values of the performances indicated above corresponding to the β_n of minimum EBSFC and to the β_n of maximum equivalent specific power.

Here below an example of "Summary" file:

File Modifica Formato Visualizza ?

```
 ENGINE EFFICIENCIES: eta_c1 =  0.84999999999999998      eta_c2 =  0.84999999999999998      eta_mc1 =  0.97999999999999998
     eta_mc2 =  0.97999999999999998      eta_t1 =  0.88000000000000000      eta_t2 =  0.92000000000000004      eta_mt1 =
0.97999999999999998      eta_mt2 =  0.97999999999999998      eta_b =  0.97999999999999998      eta_n =
0.97999999999999998      eta_bg =  0.98999999999999999      eta_p_prop =  0.84999999999999998
 eps_d =  0.94999999999999996      eps_b =  0.94999999999999996      eps_i =  0.94999999999999996      esp_r =
0.94999999999999996

 BETA_N CONSIDERED:
   1.0000000000000000        1.1000000000000001        1.2000000000000000
 ----------------------------------------------------------------------------------------------------
 ****************************************************************************************************
 ----------------------------------------------------------------------------------------------------
 EBSFC values [kg/kWh]:
  0.28615706457759504       0.25864337876264515       0.25722949633544634
  0.26828085288772319       0.24409002354401069       0.24239836041646864
  0.24717109838043216       0.22646066690259831       0.22461038054067695
  0.22326908358988218       0.20606297957356226       0.20412193190758082
  0.19690893077504085       0.18311861307806379       0.18110849769946469
 Equivalent Specific Power values [kJ/kg]:
   255.63133893875224        281.73122389755315        282.25314311934039
   272.73318175547791        297.45178707673500        297.35458720778797
   289.46823809425456        312.21431208238135        311.27760516598903
   305.84089521183472        325.93147268819507        323.89594854185248
   321.85505217076741        338.45021604410152        334.98997394868445
 Lambda values:
   1.0000000000000000       0.94132250149065166       0.88716090616239329
   1.0000000000000000       0.94779098246789595       0.89954421335040291
   1.0000000000000000       0.95474999858944831       0.91282982954403091
   1.0000000000000000       0.96218363854956979       0.92704462600877491
   1.0000000000000000       0.97008414309909174       0.94222815843680097
 Specific Heat exchanged in the Regenerator [kJ/kg]:
   28.639093244722648        31.891261706613971        34.928195461649011
   76.089174868292886        82.576044200386335        88.633647218305370
   142.39099379238181        152.09606309118121        161.15896186414506
   227.58103251045233        240.48867158849231        252.54229557706742
   331.69216428743783        347.78752732500351        362.81802965590805
 Specific Heat exchanged in the Intercooler [kJ/kg]:
   29.249771568184922        29.249771568184922        29.249771568184922
   58.499543136369901        58.499543136369901        58.499543136369901
   87.749314704554820        87.749314704554820        87.749314704554820
   116.99908627273980        116.99908627273980        116.99908627273980
   146.24885784092473        146.24885784092473        146.24885784092473
 Engine Thermal Efficiency:
  0.31855027425989291       0.32170106749121918       0.32439750411448365
  0.33793999266194225       0.34111642671958964       0.34376204845157587
  0.36507042017062802       0.36807213641431030       0.37048883999962839
  0.40247063164689190       0.40520420593558287       0.40730843747077655
  0.45466026794309766       0.45723250201340038       0.45912938132178138
 ----------------------------------------------------------------------------------------------------
 ****************************************************************************************************
 ----------------------------------------------------------------------------------------------------
```

Figure 3.4: Output file "Summary.txt" - top part

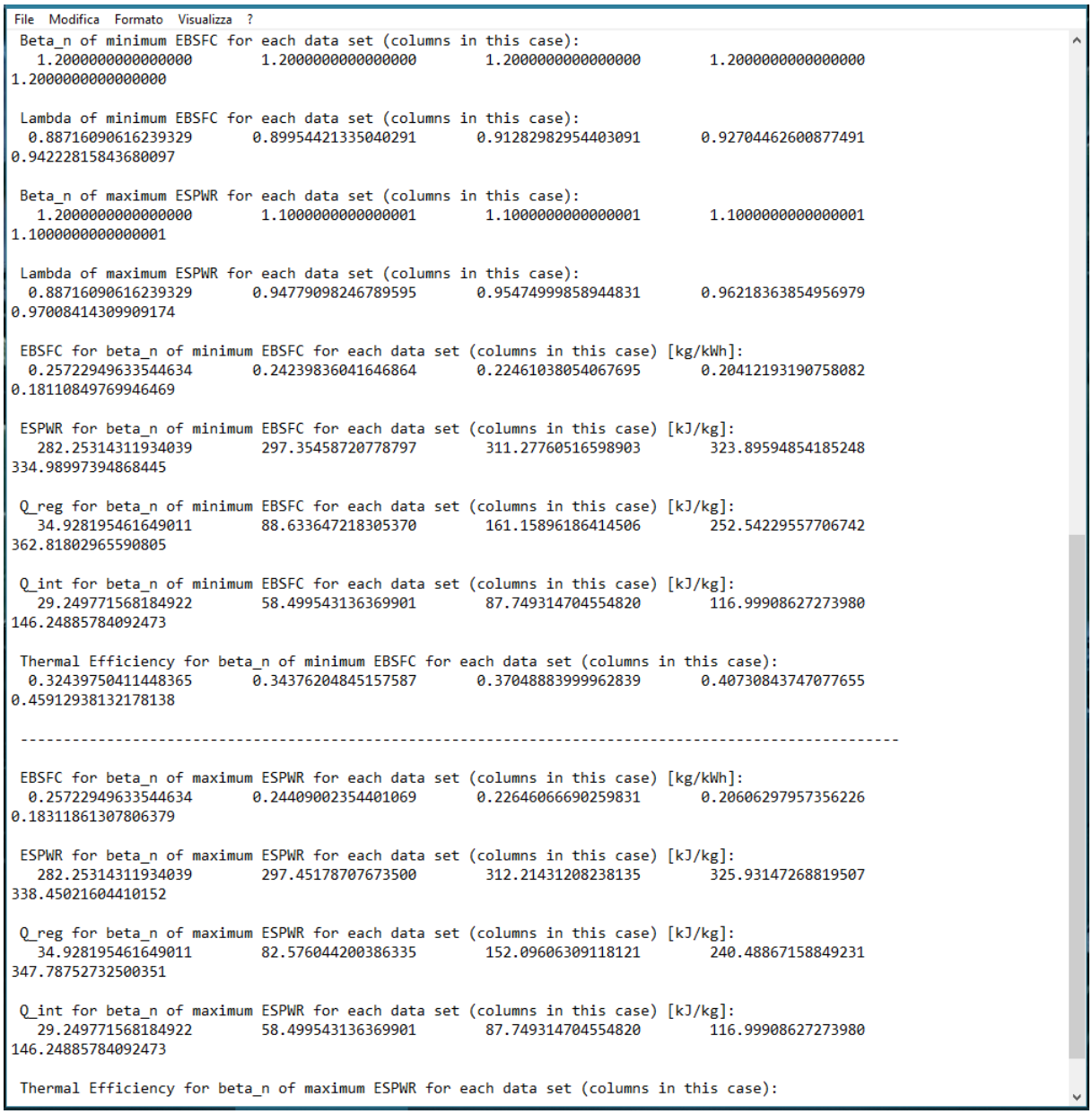

Figure 3.5: Output file "Summary.txt" - bottom part

3.2.3 Code details

The code consists in a main program and a subroutine. The subroutine has the scope to compute the air pressure, temperature and density for a given altitude.

Refer to the end of this section for additional information.

At the beginning of the code (lines 1 to 81) are declared all the variables and parameters that will be used, starting from the variables shared between main program and subroutine. Real variables are declared with double precision. Vectors and matrices which dimensions depend on the number of cases and/or β_n values are declared as "allocatable", in order to be able to size them when the total number of cases and β_n values are read from the input file.

Lines from 82 to 113 contain the user message which provides instructions and information to the user in order to run the code correctly.

Lines from 114 to 171 contain the data loading. Here the number of cases and of β_n values are read from the "Data.txt" file and the "allocatable" vectors and matrices are sized/allocated. The engine's components efficiencies and the β_n values are read and loaded in the appropriate variables.

At this point, the computation of the thermodynamic cycle's quantities and of the performances can begin.

It is achieved by means of two "DO" loops, one nested in the other. The outer one (lines 175 to 422) cycles through each of the input cases, while the inner one (lines 219 to 330) cycles through each β_n value. A "WHILE" loop is present (lines 226 to 239), nested in the inner "DO" loop. It is needed in order to compute the f parameter: in fact, the temperature at the exit of the regenerator in the air side is unknown, since it depends of the heat recovered from the combustion gases at the power turbine exit, which depends on f itself. Therefore, it is necessary to set f equal to 0 as a first value and then iterate until convergence. Convergence is assumed reached if:

$$\frac{|f_{new} - f_{old}|}{f_{new}} < 0.001 \tag{3.13}$$

in a maximum of 1000 iterations.

So, lines from 172 to 208 contain the case's data loading and the computations of the thermodynamic cycle's properties that do not depend on λ/β_n. Additionally, here the subroutine is called to compute the external air properties.

At this point the "Result X.txt" file is created and initialized (lines 210 to 218) and then starts the inner "DO" loop. At the beginning of this cycle it is found the initialization of the variables needed in the following "WHILE" loop. At the end on it, the remaining thermodynamic cycle's properties are computed.

Now that all the thermodynamic properties are known, it is possible to compute the performances (lines 251 to 291), both mass-specific and not (if the total propulsive power required was set different from 0). Here also are generated the matrices of the selected performances (see above) that later on will be written in the "Summary.txt" file.

Lines from 292 to 330 contain the writing of the results related to the current β_n value in the "Results" file. After that, the inner "DO" loop is concluded.

The following lines (from 331 to 366) contain the computation of the lowest $EBSFC$ and highest equivalent specific power and their corresponding β_n values. Right after, the performances' values corresponding to those β_n are written in the "Results file" (lines from 367 to 406), along with all the $EBSFC$, equivalent specific power and λ values in vector form (for each β_n value). At this point the current "Results" file is saved and closed.

Right after (lines from 407 to 421), the performances' values corresponding to the β_n of minimum EBSFC and of maximum equivalent specific power are saved in the corresponding vector, for each input case. At this point the outer "DO" loop is concluded.

Lines from 424 to 506 contain the generation of the "Summary.txt" file, in which the performances' matrices and vectors created above are written in a form more suitable to post-processing operations.

With line 513 the main program ends, after a brief confirmation message to the user.

Subroutine: U.S. Standard Atmosphere Model

Lines from 514 to 570 contain the last part of the code, the subroutine SAM (Standard Atmosphere Model). The subroutine takes the altitude as input and provides air temperature, pressure and density as outputs.

It employs the U.S. Standard Atmosphere Model. This model provides *"a hypothetical vertical distribution of atmospheric temperature, pressure, and density which by international agreement and for historical reasons, is roughly representative of year-round mid-latitude conditions"* [51]. This model, as provided by Sforza [51], is an idealized, steady-state representation of the atmosphere and does not account for diurnal or day-to-day variations in the characteristics of the atmosphere, nor for latitude, season, humidity and degree of solar activity.

In the model, the atmosphere up to 100 km of geometric altitude (z) is divided into nine layers. In each of these layers, the temperature profile is assumed in the following form:

$$T = T_i + \lambda_i\big(h - h_i\big) \tag{3.14}$$

where T_i is the temperature at the start of the i-th layer, λ_i is the lapse rate dT/dh in that layer, and h_i is the geopotential altitude at the start of the i-th layer:

$$h = z\frac{1}{1 + \frac{z}{R_E}} \tag{3.15}$$

where R_E is Earth's radius.
The temperature at the Earth's surface ($h = z = 0$) is assumed equal to $288.15K$.
Here below the λ_i values for each layer:

Layer	h **(km)**	z **(km)**	λ_i **(K/km)**	**Thermal type**
1	0	0	-6.5	Neutral
2	11	11.019	0	Isothermal
3	20	20.063	$+1.0$	Inversion
4	32	32.162	$+2.8$	Inversion
5	47	47.351	0	Isothermal
6	51	51.413	-2.8	Neutral
7	71	71.802	-2.0	Neutral
8	84.85	86	0	Isothermal
9	90.69	92	$+1.03$	Inversion
10 on	98.45	100	Increasing	Inversion

Table 3.4: Definitions of the layers in the U.S. Standard Atmosphere Model

Atmospheric pressure is obtained by integration of the hydrostatic equation:

$$dP = -\rho g dz \tag{3.16}$$

After integration, in non-isothermal layers:

$$P = P_i\left[\frac{T_i}{T_i + \lambda_i\big(h - hi\big)}\right]^{\frac{g_E}{R\lambda_i}} \tag{3.17}$$

while, in isothermal layers:

$$P = P_i \cdot exp\left[-\frac{g_E}{RT_i}\big(h - h_i\big)\right] \tag{3.18}$$

where R is the air specific gas constant and g_E is the gravitational acceleration at the Earth's surface.

Air density is then obtained by applying the state equation for perfect gases.

In the code, the air molecular weight is assumed equal to 28.96 g/mol up to 86 km of altitude, and equal to 28.40 g/mol from 86 km to 100 km of altitude, due to the changes in the atmosphere composition at high altitude. Furthermore, since at these altitudes the difference between geopotential and geometric altitudes is small, it was assumed $z = h$.

For further details refer to [51], chapter 2.

Full code

Finally, here below is reported the full code:

```
1  MODULE ambient !Variables shared with the subroutine SAM
2  IMPLICIT NONE
3  SAVE
4  REAL*8 :: T_0, P_0, rho_0, z, R_a
5  END MODULE ambient
6  !----------------------------------------------------------------------
7  !----------------------------------------------------------------------
8  PROGRAM turboprop_reg
9  USE ambient
10 IMPLICIT NONE
11 !----------------------------------------------------------------------
12 !Parameters declaration
13 !----------------------------------------------------------------------
14 REAL*8, PARAMETER :: treshold = 0.001
15 REAL*8, PARAMETER :: cp_a_cold = 1011.73 ![J/kgK]
16 REAL*8, PARAMETER :: cp_a_hot = 1059.69 ![J/kgK]
17 REAL*8, PARAMETER :: cp_g_cold = 1043.50 ![J/kgK]
18 REAL*8, PARAMETER :: cp_g_hot = 1145.65 ![J/kgK]
19 REAL*8, PARAMETER :: cp_f = 1920 ![J/kgK]
20 REAL*8, PARAMETER :: H_f = 43200000 ![J/kg]
21 REAL*8, PARAMETER :: T_tf = 288.15 ![K]
22 REAL*8, PARAMETER :: gamma_a_cold = 1.40
23 REAL*8, PARAMETER :: gamma_a_hot = 1.37
24 REAL*8, PARAMETER :: gamma_g_cold = 1.38
25 REAL*8, PARAMETER :: gamma_g_hot = 1.33
26 REAL*8, PARAMETER :: R_g = 287.21 ![J/kgK]
27 REAL*8, PARAMETER :: PI = 3.1415926535
28 !----------------------------------------------------------------------
29 !Variables declaration
30 !----------------------------------------------------------------------
31 REAL*8 :: eta_c1, eta_c2, eta_mc1, eta_mc2, eta_b, eta_t1, eta_t2,
      eta_mt1, eta_mt2, eta_n, eta_gb, eta_p_prop !Engine efficiencies
      variables
32 REAL*8 :: eps_d, eps_b, eps_i, eps_r !Engine efficiencies variables
33 REAL*8 :: M_0, T_t4, beta_c1, beta_c2, E, R, D_prop, L_p_tot !Input
      variables
34 REAL*8 :: V_inf, T_t0, P_t0 !Ambient variables
35 REAL*8 :: T_t2, P_t2 !Diffuser variables
36 REAL*8 :: T_t25, P_t25 !LPC variables
37 REAL*8 :: T_t27, P_t27 !Intercooler variables
38 REAL*8 :: T_t3, P_t3 !HPC variables
39 REAL*8 :: T_t35, P_t35 !Regenerator (air side) variables
40 REAL*8 :: P_t4, f, f_new !Combustor variables
```

```
41 REAL*8 :: T_t45, P_t45 !HPT variables
42 REAL*8 :: deltah_av, lambda, T_t5_is, T_t5, P_t5, deltah_pt_is !Power
   turbine variables
43 REAL*8 :: T_t7, P_t7 !Regenerator (gas side) variables
44 REAL*8 :: T_9_is, T_9, v_9, P_9, deltah_noz_is, beta_n !Nozzle variables
45 !Performance variables:
46 REAL*8 :: m_a, m_f !Engine mass flow rates
47 REAL*8 :: m_a_prop, v_wake !Propeller variables
48 REAL*8 :: Thrust_prop, Thrust_jet, Thrust_total !Thrust variables
49 REAL*8 :: EBSFC, L_j_eq !EBSFC variables
50 REAL*8 :: L_av, L_j_prop, L_j_jet, L_j_total, L_p_tot_spec, eta_th,
   eta_p, eta_o !Efficiencies variables
51 REAL*8 :: Q_reg, Q_int, Q_comb, L_lpc, L_hpc, L_hpt, L_pwt !Powers and
   heats exchanged
52 !Service variables:
53 REAL*8 :: beta_n_max, EBSFC_min, delta, ESPWR_max
54 INTEGER :: pos_min, l, iter, i, j, k, kk, ll, jj, ii, n_max, data_max,
   pos_max, iii, kkk, jjj, x, y, xx
55 REAL*8, DIMENSION(:), ALLOCATABLE :: beta_n_vect !Vector where to load
   the beta_n values from file
56 REAL*8, DIMENSION(:,:), ALLOCATABLE :: lambda_vect
57 REAL*8, DIMENSION(:,:), ALLOCATABLE :: EBSFC_vect
58 REAL*8, DIMENSION(:,:), ALLOCATABLE :: L_j_eq_vect
59 REAL*8, DIMENSION(:,:), ALLOCATABLE :: Q_reg_vect
60 REAL*8, DIMENSION(:,:), ALLOCATABLE :: Q_int_vect
61 REAL*8, DIMENSION(:,:), ALLOCATABLE :: eta_th_vect
62 REAL*8, DIMENSION(:), ALLOCATABLE :: pos_equiv
63 REAL*8, DIMENSION(:), ALLOCATABLE :: pos_equiv2
64 REAL*8, DIMENSION(:), ALLOCATABLE :: beta_n_ebsfc
65 REAL*8, DIMENSION(:), ALLOCATABLE :: beta_n_espwr
66 REAL*8, DIMENSION(:), ALLOCATABLE :: lambda_ebsfc
67 REAL*8, DIMENSION(:), ALLOCATABLE :: lambda_espwr
68 REAL*8, DIMENSION(:), ALLOCATABLE :: EBSFC_vect_min
69 REAL*8, DIMENSION(:), ALLOCATABLE :: ESPWR_vect_min
70 REAL*8, DIMENSION(:), ALLOCATABLE :: Q_reg_min
71 REAL*8, DIMENSION(:), ALLOCATABLE :: Q_int_min
72 REAL*8, DIMENSION(:), ALLOCATABLE :: eta_th_min
73 REAL*8, DIMENSION(:), ALLOCATABLE :: EBSFC_vect_max
74 REAL*8, DIMENSION(:), ALLOCATABLE :: ESPWR_vect_max
75 REAL*8, DIMENSION(:), ALLOCATABLE :: Q_reg_max
76 REAL*8, DIMENSION(:), ALLOCATABLE :: Q_int_max
77 REAL*8, DIMENSION(:), ALLOCATABLE :: eta_th_max
78 REAL*8, DIMENSION(9) :: data !Vector where to load the input data from
   file
79 REAL*8, DIMENSION(16) :: efficiencies !Vector where to load the engine
   efficiencies
80 INTEGER, DIMENSION(2) :: vect_dim !Vector where to load other vectors
   dimensions
81 CHARACTER(22) :: filename !For output file generation
82 !------------------------------------------------------------------------
83 !User message
84 !------------------------------------------------------------------------
85 WRITE(*,*) "Code to compute the thermodynamic cycle and performances of
   a turbopropeller with regeneration and intercooling."
86 WRITE(*,*) "The program needs an input file named 'Data.txt'. It must be
    in the same directory of the executable."
87 WRITE(*,*) "Follow the instructions on that file to provide the data
   requested:"
```

```
88  WRITE(*,*) "number of cases to analyze/number of nozzle expansion ratios
        to consider, engine efficiencies"
89  WRITE(*,*) "(eta = efficiency, eps = pneumatic eff, _m = mechanical eff,
        _gb = gearbox, eta_p_prop = propeller prop eff, &
90  _c = compressor, _t = turbine, _n = nozzle, _d = diffuser, _b = burner,
       _i = intercooler, _r = regenerator), &
91  nozzle pressure ratio values and the following case-dependant data:"
92  WRITE(*,*) "flight altitude (in meters), flight Mach number, maximum
       temperature of the cycle[K], compression ratio of &
93  first compressor, compression ratio of second compressor, intercooling
       effectiveness, degree of regeneration, &
94  propeller diameter[m], total propulsive power desired[Kw]."
95  WRITE(*,*) "If interested only in mass-specific quantities, set
       propeller diameter and equivalent propulsive power to 0."
96  WRITE(*,*) "It is possible to specify multiple data sets, one on each
       line (MAX 999 sets): &
97  the code will create an output file for each of them."
98  WRITE(*,*) "If interested in the study of a traditional engine (no
       regenerator and intercooler) please set E and R to 0, and &
99  the intercooler and regenerator pneumatic efficiencies to 1."
100 WRITE(*,*) "The output of this program is a file,'Results.txt', for each
        data set specified in the 'Data.txt' file. In each row &
101 are written the results of calculations for a given beta_n value. The
       Result.txt files are located in the Results folder, that &
102 must be present in the program directory."
103 WRITE(*,*) "At the end of each file all EBSFC, specific power and beta_n
        values are written, along with the lowest EBSFC &
104 and highest Equivalent Specific Power and the corresponding beta_n
       values, with the indication of the corresponding set or sets &
105 (e.g. in case of multiple 'lowest' EBSFC values) of results."
106 WRITE(*,*) "In addition, a 'Summary.txt' file is created in the 'Results
       ' folder. There can be found performances values &
107 arranged in matrix form, for each beta_n(columns) and for each data_set(
       rows), along with the beta_n and lambda values &
108 corresponding to minimum EBSFC/maximum Equiv. Spec. Power and their
       corresponding EBSFC and Equiv. Spec. Power values."
109 WRITE(*,*) "It is suggested to open the Summary file with Notepad++."
110 WRITE(*,*) "Delete any existing 'Result' and 'Summary' files in the
       Results folder before re-launching the code."
111 WRITE(*,*)
112 WRITE(*,*) "Press ENTER when ready."
113 READ(*,*)
114 !-----------------------------------------------------------------------
115 !Data loading
116 !-----------------------------------------------------------------------
117 OPEN(UNIT=11, FILE="Data.txt", STATUS="OLD", ACTION="READ")
118 READ(11,*)
119 READ(11,*) vect_dim
120 IF (vect_dim(1) > 999) THEN
121     WRITE(*,*) "ERROR: Too many data sets (max 999)"
122     WRITE(*,*) "Press ENTER to close this window."
123     READ(*,*)
124     STOP
125 END IF
126 data_max = vect_dim(1)
127 n_max = vect_dim(2)
128 ALLOCATE(lambda_vect(data_max,n_max))
129 ALLOCATE(EBSFC_vect(data_max,n_max))
```

```
ALLOCATE(L_j_eq_vect(data_max,n_max))
ALLOCATE(Q_reg_vect(data_max,n_max))
ALLOCATE(Q_int_vect(data_max,n_max))
ALLOCATE(eta_th_vect(data_max,n_max))
ALLOCATE(beta_n_vect(n_max))
ALLOCATE(pos_equiv(n_max))
ALLOCATE(pos_equiv2(n_max))
ALLOCATE(beta_n_ebsfc(data_max))
ALLOCATE(beta_n_espwr(data_max))
ALLOCATE(lambda_ebsfc(data_max))
ALLOCATE(lambda_espwr(data_max))
ALLOCATE(EBSFC_vect_min(data_max))
ALLOCATE(ESPWR_vect_min(data_max))
ALLOCATE(Q_reg_min(data_max))
ALLOCATE(Q_int_min(data_max))
ALLOCATE(eta_th_min(data_max))
ALLOCATE(EBSFC_vect_max(data_max))
ALLOCATE(ESPWR_vect_max(data_max))
ALLOCATE(Q_reg_max(data_max))
ALLOCATE(Q_int_max(data_max))
ALLOCATE(eta_th_max(data_max))
READ(11,100)
READ(11,*) efficiencies
eps_d = efficiencies(1)
eta_c1 = efficiencies(2)
eta_c2 = efficiencies(3)
eta_mc1 = efficiencies(4)
eta_mc2 = efficiencies(5)
eta_b = efficiencies(6)
eps_b = efficiencies(7)
eta_t1 = efficiencies(8)
eta_t2 = efficiencies(9)
eta_mt1 = efficiencies(10)
eta_mt2 = efficiencies(11)
eta_n = efficiencies(12)
eta_gb = efficiencies(13)
eta_p_prop = efficiencies(14)
eps_i = efficiencies(15)
eps_r = efficiencies(16)
READ(11,*)
READ(11,*) beta_n_vect
READ(11,101)
!-------------------------------------------------------------------------
!COMPUTATIONS
!-------------------------------------------------------------------------
DO ii = 1, data_max
    WRITE (filename, '("Results/Results", I3, ".txt")' )  ii
    READ(11,*) data
    z = data(1)
    M_0 = data(2)
    T_t4 = data(3)
    beta_c1 = data(4)
    beta_c2 = data(5)
    E = data(6)
    R = data(7)
    D_prop = data(8)
    L_p_tot = data(9)*1000 !to have Watts
    !Ambient
```

```
188     CALL SAM
189     P_9 = P_0
190     V_inf = SQRT(gamma_a_cold*R_a*T_0)*M_0
191     T_t0 = T_0*(1+(((gamma_a_cold-1)/2)*M_0**2))
192     P_t0 = P_0*((1+(((gamma_a_cold-1)/2)*M_0**2))**(gamma_a_cold/(
            gamma_a_cold-1)))
193     !Diffuser
194     T_t2 = T_t0
195     P_t2 = eps_d*P_t0
196     !LPC
197     P_t25 = beta_c1*P_t2
198     T_t25 = T_t2*(1+((beta_c1**((gamma_a_cold-1)/gamma_a_cold)-1)/eta_c1
            ))
199     !Intercooler
200     P_t27 = eps_i*P_t25
201     T_t27 = T_t25-(E*(T_t25-T_t2))
202     !HPC
203     P_t3 = beta_c2*P_t27
204     T_t3 = T_t27*(1+((beta_c2**((gamma_a_cold-1)/gamma_a_cold)-1)/eta_c2
            ))
205     !Regenerator - part1
206     P_t35 = eps_r*P_t3
207     !Combustor - part1
208     P_t4 = eps_b*P_t35
209     !2. Beta_n-dependant computations
210     OPEN(UNIT=12, FILE=filename, STATUS="NEW", ACTION="WRITE") !Creating
             new file to save the results
211     WRITE(12,*) "ENGINE EFFICIENCIES: eta_c1 =",eta_c1,"eta_c2 =",eta_c2
            ,"eta_mc1 =",eta_mc1,"eta_mc2 =",eta_mc2,&
212     "eta_t1 =",eta_t1,"eta_t2 =",eta_t2,"eta_mt1 =",eta_mt1,"eta_mt2 =",
            eta_mt2,"eta_b =",eta_b,"eta_n =",eta_n,&
213     "eta_gb =",eta_gb,"eta_p_prop =",eta_p_prop
214     WRITE(12,*)"eps_d =",eps_d,"eps_b =",eps_b,"eps_i =",eps_i,"esp_r ="
            ,eps_r
215     WRITE(12,*)
216     WRITE(12,*) "CASE INPUTS: Altitude[m] =",z,"T_0[K] =",T_0,"P_0[Pa] =
            ",P_0,"M_0 =",M_0,"T_max[K] =",T_t4,"Beta_c1 =",beta_c1,&
217     "Beta_c2 =",beta_c2,"E =",E,"R =",R,"D_prop[m] =",D_prop,"L_p,tot[kW
            ] =",L_p_tot/1000
218     WRITE(12,100)
219     DO i = 1, SIZE(beta_n_vect)
220         f = 0
221         iter = 0
222         delta = 100
223         beta_n = beta_n_vect(i)
224         P_t7 = beta_n*P_9
225         P_t5 = P_t7/eps_r
226         DO WHILE ((delta > treshold) .AND. (iter <= 1000))
227             !HPT
228             T_t45 = T_t4-(((((T_t3-T_t27)/eta_mc2)+((T_t25-T_t2)/eta_mc1
                    ))/(eta_mt1*(1+f)))*(cp_a_cold/cp_g_hot))
229             P_t45 = P_t4*((1-((1-(T_t45/T_t4))/eta_t1))**(gamma_g_hot/(
                    gamma_g_hot-1)))
230             !Power turbine
231             T_t5_is = T_t45*((P_t5/P_t45)**((gamma_g_hot-1)/gamma_g_hot)
                    )
232             T_t5 = T_t45-(eta_t2*(T_t45-T_t5_is))
233         !Regenerator and combustor - part 2
```

```
234             T_t35 = T_t3+(R*(T_t5-T_t3))
235             f_new = ((cp_g_hot*T_t4)-(cp_a_hot*T_t35))/((cp_f*T_tf)+(H_f
                    *eta_b)-(cp_g_hot*T_t4))
236             delta = ABS(f_new-f)/f_new
237             f = f_new
238             iter = iter+1
239         END DO
240         T_t7 = T_t5-(((T_t35-T_t3)/(1+f))*(cp_a_hot/cp_g_hot))
241         beta_n_max = (P_t45*eps_r)/P_9
242         !Nozzle
243         T_9_is = T_t7*((P_9/P_t7)**((gamma_g_cold-1)/gamma_g_cold))
244         T_9 = T_t7-(eta_n*(T_t7-T_9_is))
245         v_9 = SQRT(2*cp_g_cold*(T_t7-T_9))
246         !Lambda computation
247         deltah_pt_is = cp_g_hot*(T_t45-T_t5_is)
248         deltah_noz_is = cp_g_cold*(T_t7-T_9_is)
249         deltah_av = deltah_pt_is+deltah_noz_is
250         lambda = deltah_pt_is/deltah_av
251         !PERFORMANCES - mass-specific quantities
252         !Efficiencies
253         L_av = f*(H_f+((V_inf**2)/2))
254         L_j_prop = eta_gb*eta_t2*eta_mt2*(1+f)*lambda*deltah_av
255         L_j_jet = 0.5*(((1+f)*(v_9**2))-((1-f)*(V_inf**2)))
256         L_j_total = L_j_prop+L_j_jet
257         L_p_tot_spec = (eta_p_prop*eta_t2*eta_mt2*eta_gb*(1+f)*lambda*
                    deltah_av)+(V_inf*(((1+f)*v_9)-V_inf)) !Mass-specific L_p_tot
258         eta_th = L_j_total/L_av
259         eta_p =  L_p_tot_spec/L_j_total
260         eta_o = eta_p*eta_th
261         !EBSFC
262         L_j_eq = L_j_prop + ((V_inf*(((1+f)*v_9)-V_inf))/eta_p_prop)
263         EBSFC = (f/L_j_eq)*3.6*1000000 !kg/kWh
264         !Powers and heats exchanged
265         Q_reg = cp_a_hot*(T_t35-T_t3)
266         Q_int = cp_a_cold*(T_t25-T_t27)
267         Q_comb = f*eta_b*H_f
268         L_lpc = (cp_a_cold*(T_t25-T_t2))/eta_mc1
269         L_hpc = (cp_a_cold*(T_t3-T_t27))/eta_mc2
270         L_hpt = (1+f)*cp_g_hot*(T_t4-T_t45)*eta_mt1
271         L_pwt = (1+f)*cp_g_hot*(T_t45-T_t5)*eta_mt2
272         !Performances vectors
273         EBSFC_vect(ii,i) = EBSFC
274         lambda_vect(ii,i) = lambda
275         L_j_eq_vect(ii,i) = L_j_eq
276         Q_reg_vect(ii,i) = Q_reg
277         Q_int_vect(ii,i) = Q_int
278         eta_th_vect(ii,i) = eta_th
279         !PERFORMANCES - whole quantities
280         IF (L_p_tot /= 0) THEN
281             !Mass flow rates
282             m_a = L_p_tot/((eta_p_prop*eta_t2*eta_mt2*eta_gb*(1+f)*
                        lambda*deltah_av)+(V_inf*(((1+f)*v_9)-V_inf)))
283             m_f = f*m_a
284             !Propeller properties
285             m_a_prop = rho_0*V_inf*PI*((D_prop**2)/4)
286             v_wake = SQRT(((2*eta_t2*eta_mt2*eta_gb*m_a*(1+f)*lambda*
                        deltah_av)/m_a_prop)+(V_inf**2))
287             !Thrust
```

```
288             Thrust_prop = m_a_prop*(v_wake-V_inf)
289             Thrust_jet = m_a*(((1+f)*v_9)-V_inf)
290             Thrust_total = Thrust_prop+Thrust_jet
291         END IF
292         !Writing i-th cycle results
293         WRITE(12,*) "-----------------------------------------------------"
294         WRITE(12,*) "-----------------------------------------------------"
295         WRITE(12,*) "Set",i,", Beta_n =",beta_n,", Lambda =",lambda
296         IF (beta_n > beta_n_max) THEN
297             WRITE(12,*) "NOZZLE PRESSURE RATIO TOO BIG, YOU ARE
                EXPANDING TOO MUCH!"
298         END IF
299         WRITE(12,100)
300         WRITE(12,*)
301         WRITE(12,*) "[K] T_t0 = T_t2 = ",T_t0,"T_t25 =",T_t25,"T_t27 =",
            T_t27,"T_t3 =",T_t3,"T_t35 =",T_t35,"T_t4 =",T_t4,&
302         "T_t45 =",T_t45,"T_t5 =",T_t5,"T_t7 = T_t9 =",T_t7,"T_9 =",T_9
303         WRITE(12,*) "[Pa] P_t0 =",P_t0,"P_t2 =",P_t2,"P_t25 =",P_t25,"
            P_t27 =",P_t27,"P_t3 =",P_t3,&
304         "P_t35 =",P_t35,"P_t4 =",P_t4,"P_t45 =",P_t45,"P_t5 =",P_t5,"
            P_t7 =",P_t7,"P_9 =",P_9
305         WRITE(12,*) "[m/s] V_inf =",V_inf,"v_exit =",v_9
306         WRITE(12,*)
307         WRITE(12,*) "***MASS-SPECIFIC PERFORMANCES***"!/1000 is in order
             to have kJ
308         WRITE(12,*) "[kJ/kg] L_av =",L_av/1000,"L_j,eq =",L_j_eq/1000,"
            L_j,prop =",L_j_prop/1000,"L_j,jet =",L_j_jet/1000,&
309         "L_p,tot =",L_p_tot_spec/1000,"L_lpc =",L_lpc/1000,"L_hpc =",
            L_hpc/1000,"L_hpt =",L_hpt/1000,"L_pwt =",L_pwt/1000,&
310         "Q_reg =",Q_reg/1000,"Q_int =",Q_int/1000,"Q_comb =",Q_comb
            /1000,"Delta_h_av =",deltah_av/1000
311         WRITE(12,*) "eta_th =",eta_th,"eta_p =",eta_p,"eta_o =",eta_o,"f
             =",f
312         WRITE(12,*) "EBSFC[kg/kWh] =",EBSFC
313         IF (L_p_tot /= 0) THEN
314             WRITE(12,*)
315             WRITE(12,*) "***PERFORMANCES***"
316             WRITE(12,*) "[m/s] v_wake =",v_wake
317             WRITE(12,*) "[kg/s] m_a =",m_a,"m_f =",m_f,"m_a,prop =",
                m_a_prop
318             WRITE(12,*) "[kN] Thrust(total) =",Thrust_total/1000,"
                Thrust_prop =",Thrust_prop/1000,"Thrust_jet =",Thrust_jet
                /1000
319             WRITE(12,*) "[kW] L_av =",(m_a*L_av)/1000,"L_j,eq =",(m_a*
                L_j_eq)/1000,"L_j,prop =",(m_a*L_j_prop)/1000,&
320             "L_j,jet =",(m_a*L_j_jet)/1000,"L_p,tot =",L_p_tot/1000,"
                L_lpc =",(m_a*L_lpc)/1000,"L_hpc =",(m_a*L_hpc)/1000,&
321             "L_hpt =",(m_a*L_hpt)/1000,"L_pwt =",(m_a*L_pwt)/1000,"Q_reg
                 =",(m_a*Q_reg)/1000,"Q_int =",(m_a*Q_int)/1000,&
322             "Q_comb =",(m_a*Q_comb)/1000
323         END IF
324         WRITE(12,*)
325         WRITE(12,*) "Number of iterations in the f computation (>1000
            means no convergence) :",iter
326         WRITE(12,*) "-----------------------------------------------------"
327         WRITE(12,*) "-----------------------------------------------------"
328         WRITE(12,100)
329         WRITE(12,100)
```

```
330     END DO
331     !Computation of the lowest EBSFC and its corresponding beta_n and
            its location in file Results.txt
332     EBSFC_min = EBSFC_vect(ii,1)
333     pos_min = 1
334     DO j = 2,  SIZE(EBSFC_vect,2)
335         IF (EBSFC_vect(ii,j) < EBSFC_min) THEN
336             EBSFC_min = EBSFC_vect(ii,j)
337             pos_min = j
338         END IF
339     END DO
340     !Checking for multiple lowest EBSFC values and tracking their
            position
341     l = 1
342     pos_equiv = 0
343     DO k = 1, SIZE(EBSFC_vect,2)
344         IF (EBSFC_vect(ii,k) == EBSFC_min .AND. k /= pos_min) THEN
345             pos_equiv(l) = k
346             l = l+1
347         END IF
348     END DO
349     !Computation of the highest Equiv. Spec. Power and its corresponding
            beta_n and its location in file Results.txt
350     ESPWR_max = L_j_eq_vect(ii,1)
351     pos_max = 1
352     DO jj = 2,  SIZE(L_j_eq_vect,2)
353         IF (L_j_eq_vect(ii,jj) > ESPWR_max) THEN
354             ESPWR_max = L_j_eq_vect(ii,jj)
355             pos_max = jj
356         END IF
357     END DO
358     !Checking for multiple highest ESPWR values and tracking their
            position
359     ll = 1
360     pos_equiv2 = 0
361     DO kk = 1, SIZE(L_j_eq_vect,2)
362         IF (L_j_eq_vect(ii,kk) == ESPWR_max .AND. kk /= pos_max) THEN
363             pos_equiv2(ll) = kk
364             ll = ll+1
365         END IF
366     END DO
367     !Writing EBSFC/ESPWR and corresponding lambda and min/max values
368     WRITE(12,100)
369     WRITE(12,*) "-------------------------------------------------------"
370     WRITE(12,*) "*******************************************************"
371     WRITE(12,*) "-------------------------------------------------------"
372     WRITE(12,*) "Nozzle pressure ratios considered (check above if any
            value was too big):"
373     WRITE(12,*) beta_n_vect
374     WRITE(12,*)
375     WRITE(12,*) "Lambda values obtained:"
376     WRITE(12,*) lambda_vect(ii,:)
377     WRITE(12,*)
378     WRITE(12,*) "EBSFC [kg/kWh] values obtained:"
379     WRITE(12,*) EBSFC_vect(ii,:)
380     WRITE(12,*)
381     WRITE(12,*) "Equivalent Specific Power [kJ/kg] values obtained:"
382     WRITE(12,*) L_j_eq_vect(ii,:)/1000
```

```
383     WRITE(12,*)
384     WRITE(12,*) "-------------------------------------------------------"
385     WRITE(12,*) "-------------------------------------------------------"
386     WRITE(12,*) "***EBSFC_MIN [kg/kWh] =",EBSFC_min,"   --->
           Beta_n_min =",beta_n_vect(pos_min),"   --->    &
387     lambda_min =",lambda_vect(ii,pos_min),"***","    Corresponding to
           SET:",pos_min
388     Write(12,*) "Corresponding Specific Power [kJ/kg] ---> L_j_eq =",
           L_j_eq_vect(ii,pos_min)/1000
389     Write(12,*) "Corresponding Specific Heats Exchanged [kJ/kg] --->
           Q_reg =",Q_reg_vect(ii,pos_min)/1000," &
390     Q_int =",Q_int_vect(ii,pos_min)/1000
391     WRITE(12,*) "Corresponding Thermal Efficiency ---> eta_th =",
           eta_th_vect(ii,pos_min)
392     IF (pos_equiv(1) /= 0) THEN
393         WRITE(12,*) "Other lambda/beta_n values that give EBSFC_MIN are
               those of SETS:",pos_equiv
394     END IF
395     WRITE(12,*)
396     WRITE(12,*)
397     WRITE(12,*) "***ESPWR_MAX [kJ/kg] =",ESPWR_max/1000,"   --->
           Beta_n_max =",beta_n_vect(pos_max),"   --->    &
398     lambda_max =",lambda_vect(ii,pos_max),"***","    Corresponding to
           SET:",pos_max
399     WRITE(12,*) "Corresponding EBSFC ---> EBSFC [kg/kWh] =",EBSFC_vect(
           ii,pos_max)
400     Write(12,*) "Corresponding Specific Heats Exchanged [kJ/kg] --->
           Q_reg =",Q_reg_vect(ii,pos_max)/1000," &
401     Q_int =",Q_int_vect(ii,pos_max)/1000
402     WRITE(12,*) "Corresponding Thermal Efficiency ---> eta_th =",
           eta_th_vect(ii,pos_max)
403     IF (pos_equiv2(1) /= 0) THEN
404         WRITE(12,*) "Other lambda/beta_n values that give ESPWR_max are
               those of SETS:",pos_equiv2
405     END IF
406     CLOSE(12)
407     !Tracking best EBSFC and ESPWR and their corresponding beta_n and
           lambda, for each data set
408     beta_n_ebsfc(ii) = beta_n_vect(pos_min)
409     lambda_ebsfc(ii) = lambda_vect(ii,pos_min)
410     beta_n_espwr(ii) = beta_n_vect(pos_max)
411     lambda_espwr(ii) = lambda_vect(ii,pos_max)
412     EBSFC_vect_min(ii) = EBSFC_vect(ii,pos_min) !Values corresponding to
           beta_n of min EBSFC
413     ESPWR_vect_min(ii) = L_j_eq_vect(ii,pos_min)
414     EBSFC_vect_max(ii) = EBSFC_vect(ii,pos_max) !Values corresponding to
           beta_n of max ESPWR
415     ESPWR_vect_max(ii) = L_j_eq_vect(ii,pos_max)
416     Q_reg_min(ii) = Q_reg_vect(ii,pos_min) !Values corresponding to
           beta_n of min EBSFC
417     Q_int_min(ii) = Q_int_vect(ii,pos_min)
418     Q_reg_max(ii) = Q_reg_vect(ii,pos_max) !Values corresponding to
           beta_n of max ESPWR
419     Q_int_max(ii) = Q_int_vect(ii,pos_max)
420     eta_th_min(ii) = eta_th_vect(ii,pos_min) !Values corresponding to
           beta_n of min EBSFC
421     eta_th_max(ii) = eta_th_vect(ii,pos_max) !Values corresponding to
           beta_n of max ESPWR
```

```
422 END DO
423 CLOSE(11)
424 !Writing a summary file with performances values arranged in matrix form
    , for each beta_n(columns) and for each data_set(rows)
425 OPEN(UNIT=13, FILE="Results/Summary.txt", STATUS="NEW", ACTION="WRITE")
    !Creating new file to save a summary of the results
426 WRITE(13,*) "ENGINE EFFICIENCIES: eta_c1 =",eta_c1,"eta_c2 =",eta_c2,"
    eta_mc1 =",eta_mc1,"eta_mc2 =",eta_mc2,&
427 "eta_t1 =",eta_t1,"eta_t2 =",eta_t2,"eta_mt1 =",eta_mt1,"eta_mt2 =",
    eta_mt2,"eta_b =",eta_b,"eta_n =",eta_n,&
428 "eta_gb =",eta_gb,"eta_p_prop =",eta_p_prop
429 WRITE(13,*)"eps_d =",eps_d,"eps_b =",eps_b,"eps_i =",eps_i,"esp_r =",
    eps_r
430 WRITE(13,*)
431 WRITE(13,*) "BETA_N CONSIDERED:"
432 WRITE(13,*) beta_n_vect
433 WRITE(13,*) "------------------------------------------------------------"
434 WRITE(13,*) "************************************************************"
435 WRITE(13,*) "------------------------------------------------------------"
436 WRITE(13,*) "EBSFC values [kg/kWh]:"
437 DO iii = 1, SIZE(EBSFC_vect,1)
438     WRITE(13,*) EBSFC_vect(iii,:)
439 END DO
440 WRITE(13,*) "Equivalent Specific Power values [kJ/kg]:"
441 DO kkk = 1, SIZE(L_j_eq_vect,1)
442     WRITE(13,*) L_j_eq_vect(kkk,:)/1000
443 END DO
444 WRITE(13,*) "Lambda values:"
445 DO jjj = 1, SIZE(lambda_vect,1)
446     WRITE(13,*) lambda_vect(jjj,:)
447 END DO
448 WRITE(13,*) "Specific Heat exchanged in the Regenerator [kJ/kg]:"
449 DO x = 1, SIZE(Q_reg_vect,1)
450     WRITE(13,*) Q_reg_vect(x,:)/1000
451 END DO
452 WRITE(13,*) "Specific Heat exchanged in the Intercooler [kJ/kg]:"
453 DO y = 1, SIZE(Q_int_vect,1)
454     WRITE(13,*) Q_int_vect(y,:)/1000
455 END DO
456 WRITE(13,*) "Engine Thermal Efficiency:"
457 DO xx = 1, SIZE(eta_th_vect,1)
458     WRITE(13,*) eta_th_vect(xx,:)
459 END DO
460 WRITE(13,*) "------------------------------------------------------------"
461 WRITE(13,*) "************************************************************"
462 WRITE(13,*) "------------------------------------------------------------"
463 WRITE(13,*) "Beta_n of minimum EBSFC for each data set (columns in this
    case):"
464 WRITE(13,*) beta_n_ebsfc
465 WRITE(13,*)
466 WRITE(13,*) "Lambda of minimum EBSFC for each data set (columns in this
    case):"
467 WRITE(13,*) lambda_ebsfc
468 WRITE(13,*)
469 WRITE(13,*) "Beta_n of maximum ESPWR for each data set (columns in this
    case):"
470 WRITE(13,*) beta_n_espwr
471 WRITE(13,*)
```

```
472 WRITE(13,*) "Lambda of maximum ESPWR for each data set (columns in this
       case):"
473 WRITE(13,*) lambda_espwr
474 WRITE(13,*)
475 WRITE(13,*) "EBSFC for beta_n of minimum EBSFC for each data set (
       columns in this case) [kg/kWh]:"
476 WRITE(13,*) EBSFC_vect_min
477 WRITE(13,*)
478 WRITE(13,*) "ESPWR for beta_n of minimum EBSFC for each data set (
       columns in this case) [kJ/kg]:"
479 WRITE(13,*) ESPWR_vect_min/1000
480 WRITE(13,*)
481 WRITE(13,*) "Q_reg for beta_n of minimum EBSFC for each data set (
       columns in this case) [kJ/kg]:"
482 WRITE(13,*) Q_reg_min/1000
483 WRITE(13,*)
484 WRITE(13,*) "Q_int for beta_n of minimum EBSFC for each data set (
       columns in this case) [kJ/kg]:"
485 WRITE(13,*) Q_int_min/1000
486 WRITE(13,*)
487 WRITE(13,*) "Thermal Efficiency for beta_n of minimum EBSFC for each
       data set (columns in this case):"
488 WRITE(13,*) eta_th_min
489 WRITE(13,*)
490 WRITE(13,*) "------------------------------------------------------------"
491 WRITE(13,*)
492 WRITE(13,*) "EBSFC for beta_n of maximum ESPWR for each data set (
       columns in this case) [kg/kWh]:"
493 WRITE(13,*) EBSFC_vect_max
494 WRITE(13,*)
495 WRITE(13,*) "ESPWR for beta_n of maximum ESPWR for each data set (
       columns in this case) [kJ/kg]:"
496 WRITE(13,*) ESPWR_vect_max/1000
497 WRITE(13,*)
498 WRITE(13,*) "Q_reg for beta_n of maximum ESPWR for each data set (
       columns in this case) [kJ/kg]:"
499 WRITE(13,*) Q_reg_max/1000
500 WRITE(13,*)
501 WRITE(13,*) "Q_int for beta_n of maximum ESPWR for each data set (
       columns in this case) [kJ/kg]:"
502 WRITE(13,*) Q_int_max/1000
503 WRITE(13,*)
504 WRITE(13,*) "Thermal Efficiency for beta_n of maximum ESPWR for each
       data set (columns in this case):"
505 WRITE(13,*) eta_th_max
506 CLOSE(13)
507 WRITE(*,*) "***Task completed***"
508 WRITE(*,*) "Press ENTER to close this window."
509 READ(*,*)
510 100 FORMAT(/) !New line
511 101 FORMAT(2/) !Skip first 3 lines
512 STOP
513 END PROGRAM turboprop_reg
514 !------------------------------------------------------------------------
515 !Subroutine
516 !------------------------------------------------------------------------
517 SUBROUTINE SAM !Air temperature, pressure and density as a function of
       altitude z, using the Standard Atmospheric Model
```

```
518 USE ambient
519 IMPLICIT NONE
520 REAL*8 :: h
521 h=z/1000
522 IF (h <= 86) THEN !Considering variation of air composition above 86km
523     R_a = 8314.46262/28.96
524 ELSE
525     R_a = 8314.46262/28.40
526 END IF
527 IF (h < 11.019 .AND. h >= 0) THEN !Computing air T and P
528     T_0 = 288.15 + ((-6.5)*(h))
529     P_0 = 101.33*((288.15/(288.15 + ((-6.5)*(h))))**(34.17/(-6.5)))
530     P_0 = P_0*1000
531 ELSE IF (h >= 11.019 .AND. h < 20.063) THEN
532     T_0 = 216.65
533     P_0 = 22.64*(EXP((((-34.17)*(h-11.019))/216.65)))
534     P_0 = P_0*1000
535 ELSE IF (h >= 20.063 .AND. h < 32.162) THEN
536     T_0 = 216.65 + (h-20.063)
537     P_0 = 5.474*((216.65/(216.65 + (h-20.063)))**(34.17))
538     P_0 =P_0*1000
539 ELSE IF (h >= 32.162 .AND. h < 47.351) THEN
540     T_0 = 228.65 + ((2.8)*(h-32.162))
541     P_0 = 0.8680*((228.65/(228.65 + ((2.8)*(h-32.162))))**(34.17/(2.8)))
542     P_0 = P_0*1000
543 ELSE IF (h >= 47.351 .AND. h < 51.413) THEN
544     T_0 = 270.65
545     P_0 = 0.1109*(EXP((((-34.17)*(h-47.351))/270.65)))
546     P_0 = P_0*1000
547 ELSE IF (h >= 51.413 .AND. h < 71.802) THEN
548     T_0 = 270.65 + ((-2.8)*(h-51.413))
549     P_0 = 0.006694*((270.65/(270.65 + ((-2.8)*(h-51.413))))
        **(34.17/(-2.8)))
550     P_0 = P_0*1000
551 ELSE IF (h >= 71.802 .AND. h < 86) THEN
552     T_0 = 214.65 + ((-2.0)*(h-71.802))
553     P_0 = 0.003957*((214.65/(214.65 + ((-2.0)*(h-71.802))))
        **(34.17/(-2.0)))
554     P_0 = P_0*1000
555 ELSE IF (h >= 86 .AND. h < 92) THEN
556     T_0 = 186.95
557     P_0 = 0.0003733*(EXP((((-34.17)*(h-86))/186.95)))
558     P_0  = P_0*1000
559 ELSE IF (h >= 92 .AND. h <= 100) THEN
560     T_0 = 186.95 + ((1.03)*(h-92))
561     P_0 = 0.0001288*((186.95/(186.95 + ((1.03)*(h-92))))**(34.17/(1.03))
        )
562     P_0 = P_0*1000
563 ELSE
564     WRITE(*,*) "ERROR: Incorrect altitude (0 <= Z <= 100 km)"
565     WRITE(*,*) "Press ENTER to close this window."
566     READ(*,*)
567     STOP
568 END IF
569 rho_0 = P_0/(R_a*T_0)
570 END SUBROUTINE SAM
```

Here below how the code looks like when running:

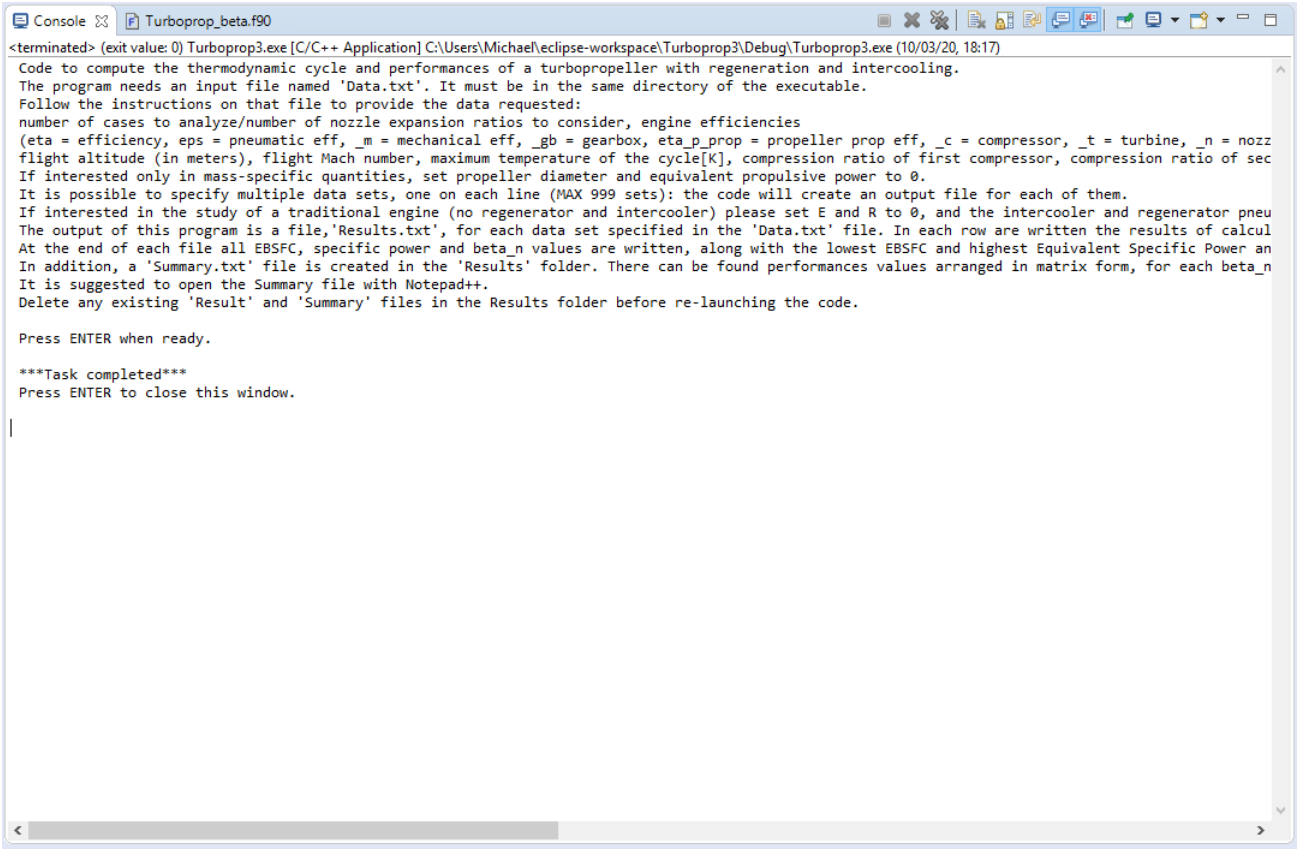

Figure 3.6: Terminal view (Eclipse [13]) of the code running

Chapter 4

Numerical simulation

As soon as the code described in chapter 3 has been developed, the tool needed to simulate the engine behaviour was finally available.

It was of interest to numerically evaluate the performances of the engine with and without heat exchange, to confront those performances, and to assess the effect of different parameters.

It was also of interest to assess how the performances vary with the nozzle expansion ratio, which β_n value generally gives the best performances and the effect of heat exchange and other parameters on it.

Finally, it was also studied the effect of intercooling and regeneration, alone and combined, on the performances. This was done in order to have an insight on the effect of the degree of regeneration/intercooling effectiveness on the performances and also to assess when heat exchange really improves the performances, in different conditions, and how intercooling and regeneration affect each other.

The simulation was done using the code described in section 3.2.3. Different input files, each with several cases, were used in order to be able to easily obtain different plots of the performances for different conditions, both for a traditional engine and for one with heat exchange:

- Performances vs overall compression ratio β_c
- Performances vs β_n
- Performances vs E and/or R
- β_n of minimum $EBSFC$/maximum equivalent specific power vs β_c

The engine components' efficiencies used in the simulation are those reported in table 3.1.

4.1 Results

In this section are reported the results of the numerical simulation in form of plots, generated using an ad hoc Matlab [53] script.

Performances were computed for the following β_c, β_n, E and R values:

- β_c: from 6 to 45, in steps of 3

- β_n: from 1 to 2, in steps of 0.1
- E and R: from 0 to 1, in steps of 0.1

4.1.1 Determination of the best β_n condition

In order to produce plots of the performances as a function of β_c it is necessary to fix a value for the nozzle expansion ratio β_n.

Since when dealing with intercooling and regeneration the parameter of most interest is the specific fuel consumption, it was decided to use in the simulation the β_n that gives the minimum $EBSFC$.

To that end, for each operating condition the performances were computed for different β_n values in order to determine which o them gives the lowest $EBSFC$.

As can be seen in fig. 4.1, 4.2 and 4.3, for turbopropellers' typical β_c values (~ 15) and operating conditions the β_n value that minimizes the specific fuel consumption is 1.2.

It can be observed also that in presence of intercooling and regeneration (fig. 4.1 and 4.2) the β_n value that minimizes the specific fuel consumption assumes higher values as β_c, E and R increase. In fact, as β_c increases, the temperature at which the air exits the compression increases and thus the heat that can be recovered with regeneration decreases. For this reason it is convenient to expand less in the power turbine in order to have combustion gases at a higher temperature. Similarly, as R increases the combustion gases can be cooled to a lower temperature and therefore it is beneficial to have combustion gases entering the regenerator at an higher temperature.

In the case of a traditional engine (fig. 4.3), the optimal β_n value remains equal to 1.2 as the β_c increases, except for very small β_c values, where the kinetic energy of the combustion gases is particularly low and thus is more beneficial to expand in the power turbine. In fact, starting from β_c values ~ 12, an increment in the compression ratio yields lower Δh_{av} values and so the optimal λ value decreases, according to eqn. 2.38. But also the λ value at which the engine operates decreases, if β_n is kept constant. So, in the end, it is consistent that the optimal β_n remains more or less the same for most β_c values.

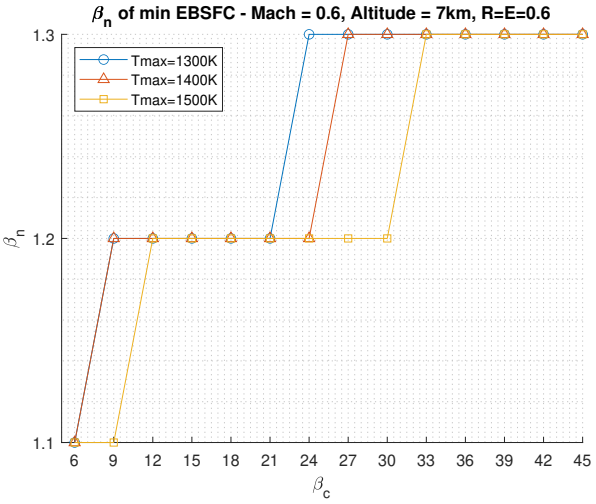

Figure 4.1: Optimal β_n - $R/E = 0.6$

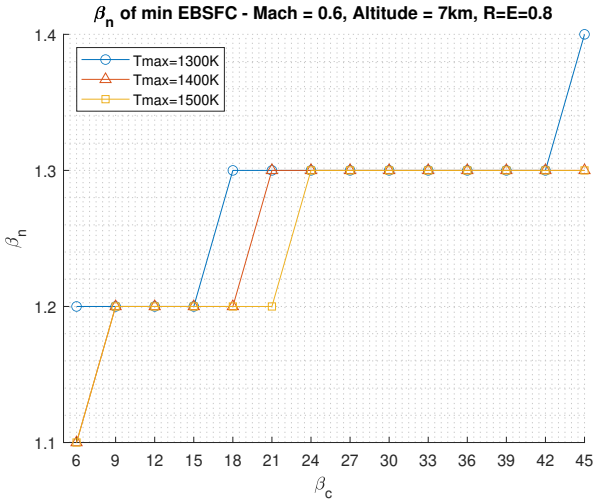

Figure 4.2: Optimal β_n - $R/E = 0.8$

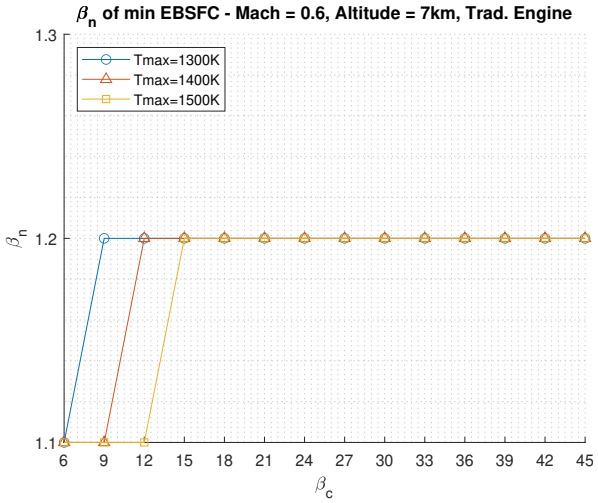

Figure 4.3: Optimal β_n - $R/E = 0$

It can be observed that the minimum $EBSFC$ and the maximum equivalent specific power are not obtained for the same β_n value, except for the case of a traditional engine (fig. 4.4 and 4.5). In fact, in presence of regeneration it is beneficial in terms of specific equivalent power to expand more in the power turbine (optimal $\beta_n = 1.1$) with respect to the optimal condition in terms of specific fuel consumption (optimal $\beta_n = 1.2$), since the gases exiting the regenerator are at low temperature and therefore the nozzle contribution to the equivalent specific power is lower.

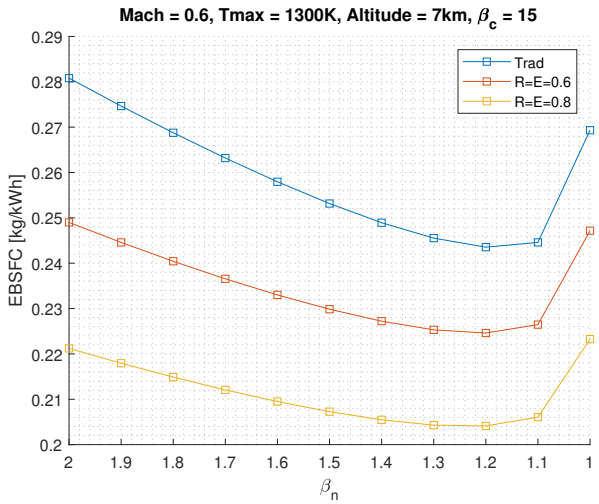

Figure 4.4: $EBSFC - \beta_n$

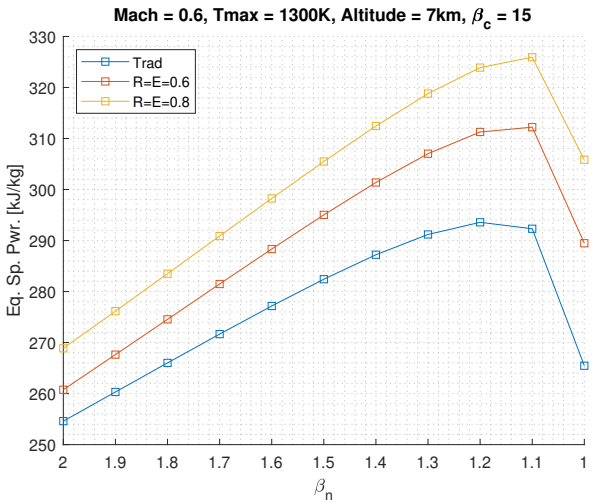

Figure 4.5: Power$-\beta_n$

4.1.2 Performances vs β_c

Once the β_n value was set, it was possible to produce plots of the performances as a function of β_c.

Here below are reported the plots for $EBSFC$, equivalent specific power and thermal efficiency. In each plot can be found three curves. The blue one corresponds to a traditional engine, i.e. without intercooling and regeneration. The red and yellow curves instead correspond to an engine with intercooling and regeneration with parameters E and R each equal to 0.6 (red curve) and 0.8 (yellow curve). Plots of the performances are reported for

different operating conditions. First of all, it was decided a reference operating regime, typical of turbopropeller engines. Then the performances were recomputed for different flight Mach numbers, maximum temperature of thermodynamic cycle and flight altitude. The parameters were modified one at a time with respect to the reference condition.

Here below the values considered in the simulation:

- Reference condition: $T_{max} = 1300K$, flight Mach number = 0.6, flight altitude = 7000m
- Other T_{max} values considered: 1400K, 1500K
- Other flight altitude values considered: 5000m, 10000m
- Other Mach number values considered: 0.5, 0.7

EBSFC

Here below the $EBSFC - \beta_c$ plots:

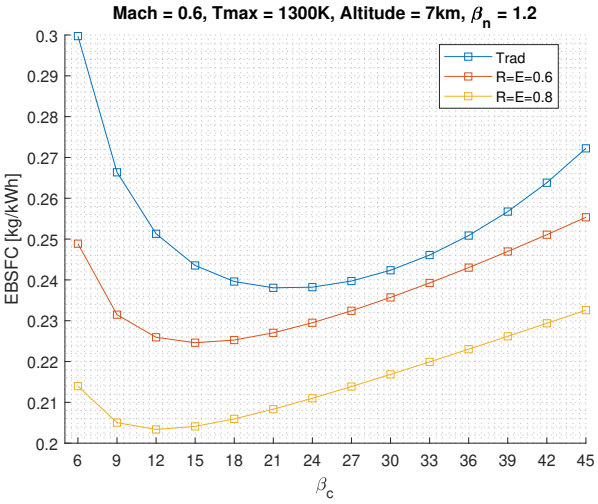

Figure 4.6: $EBSFC - \beta_c$, reference

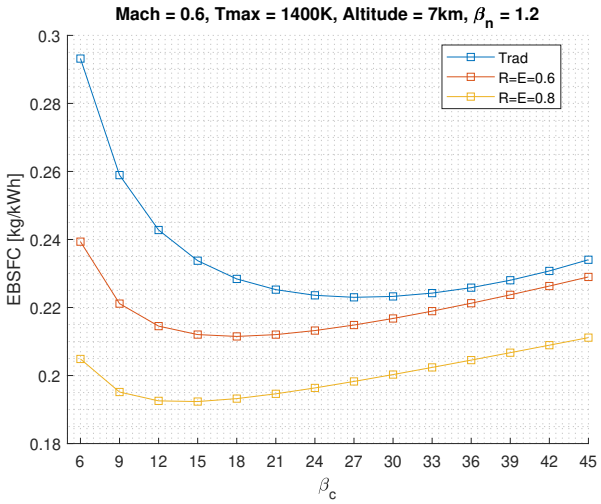

Figure 4.7: $EBSFC - \beta_c$, T_{max} (a)

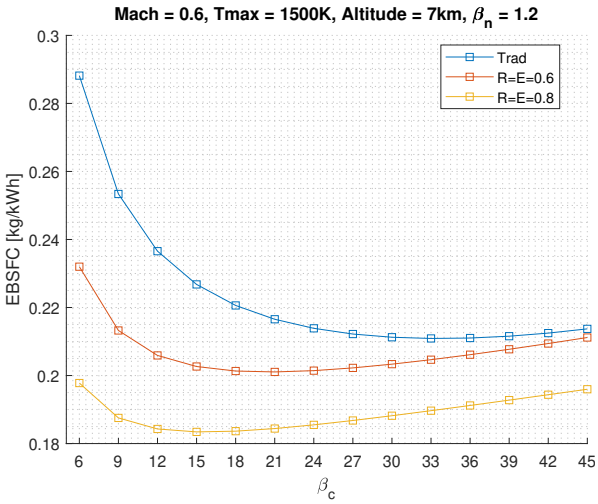

Figure 4.8: $EBSFC - \beta_c$, T_{max} (b)

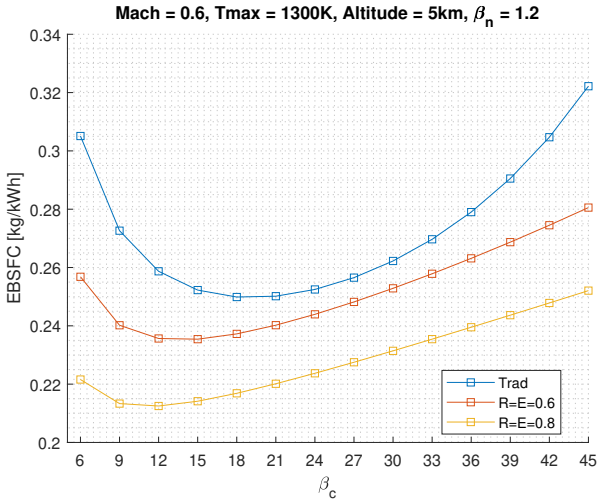

Figure 4.9: $EBSFC - \beta_c$, alt. (a)

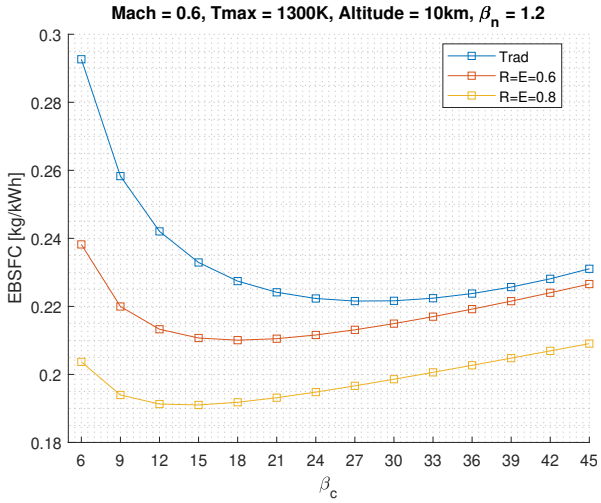

Figure 4.10: $EBSFC - \beta_c$, alt. (b)

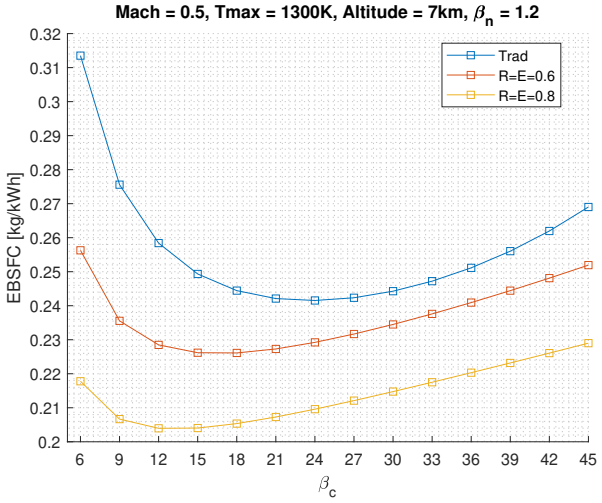

Figure 4.11: $EBSFC - \beta_c$, M (a)

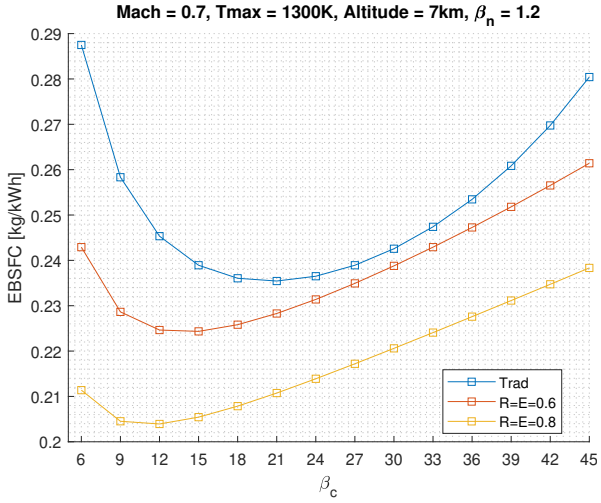

Figure 4.12: $EBSFC - \beta_c$, M (b)

From the curves above it is possible to make the following considerations:

- As T_{max} increases: $EBSFC$ decreases, is less sensitive to β_c and the minimum $EBSFC$ value is obtained at higher β_c values (see fig. 4.7, 4.8)
- As flight altitude increases: $EBSFC$ decreases, tends to grow less at high β_c and the minimum $EBSFC$ value is obtained at higher β_c values (see fig. 4.9, 4.10)
- As flight Mach number increases: $EBSFC$ decreases a bit, but is more sensitive to β_c and thus is higher at high β_c values. This effect is less evident as R and E increase. Additionally, the the minimum $EBSFC$ value is obtained at lower β_c values (see fig. 4.11, 4.12)

It is observed that the specific fuel consumption decreases as R and E increase, for each condition and β_c values considered. Also, as R increases the minimum specific fuel consumption is obtained for lower β_c values. The biggest fuel saving with respect to the traditional engine is obtained for medium-low β_c values, which are often adopted in turbopropellers.

It is also important to note that the fuel consumption reduction depends heavily on R/E and that in the presence of heat exchange the minimum $EBSFC$ value is obtained at lower β_c values with respect to the traditional engine.

Equivalent specific power

Here below the equivalent specific power$-\beta_c$ plots:

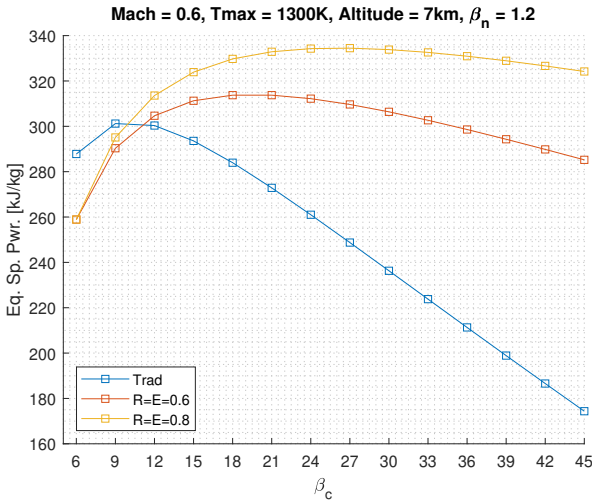

Figure 4.13: Power$-\beta_c$, reference

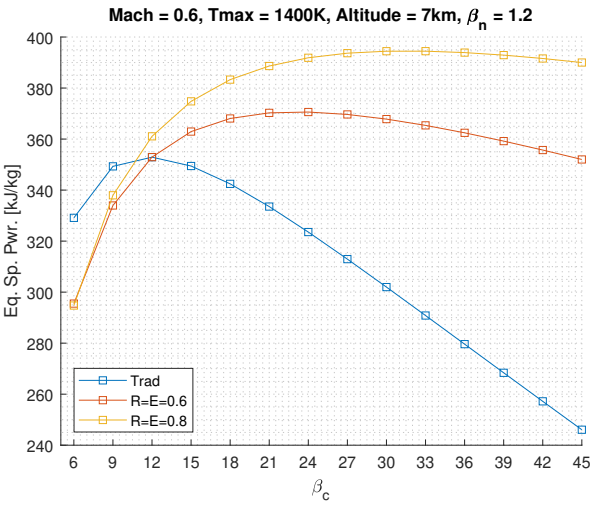

Figure 4.14: Power$-\beta_c$, T_{max} (a)

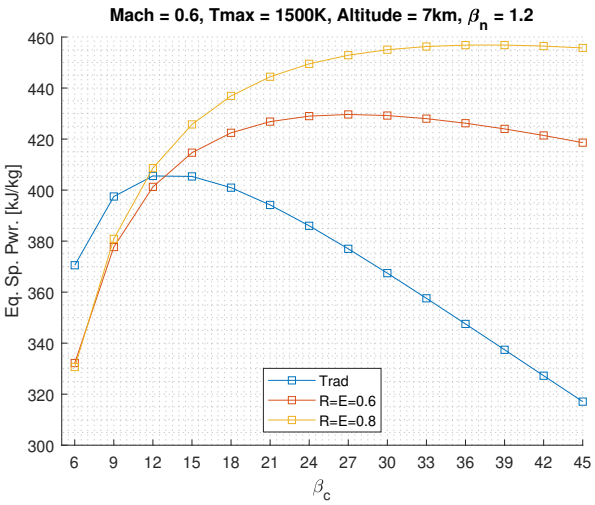

Figure 4.15: Power$-\beta_c$, T_{max} (b)

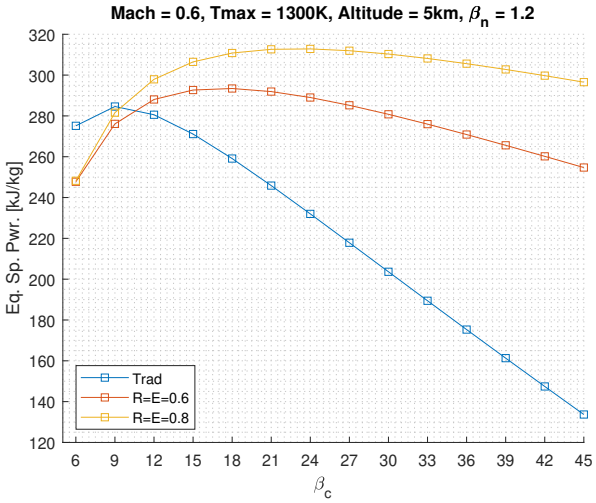

Figure 4.16: Power$-\beta_c$, alt. (a)

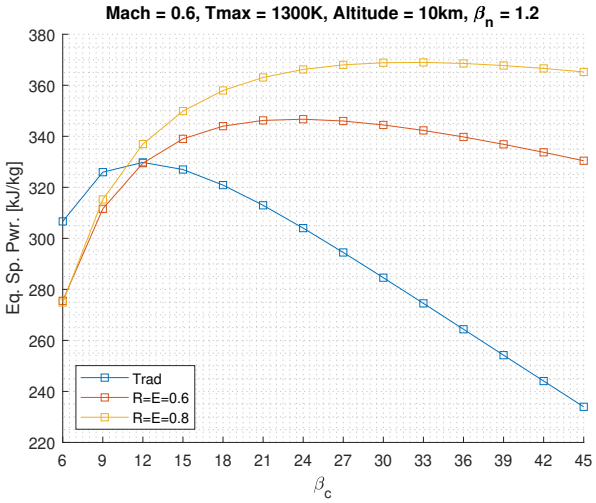

Figure 4.17: Power$-\beta_c$, alt. (b)

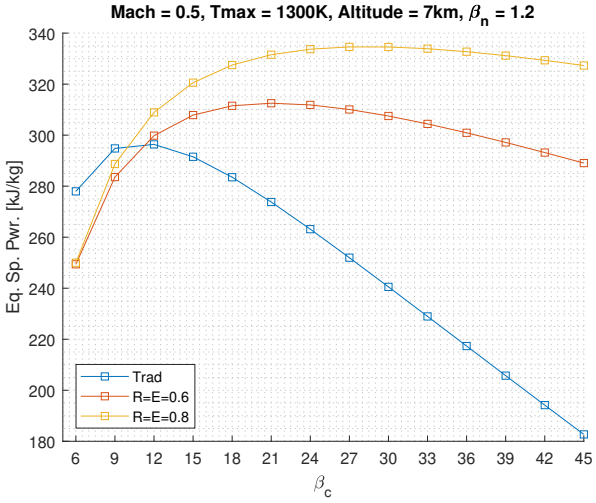

Figure 4.18: Power$-\beta_c$, M (a)

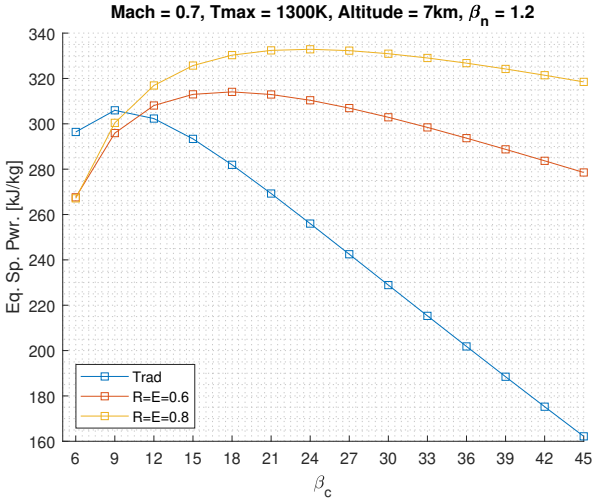

Figure 4.19: Power$-\beta_c$, M (b)

From the curves above it is possible to make the following considerations:

- As T_{max} increases: equivalent specific power increases sensibly and its maximum value is obtained at higher β_c values (see fig. 4.14, 4.15)
- As flight altitude increases: equivalent specific power increases and its maximum value is obtained at higher β_c values (see fig. 4.16, 4.17)
- As flight Mach number increases: equivalent specific power's maximum value is obtained at lower β_c values. Additionally, its sensitivity to β_c increases: higher specific powers are obtained at very low β_c values and slightly lower specific powers are obtained at very high β_c values (see fig. 4.18, 4.19)

It is observed that for very low β_c values a traditional engine yields higher equivalent specific powers with respect to an engine with heat exchange, since the pressure losses introduces by the heat exchangers are not compensated by the reduction of the compression work due to intercooling. This effect is bigger when E/R are low.

On the other hand, starting from $\beta_c \sim 10$ the engine with intercooling and regeneration yields higher equivalent specific powers with respect to the traditional engine, increasing as E/R increase, since as E increases the power required by the compression process decreases.

It is also observed that in the presence of heat exchange the maximum equivalent specific power value is obtained at higher β_c values with respect to the traditional engine. Since the minimum $EBSFC$ values instead is obtained at lower β_c values, it is impossible to operate at a point optimal both in terms of fuel consumption and power output: a choice or a trade-off must be made.

Thermal efficiency

Here below the $\eta_{th} - \beta_c$ plots:

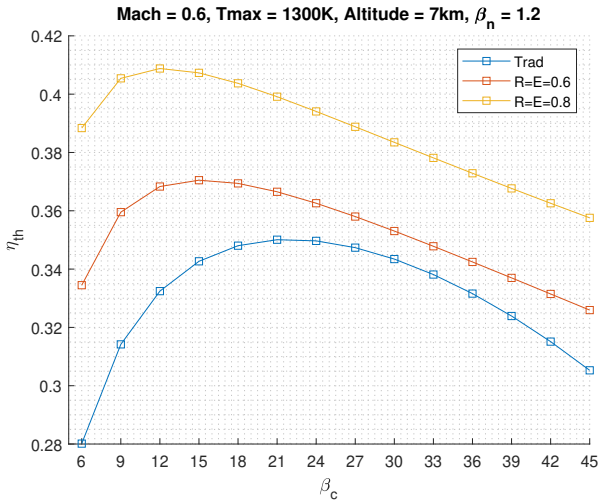

Figure 4.20: $\eta_{th} - \beta_c$, reference

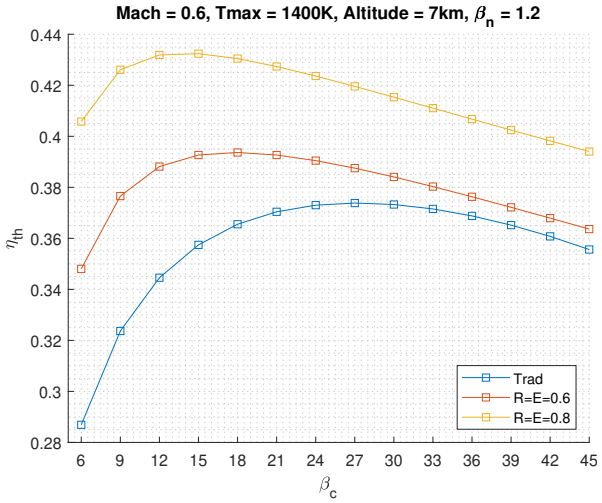

Figure 4.21: $\eta_{th} - \beta_c$, T_{max} (a)

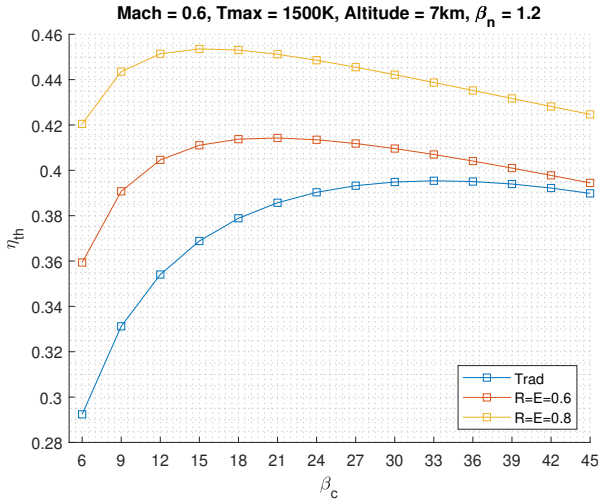

Figure 4.22: $\eta_{th} - \beta_c$, T_{max} (b)

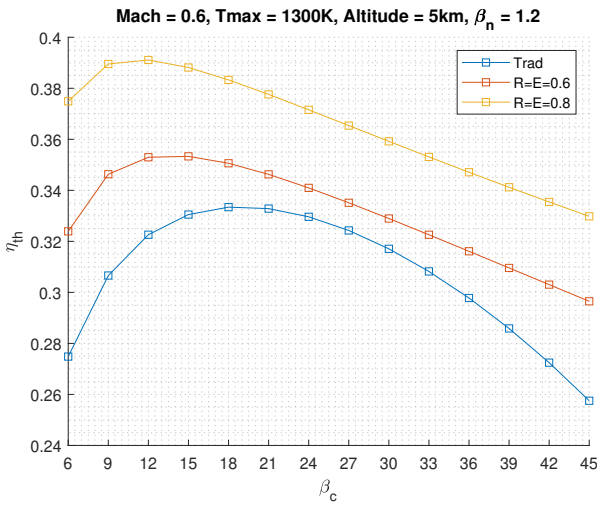

Figure 4.23: $\eta_{th} - \beta_c$, alt. (a)

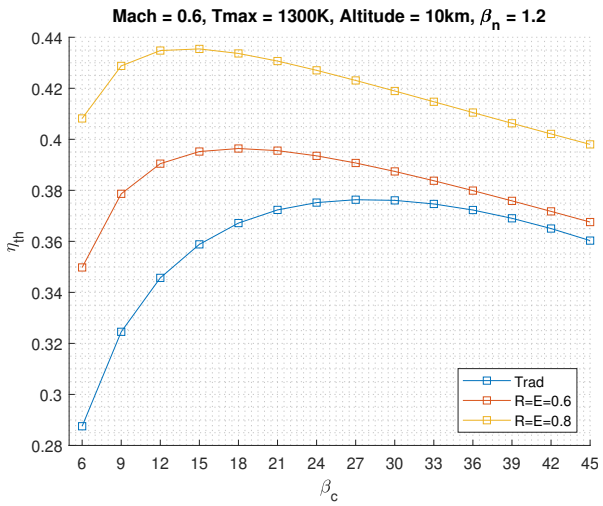

Figure 4.24: $\eta_{th} - \beta_c$, alt. (b)

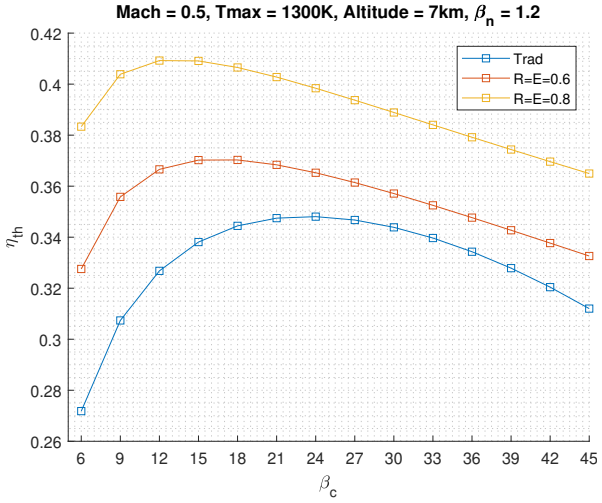

Figure 4.25: $\eta_{th} - \beta_c$, M (a)

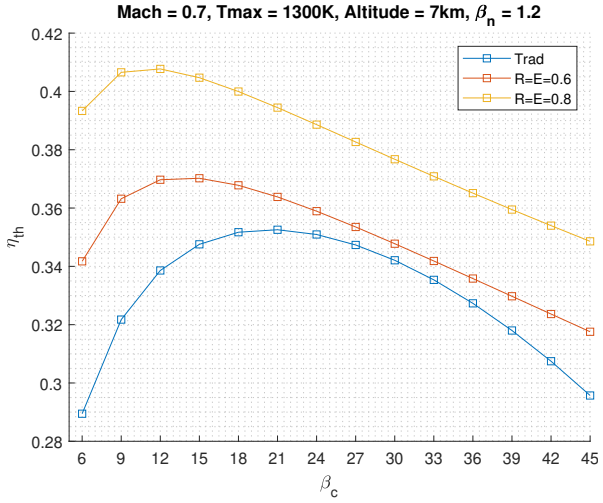

Figure 4.26: $\eta_{th} - \beta_c$, M (b)

From the curves above it is possible to make the following considerations:

- As T_{max} increases: η_{th} increases, its maximum value is obtained at higher β_c values and it decreases less at high β_c values (see fig. 4.21, 4.22)
- As flight altitude increases: η_{th} increases, its maximum value is obtained at higher β_c values and it decreases less at high β_c values (see fig. 4.23, 4.24)
- As flight Mach number increases: η_{th} slightly increases at very low β_c values, but decreases at very high β_c values. Additionally, its maximum value is obtained at slightly lower β_c values (see fig. 4.25, 4.26)

It is observed that the thermal efficiency of the engine with intercooling and regeneration is always higher with respect to the traditional engine, for all the cases considered. Similarly to the $EBSFC$, the maximum difference between the engine with heat exchange and the tradtional one, in terms of η_{th}, is obtained at medium-low β_c values. As the compression ratio increases, since the possibility of regeneration decreases, the difference between the

engine with interccoling and regeneration and the traditional one decreases. As a result, for low R/E values and high β_c values it might be more convenient to use a traditional engine, in terms of thermal efficiency: as for the $EBSFC$, η_{th} heavily depends on R and E.

4.1.3 Performances vs E and R

In this section are reported the plots of $EBSFC$, equivalent specific power and η_{th} as a function of E, R and $E + R$.

This analysis has the scope to study the effects of intercooling and regeneration on the engine performances, both alone and together, in order to be able to evaluate how the two systems interact with each other.

The curves in the plots refer to two different T_{max} values (1300K and 1500K), but similar results are obtained if different flight Mach numbers and altitudes are considered.

EBSFC

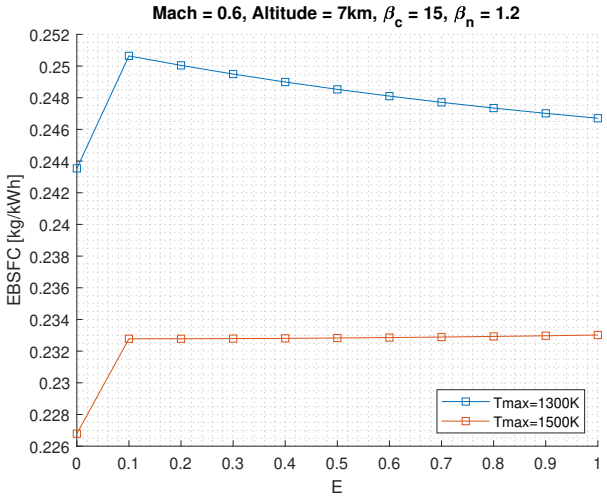

Figure 4.27: $EBSFC - E$, T_{max}

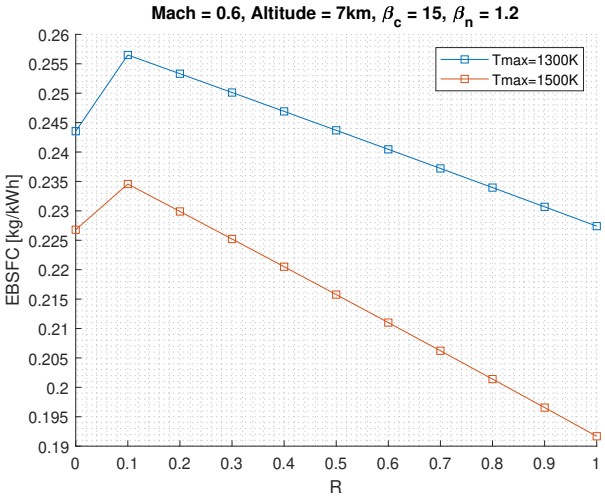

Figure 4.28: $EBSFC - R$, T_{max}

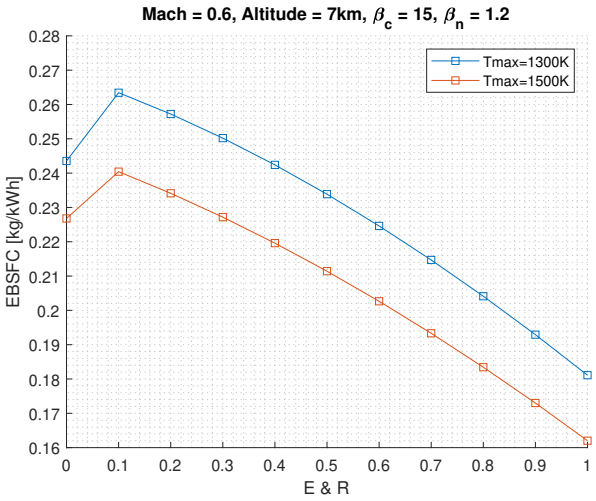

Figure 4.29: $EBSFC - E/R$, T_{max}

From the curves above it is possible to make the following considerations:

- $EBSFC$ vs E (fig. 4.27): with the introduction of intercooling ($E \neq 0$) there is an initial increment of the specific fuel consumption due to the pressure losses introduced by the heat exchanger. Subsequently, as E increases, it is observed a light decrement of the $EBSFC$ for lower T_{max} values, while for higher values there is a very faint increment. In fact, intercooling increases the heat that must be provided to the fluid in the combustion chamber in order to reach the desired T_{max}, since the temperature at which the air exits from the compressors is lower. So, for high T_{max} values the additional heat that must be provided in the combustion chamber is greater than the work saved in the compression process

- $EBSFC$ vs R (fig. 4.28): also here with the introduction of regeneration ($R \neq 0$) there is an initial increment of the specific fuel consumption due to the pressure losses introduced by the heat exchanger. Subsequently, as R increases, the $EBSFC$ decreases linearly. As T_{max} increases, its sensitivity with respect to R increases

- $EBSFC$ vs E/R (fig. 4.29): when both regeneration and intercooling are present, the $EBSFC$ decreases with R/E, but not linearly anymore. It is observed that at lower T_{max} values it is obtained a better specific fuel consumption with respect to the traditional engine ($E/R = 0$) starting from lower E/R values, with respect to the case of regeneration only. Furthermore, with respect to the case of regeneration only, at high E/R values are obtained lower $EBSFC$ values, while at low E/R values are obtained higher $EBSFC$ values

In general, it is observed that a reduction in the specific fuel consumption, with respect tot he traditional engine, is not guaranteed. In fact, for low E/R values ($< 0.3 - 0.4$) the effect of the pressure losses introduced by the heat exchangers is greater than the benefits they provide. It is then of paramount importance to be able to guarantee high E/R values, otherwise the specific fuel consumption worsens instead of improving.

Equivalent specific power

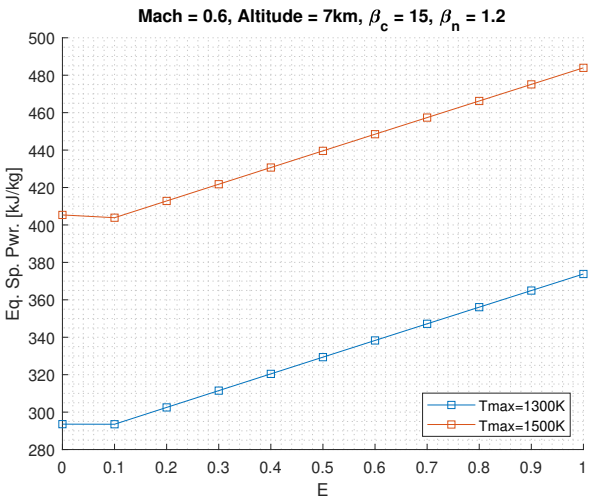

Figure 4.30: Power$-E$, T_{max}

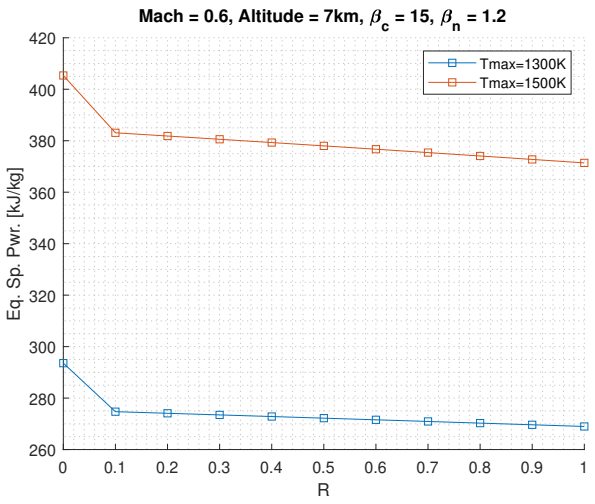

Figure 4.31: Power$-R$, T_{max}

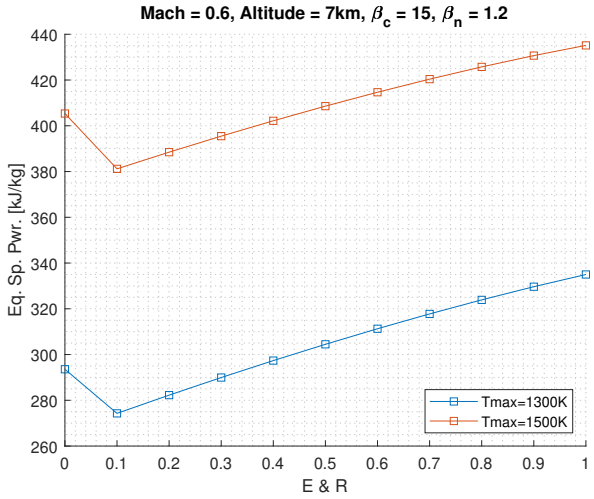

Figure 4.32: Power$-E/R$, T_{max}

From the curves above it is possible to make the following considerations:

- Equivalent specific power vs E (fig. 4.30): with the introduction of intercooling ($E \neq 0$) there is an initial faint decrement of the equivalent specific power due to the pressure losses introduced by the heat exchanger. Subsequently, as E increases, the equivalent specific power increases linearly, thanks to the reduction of the work absorbed by the compression process

- Equivalent specific power vs R (fig. 4.31): also here with the introduction of regeneration ($R \neq 0$) there is an initial decrement of the equivalent specific power due to the pressure losses introduced by the heat exchanger. Subsequently, as R increases, the equivalent specific power decreases linearly, since the combustion gases at the nozzle entrance are at lower temperatures

- Equivalent specific power vs E/R (fig. 4.32): when both regeneration and intercooling are present, the equivalent specific power increases with R/E, but less than the case with intercooling only. It is observed that by combining intercooling and regeneration it is possible to obtain an higher equivalent specific power with respect to the traditional engine, which is impossible when only regeneration is implemented

In general, it is observed that it is obtained an higher equivalent specific power with respect to the traditional engine starting from E/R values greater than ~ 0.4. As for the $EBSFC$, it is of paramount importance to be able to guarantee high E/R values in order to have an improvement with respect to the traditional engine.

Thermal efficiency

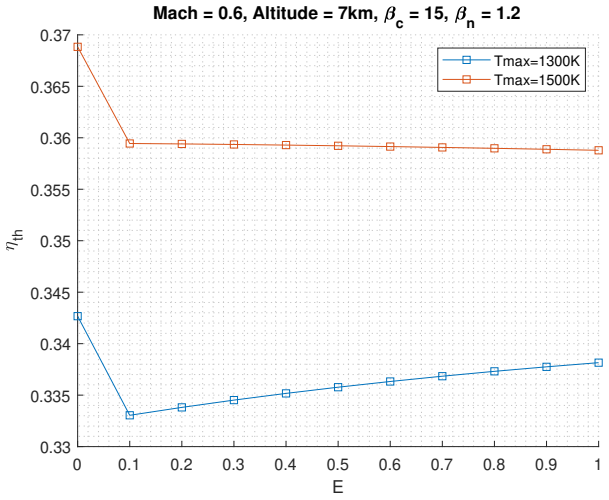

Figure 4.33: $\eta_{th} - E$, T_{max}

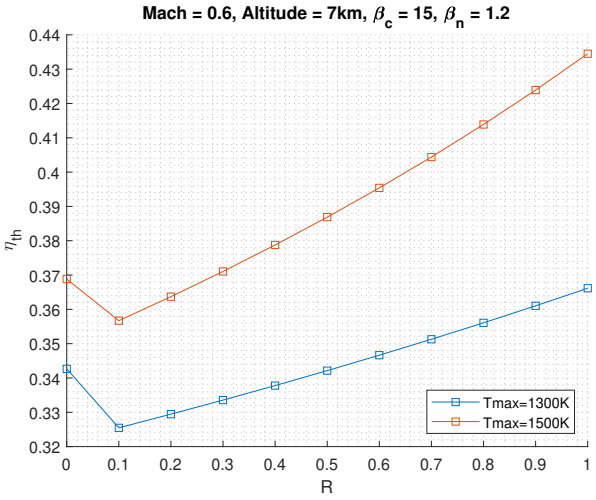

Figure 4.34: $\eta_{th} - R$, T_{max}

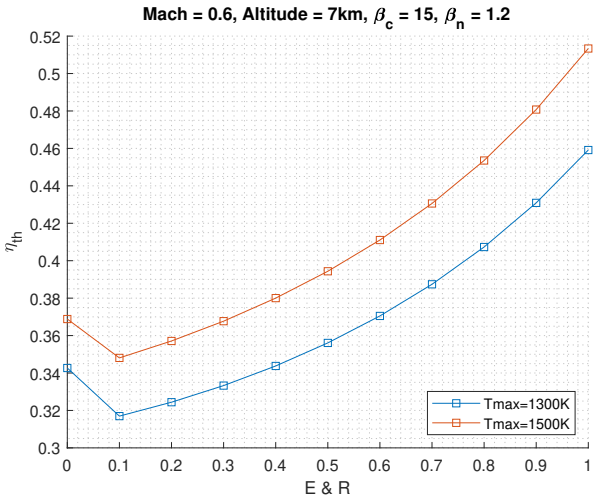

Figure 4.35: $\eta_{th} - E/R$, T_{max}

From the curves above it is possible to make the following considerations:

- η_{th} vs E (fig. 4.33): with the introduction of intercooling ($E \neq 0$) there is an initial decrement of η_{th} due to the pressure losses introduced by the heat exchanger. Subsequently, as E increases, it is observed a light increment of η_{th} for lower T_{max} values, while for higher values there is a very faint decrement. In fact, intercooling increases the heat that must be provided to the fluid in the combustion chamber in order to reach the desired T_{max}, since the temperature at which the air exits from the compressors is lower. So, for high T_{max} values the additional heat that must be provided in the combustion chamber is greater than the work saved in the compression process

- η_{th} vs R (fig. 4.34): also here with the introduction of regeneration ($R \neq 0$) there is an initial decrement of η_{th} due to the pressure losses introduced by the heat

exchanger. Subsequently, as R increases, η_{th} increases linearly. As T_{max} increases, its sensitivity with respect to R increases.

- η_{th} vs E/R (fig. 4.35): when both regeneration and intercooling are present, η_{th} increases with R/E (not linearly) up to higher values with respect to the case of regeneration only.

In general, it is observed that it is obtained an higher η_{th} with respect to the traditional engine starting from E/R values greater than $\sim 0.3 - 0.4$.

Also, $EBSFC$ and η_{th} show a very similar behaviour, if is considered that $EBSFC$ improves when it decreases while η_{th} improves when it increases.

As for the $EBSFC$, it is of paramount importance to be able to guarantee high E/R values in order to have an improvement with respect to the traditional engine.

In figures 4.36 and 4.37 is shown the peculiar behaviour of η_{th} at different flight Mach numbers (0.5 and 0.7). While for different T_{max} and flight altitude values the different curves never cross, when considering different flight Mach numbers and regeneration the curves intersect.

In particular it observed that for high R or E/R values ($> 0.5 - 0.6$) higher η_{th} values are obtained at lower flight Mach number values, while at low R or E/R values higher η_{th} values are obtained at higher flight Mach number values. This does not happen when in presence of intercooling only (see fig 4.38).

This happens because at high R values it is more convenient to have air at the end of the compression at a lower temperature, since with regeneration it is possible to recover an high amount of heat (due to the high degree of regeneration). On the other hand, when the regeneration effectiveness is too low it is more convenient to exploit the higher air's total pressure deriving from an higher flight speed.

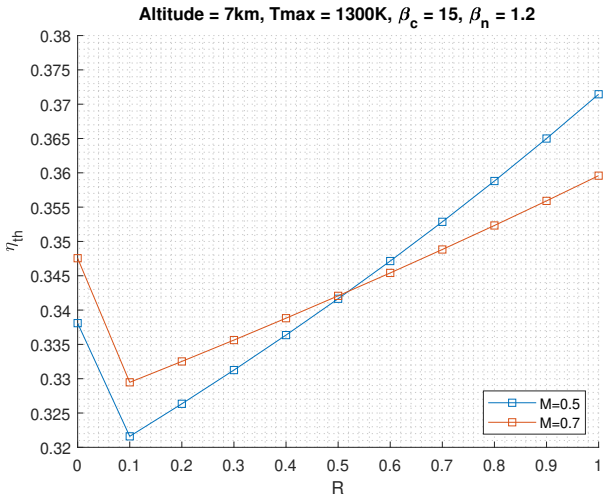

Figure 4.36: $\eta_{th} - R$, M

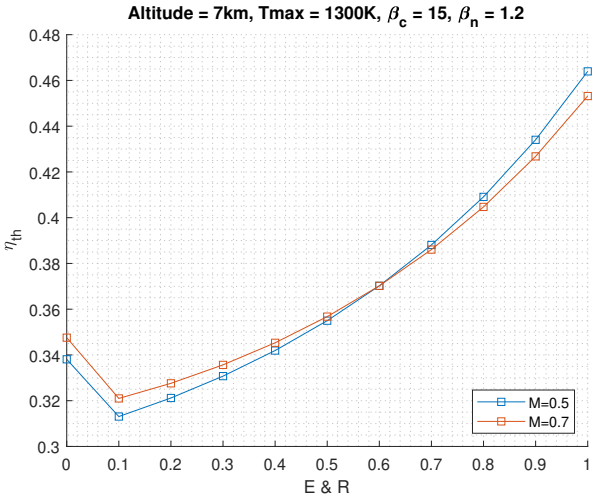

Figure 4.37: $\eta_{th} - E/R$, M

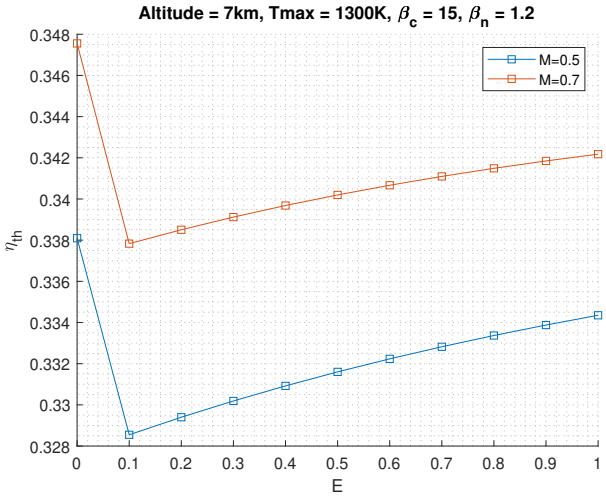

Figure 4.38: $\eta_{th} - E,\ M$

Comparison between regeneration, intercooling, and their simultaneous implementation

Finally, here below are presented plots of the engine's performance curves for different cases: traditional engine, engine with only regeneration, engine with only intercooling, intercooled and regenerated engine. This is done both in order to have an insight of the overall impact of the the two heat exchange techniques (both alone and together), and also as a mean to assess if the data is consistent with the theory.

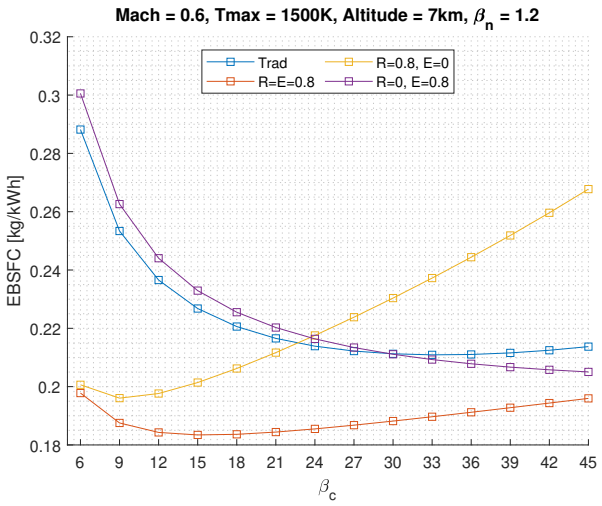

Figure 4.39: $EBSFC - \beta_c$, comparison

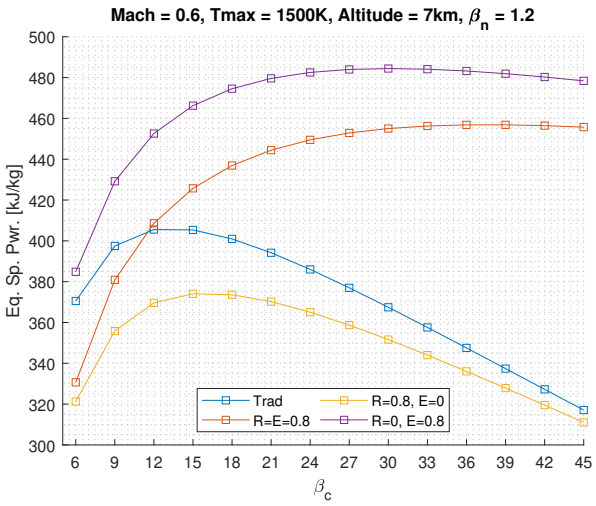

Figure 4.40: Power$-\beta_c$, comparison

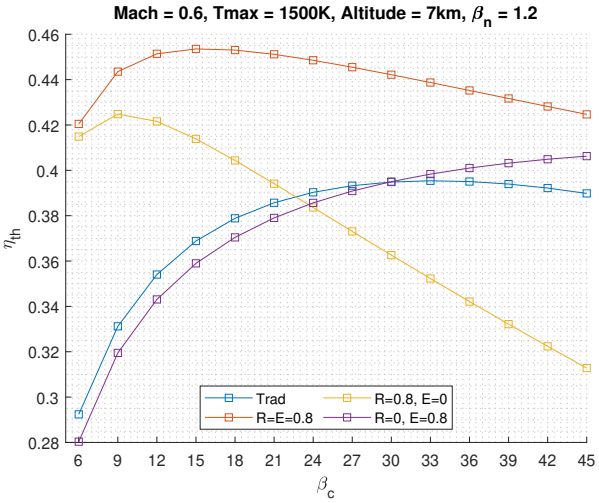

Figure 4.41: $\eta_{th} - \beta_c$, comparison

From the plots above it is possible to make the following considerations:

- Figure 4.39: the lowest $EBSFC$ is obtained by combining intercooling and regeneration. Implementing only regeneration, lower $EBSFC$ values with respect to the non-regenerated cases are obtained only for low compression ratios, since as β_c increases the heat that can be regenerated decreases. Furthermore, the minimum $EBSFC$ is obtained at lower β_c values with respect to the case of both intercooling and regeneration. The introduction of only intercooling yields slightly higher $EBSFC$ values with respect tot he traditional case, except for very high compression ratios. In fact, with intercooling the air delivered by the compressors is at a lower temperature, and therefore more fuel is needed to reach the desired turbine inlet temperature. This, along with the pressure losses introduced by the heat exchanger, overcompensates the increment in the useful power, except for high β_c values

- Figure 4.40: the highest equivalent specific power is obtained with intercooling only. In fact, in this way the additional pressure losses introduced by the heat exchangers are minimized and the useful power is maximized, since the compression process requires less power and no energy is extracted from the combustion gases. The lowest equivalent specific power is obtained with regeneration only. In fact, regeneration extracts energy from the combustion gases, which expand at a lower temperature in the nozzle, and also introduces pressure losses in the heat exchanger. Combining intercooling and regeneration it is possible to obtain very high power outputs, higher than those of the traditional engine starting from $\beta_c \sim 12$ and less sensitive to increments in the overall compression ratio

- Figure 4.41: the highest thermal efficiency is obtained with both intercooling and regeneration. Provided that E and R assume sufficiently high values, the reduction of the specific power needed for the compression and the reduction in the heat needed from combustion to reach the desired turbine inlet temperature grant the best engine efficiencies. The implementation of only regeneration yields higher efficiencies, with respect to the traditional case, only for medium-low β_c, since the efficiency of the regenerated thermodynamic cycle decreases rapidly as the compression ratio increases (see eqn. 2.2). Concerning the case of only intercooling, as anticipated in section

2.1, the efficiency is lower with respect to the traditional engine, except for high compression ratios

From these considerations, the data given by the simulations results consistent with the theory, in particular with what discussed in section 2.1.

It is also clear from these plots that the synergy between intercooling and regeneration is very strong, and thus they should be implemented together in order to obtain the best overall performances. In fact, their simultaneous implementation yields better fuel consumptions, better efficiencies, optimal conditions at higher compression ratio values with respect to regeneration only, and usually higher equivalent specific powers with respect to the traditional engine.

4.1.4 Performances vs ε_i and ε_r

It is now of interest to study how the pressure losses in the regenerator and intercooler affect the engine's performances. Figures 4.42, 4.43 and 4.44 report the results of this analysis.

The following considerations can be done (though it is not very clear by looking at the charts):

- the performances' sensitivity with respect to $\varepsilon_{i/r}$ decreases very slightly at higher $\varepsilon_{i/r}$ values
- $EBSFC$ and η_{th} sensitivity with respect to $\varepsilon_{i/r}$ decreases very slightly at higher R/E values, while equivalent specific power's sensitivity increases very slightly
- in these conditions, a 1% increment in both pneumatic efficiencies (e.g. from 0.95 to 0.96) yields a slightly more than 1% net improvement in the overall engine $EBSFC$, and approximately the same is valid for the equivalent specific power and thermal efficiency

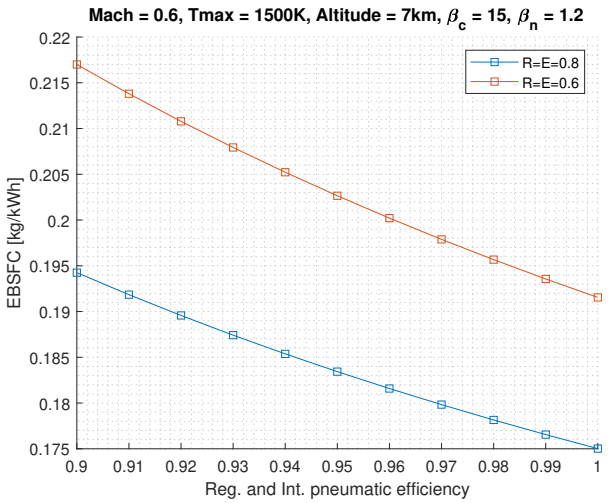

Figure 4.42: $EBSFC - \varepsilon_{i/r}$

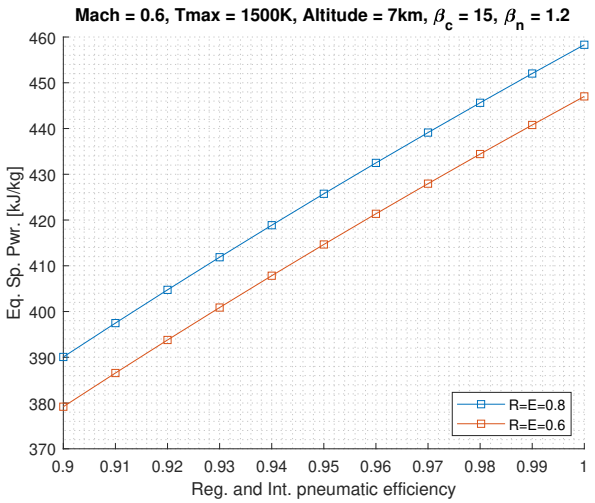

Figure 4.43: Power$-\varepsilon_{i/r}$

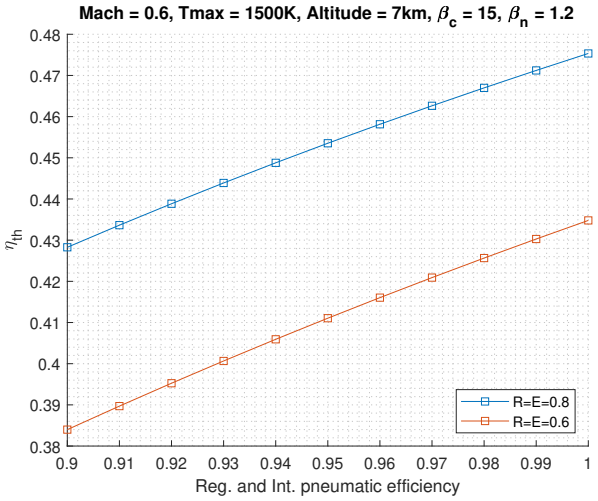

Figure 4.44: $\eta_{th} - \varepsilon_{i/r}$

So, it is observed that pressure losses in the heat exchangers have quite an impact on the overall engine performances. Thus, ε_i and ε_r are additional parameters on which to work in order to obtain ever improved engine performances. This highlights the key role that the heat exchangers' design has in the improvement of the engine performances: they must provide both high E/R and $\varepsilon_{i/r}$ values in order to fully exploit regeneration and intercooling potential.

4.1.5 Heat exchanged in the intercooler and regenerator

It is now of interest to study how the various parameters affect the heat exchanged (for unit of air mass flow rate) in the intercooler, Q_{int}, and in the regenerator, Q_{reg}. As it was done for the other engine's performances, the heats exchanged are presented for different β_c, E, R, E/R values and operating conditions. Concerning the operating conditions, the heat exchanged in the regenerator is reported only for different T_{max} values, while the heat exchanged in the intercooler is reported only for different flight altitudes.

Heat exchanged in the Intercooler

From the analysis it is observed that Q_{int} depends on the flight conditions (altitude and Mach number), but not from T_{max}, since the intercooler is ahead of the combustion chamber.

It increases as β_c increases, since the heat that can be exchanged in the intercooler increases due to the higher compressed air temperature. It decreases as the flight altitude increases (see fig. 4.45, 4.46), since the air entering the compressor is at a lower temperature and pressure. It slightly increases as the flight Mach number increases, since the air entering the compressor is at higher total temperature and pressure. It does no vary with β_n and R, since the intercooler is ahead both of the regenerator and nozzle. It increases linearly with E (see fig. 4.47).

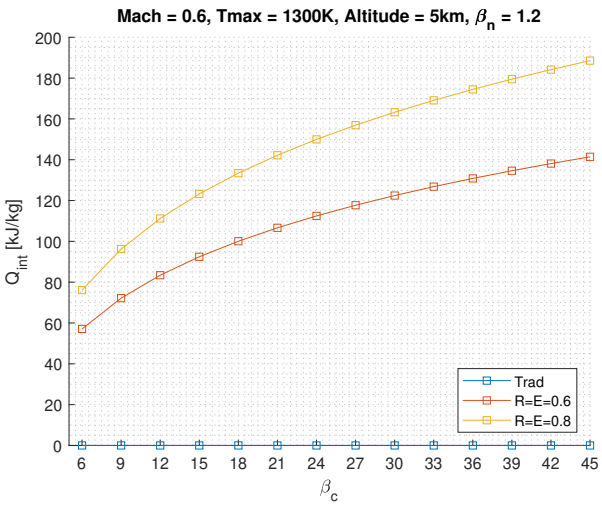

Figure 4.45: $Q_{int} - \beta_c$, alt. (a)

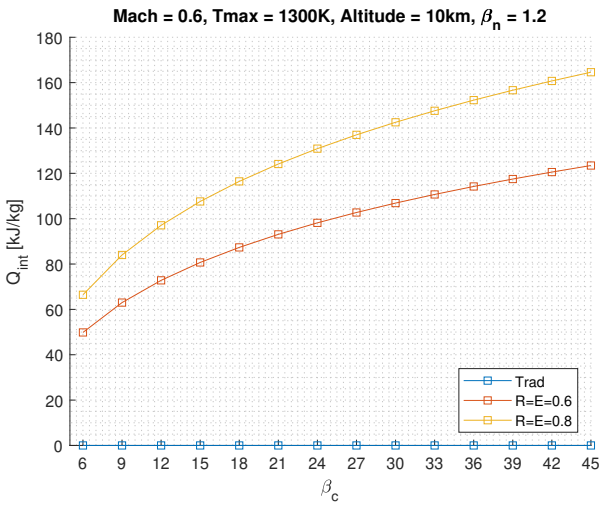

Figure 4.46: $Q_{int} - \beta_c$, alt. (b)

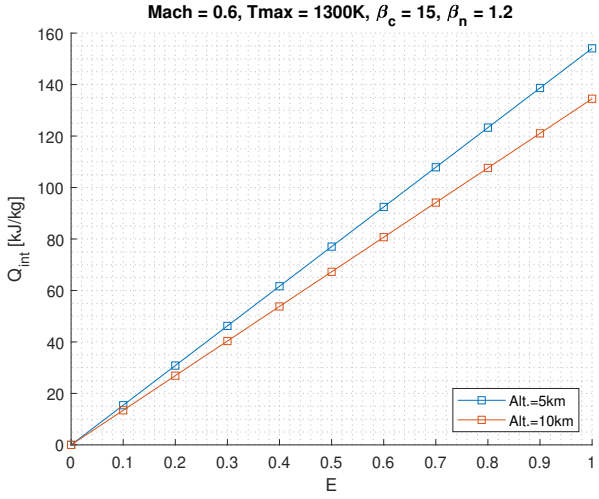

Figure 4.47: $Q_{int} - E$, alt.

Heat exchanged in the Regenerator

From the analysis it is observed that Q_{reg} depends both on the flight conditions (altitude and Mach number) and T_{max}, since the regenerator is placed after the combustion chamber.

It decreases as β_c increases, since the limits of regeneration are tighter due to the higher air temperature at the end of the compression process. It increases with the flight altitude, as the air coming from the compression is at a lower temperature (due to lower air temperature and pressure at the intake). It decreases with the flight Mach number, since the air coming from the compression is at an higher temperature (due to higher air total temperature and pressure at the intake). It increases with T_{max} (see fig. 4.48, 4.49), since the gas at the power turbine exit are at an higher temperature. It increases with β_n (see fig. 4.52), since the higher β_n is, the less the gases are expanded in the power turbine and thus are at an higher temperature.

It increases linearly with R (see fig. 4.50) and has a dependence on E (provided that $R \neq 0$) (see fig. 4.51): in fact intercooling lowers the air temperature at the end of the compression and therefore expands the limits for regeneration. Furthermore, the power

absorbed by the HPT is lower, since the compression requires less power, resulting in an higher gas temperature at the exit of the power turbine. From of all this it is clear that by combining intercooling and regeneration it is possible to obtain a huge increment in the heat recoverable in the regenerator, which in the case at hand even doubles (see fig. 4.50, 4.51).

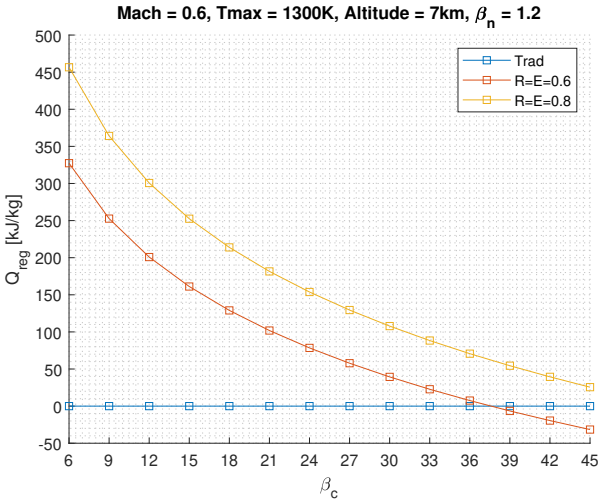

Figure 4.48: $Q_{reg} - \beta_c$, T_{max} (a)

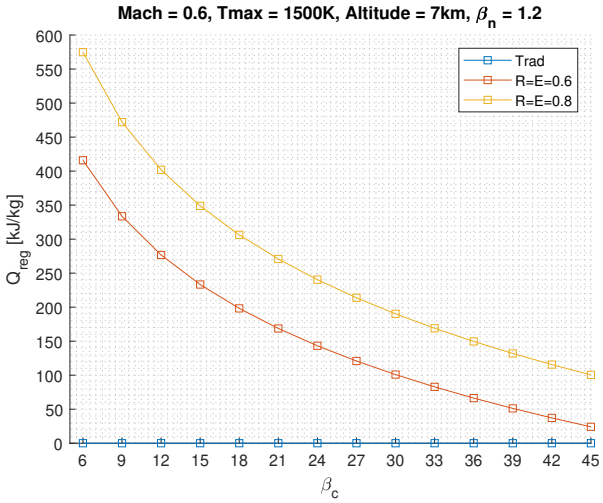

Figure 4.49: $Q_{reg} - \beta_c$, T_{max} (b)

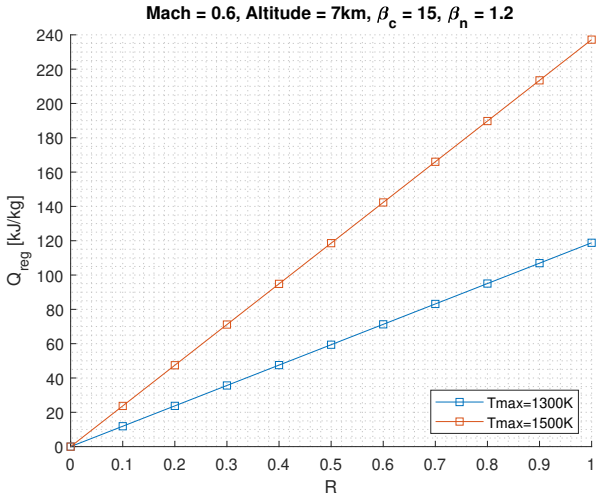

Figure 4.50: $Q_{reg} - R$, T_{max}

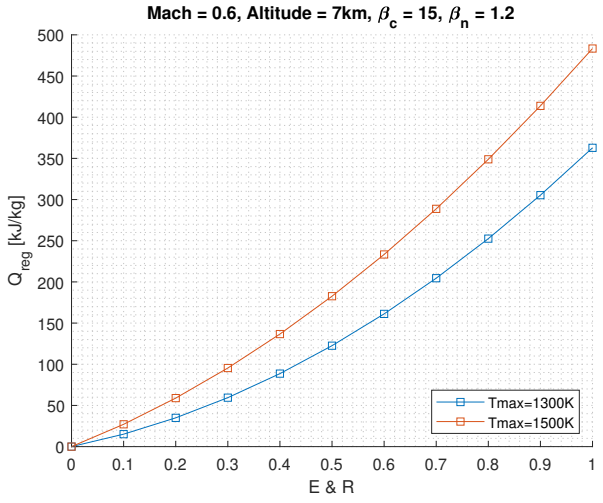

Figure 4.51: $Q_{reg} - E/R$, T_{max}

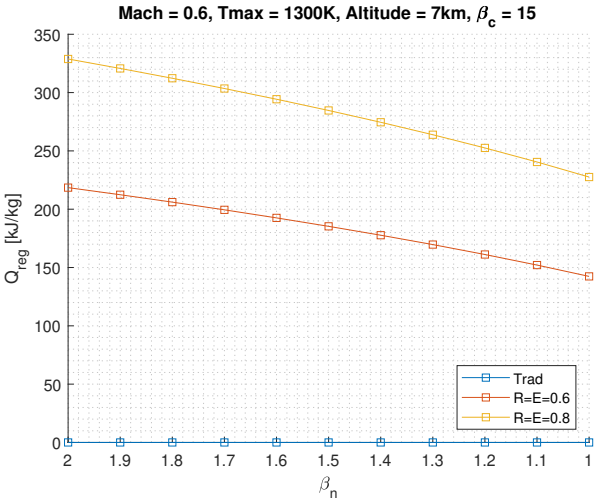

Figure 4.52: $Q_{reg} - \beta_n$

4.1.6 $\lambda - \beta_n$ correspondence

It is now of interest to study the relationship between the nozzle expansion ratio β_n and the λ parameter defined in section 2.2.2.

From the analysis it is observed that the $\lambda - \beta_n$ correspondence is not constant, but varies with the flight conditions and the engine parameters. As an example, figures 4.53 and 4.54 show the dependence of the $\lambda - \beta_n$ correspondence on the flight Mach number and E/R parameters.

Additionally, it is observed that $\beta_n = 1.2$, which usually gives the minimum the specific fuel consumption, always corresponds to very high λ values, around 0.9. This value also gives the maximum equivalent specific power in a traditional engine and is consistent with typical λ_{opt} values (see eqn. 2.38) obtained for traditional turbopropellers [12]. On the other hand, in the case of an engine with heat exchange the β_n value that gives the maximum equivalent specific power is lower, usually 1.1, and corresponds to λ values around 0.95. In fact, regeneration extracts energy from the combustion gases, reducing their contribution to the equivalent specific power. Therefore, is more convenient to expand more in the power turbine in order to maximize the overall useful power output.

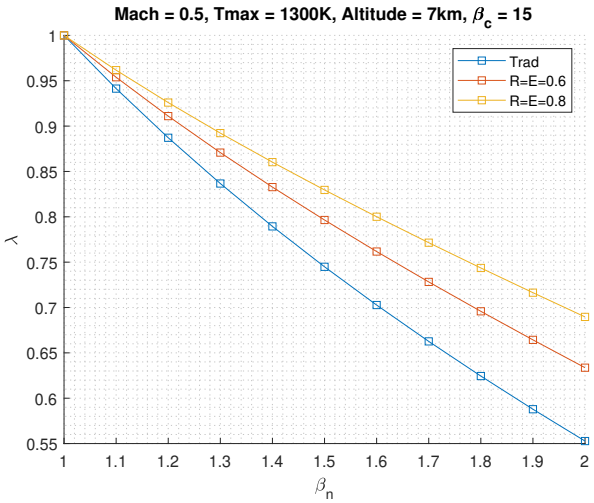

Figure 4.53: $\lambda - \beta_n$, M (a)

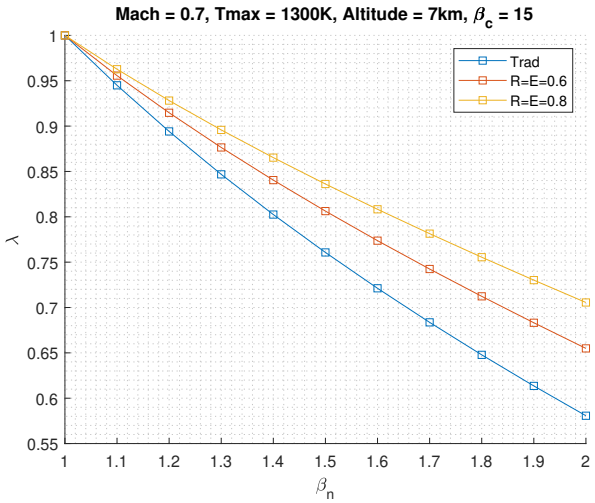

Figure 4.54: $\lambda - \beta_n$, M (b)

Chapter 5

Potential benefits of the application of regeneration and intercooling on current turbopropellers

As a conclusion of this study, it is of interest to estimate the economical and environmental benefits deriving from an hypothetical operation of a turbopropeller engine with intercooling and regeneration with respect to a traditional one. This is a crucial point, since the implementation of heat exchange techniques on commercial engines depends on whether the benefits compensate for the additional complexity, weight and cost (both of manufacture and of development) of the engine.

To this end, it is presented a comparison between two engines: a traditional turbopropeller and one with heat exchange. The traditional engine chosen is the Pratt & Whitney Canada PW150A, since it is a quite new model and can represent modern state-of-the-art turbopropellers. On the other hand, since currently there are no turbopropeller with heat exchange on the market, it was decided to use the code presented in chapter 3 to simulate one. The parameters' values chosen for the simulation are:

- Engine components' efficiencies: those reported in table 3.1
- Flight condition: cruise at $M = 0.6$, altitude = 7000m, which are typical flight condition for turbopropellers, are already mentioned
- Engine operating conditions: $\beta_c = 15$, $T_{max} = 1500$K, which are typical values for modern up-to-date turbopropellers, as already mentioned
- Nozzle expansion ratio $\beta_n = 1.2$, since the analysis conducted in chapter 4 indicated 1.2 as the value that minimizes the equivalent specific fuel consumption
- Intercooling and regeneration effectiveness: the simulation was done for different E/R values, from 0.4 to 0.8. In fact, from the analysis conducted in chapter 4 resulted that for E/R values lower than 0.4 the benefits deriving from intercooling and regeneration do not compensate for the losses they introduce. On the other hand, E/R values higher than 0.8 are not realistic in aeronautic applications [14]
- Engine equivalent power: set equal to that of the PW150A engine, in order to simulate an engine of the same class/size

5.1 Economical and environmental benefits

The principal economical benefit consists in the fuel saved. In fact, usually with regeneration and intercooling the engine has a lower $EBSFC$ and therefore less fuel is consumed, resulting in less fuel needed for each flight, reducing costs and increasing the available payload.

In this analysis only the reduced fuel costs is accounted for, since the evaluation of the benefits of the increased payload depends on the particular application, not to mention that the presence of heat exchangers might (over-)compensate the reduction in total fuel weight.

The environmental benefits are evaluated in terms of reduced emissions. In particular, only CO_2 emissions are accounted for in this analysis. In fact, CO_2 production is directly linked with fuel consumption, while other pollutants, such as NO_x, SO_x and unburned hydrocarbons, depend on many other parameters, such as the temperature in the combustion chamber, its efficiency, mixing, residence time, fuel composition etc.

CO_2 production can be estimated from the global combustion reaction of Jet A-1 fuel and oxygen.

The general hydrocarbon-oxygen combustion reaction is [46]:

$$C_aH_b + \left(a + \frac{b}{4}\right)O_2 \longrightarrow aCO_2 + \frac{b}{2}H_2O \tag{5.1}$$

Thus, since Jet A-1 approximate chemical formula is $C_{11}H_{21}$ [54]:

$$C_{11}H_{21} + 16.25\,O_2 \longrightarrow 11\,CO_2 + 10.5\,H_2O \tag{5.2}$$

So, for each mole of Jet fuel burnt, 11 moles of CO_2 are produced. In order to have the mass of CO_2 produced it necessary to pass through the molar mass $\mathcal{MM}$:

- $\mathcal{MM}$ of $C_{11}H_{21}$ = 153 g/mol
- $\mathcal{MM}$ of CO_2 = 44 g/mol

(C atomic mass = 12 u, H atomic mass = 1 u, O atomic mass = 16 u)

Thus, for each kg of Jet fuel burnt, $\frac{11 \cdot 44}{153}$ = 3.163 kg of CO_2 are produced.

5.1.1 Results

In the tables below are reported the results of the comparison between the two engines, along with their performances.

In order to estimate the reduced costs associated to the lower fuel consumption, the following data is used:

- Jet A-1 fuel price considered equal to 532.73 \$/mt (= 0.495 €/kg, 1 mt = 1000 kg), as indicated by [55] in date 14/02/2020
- U.S. Dollar−Euro change is considered equal to 0.93, as indicated by [56] in date 20/02/2020

Engine performances

Traditional engine	
Eq. Power [kW]	4039*
$EBSFC$ [kg/kWh]	0.213**
Fuel cons. [kg/hr]	860.3
Weight [kg]	717***

** source: https://www.flyradius.com/bombardier-q400/engine-pw150a*

*** estimate, source: Aviation Week and Space Technology Source Book 2006*

**** source:*

https://www.easa.europa.eu/sites/default/files/dfu/TCDS%20PW150%20series%20issue%2001_20141119_1.0.pdf

Table 5.1: Performances: traditional engine

Engine with heat exchange					
	R/E: 0.4	**R/E: 0.5**	**R/E: 0.6**	**R/E: 0.7**	**R/E: 0.8**
Eq. Power [kW]	4039				
$EBSFC$ [kg/kWh]	0.220	0.211	0.203	0.193	0.183
Fuel cons. [kg/hr]	886.9	853.9	818.5	780.8	740.9

Table 5.2: Performances: engine with heat exchange

Comparison between the two engines

	R/E: 0.4	**R/E: 0.5**	**R/E: 0.6**	**R/E: 0.7**	**R/E: 0.8**
Sp. Fuel saved [kg/kWh]	-0.007	0.002	0.010	0.020	0.030
Fuel saved [kg/hr]	-26.62	6.40	41.79	79.48	119.42
CO_2 saved [kg/hr]	-84.21	20.26	132.2	251.4	377.7
Fuel costs saved [€/hr]	-13.18	3.17	20.69	39.34	59.11
Saving [%]	-3.09	0.74	4.86	9.24	13.88

Table 5.3: Hourly savings

From table 5.3 is clear that the use of engines with regeneration and intercooling and optimized in terms of fuel consumption leads to considerable advantages compared to the engines currently in use only for high R/E values. For $R = E = 0.4$ it is observed even a

decrement in the performances, while for values of 0.5 the benefits are negligible. Still, it is comforting that there are substantial benefits even for R/E values of 0.7 and 0.6, since 0.8 is a very difficult value to obtain in aeronautical applications [14].

While in turbines for ground or marine applications it is easy to obtain regeneration effectiveness above 0.9, in aeronautical applications that is not possible, due to weight and size constraints.

That said, it is important to consider that the results shown in table 5.3 are optimistic, for the following reasons:

- the computations are valid for cruise conditions, so during take-off, landing, climb and descent it is expected a degradation in terms of savings. This also implies that the benefits are lower for shorter flights with respect to longer flights
- the performances of the engine with intercooling and regeneration are simulated, not measured. Thus, the performances of a real intercooled and regenerated engine might be (slightly hopefully) different
- the simulated engine is optimized in terms of specific fuel consumption, while nothing is known about the PW150A in that regard
- the simulated engine does not take into account its (manufacturing) price, so state-of-the-art technology is assumed. In general, trade-offs between performances and engine price/manufacturing cost are usually done

Furthermore, the implementation of regeneration and intercooling inevitably implies some disadvantages, as anticipated before: the development cost of the new engine and the additional weight of the heat exchangers, which is discussed in section 5.2.

On the other hand, nothing is know about PW150A components' efficiency and turbine inlet temperature, which might be higher than those assumed in the simulation. Also, pressure losses in the regenerator and intercooler might be lower than the 5% assumed in the simulation.

It is also important to remember that CO_2 and fuel cost reductions are proportional to the engine power. Therefore, for low power engines the reduced fuel consumption might not be worth the added engine complexity and cost, both of manufacture and maintenance. To have an idea, in a study for a 750 kW regenerated turboshaft that took place in the 1960's the engine cost was estimated to be $\sim 40\%$ higher than the non-regenerated one [14].

Overall, even if the results are optimistic, the analysis shows that this kind of engine has good potential, with projected savings up to around 13% during cruise flight, once the technology behind it is consolidated.

5.2 Heat exchangers' weight estimation

It is now of interest to estimate the weight of a regenerator for aeronautical applications.

Unfortunately, throughout the years interest in this kind of application has been intermittent, with few design concepts and even fewer actual hardware built. Thus, not much data is available in the literature and the technology has not been extensively developed.

On the other hand, technology advancements have been made in the general heat exchangers field, since the initial testing of heat exchanged gas turbines for aeronautical applications in the late 1960's. New materials and surface geometries are now available and the heat exchangers' performances, durability and efficiency improved.

Here follows a brief discussion about different surface geometries and their applicability for aeronautical purposes, as reported in [14]:

- Plate-fin surface geometry: this design is characterized by demonstrated high performance and failure-free operation even in cyclical operating conditions, such as those that characterize aeroengines. This geometry also is compatible with internal high pressure differentials, a common situation in aeronautical gas turbines. However, this design is characterized by very high weight, and thus is not suitable for aeronautical propulsion

- Primary surface geometry: in this design the matrix is composed by thin metallic foils, without secondary surfaces. This allows for a lower heat exchanger cost, weight and for easier manufacturing. On the other hand, due to the absence of supporting structural elements between the air and gas passages (due to the absence of secondary surfaces), this design does not perform well in presence of high pressure differentials, which are present in aeroengines. For this reason, this design is not suitable for aeronautical engines with a significant compression ratio

- Circular tubes geometry: this is the design used in the early studies of heat exchanged turboshafts. However, the technology of circular tubes has not advanced much in the years after, primarily due to the high complexity and cost of surfaces with tubes smaller than 4 mm and it was concluded that no technological breakthrough would come from this geometry [14]. Furthermore, while smaller tubes will enhance heat exchange, they introduce other problems, such as flow maldistribution, fouling issues and complex heat exchanger assembly

- Oval tubes geometry: this design yields high heat transfer performances on low pressure losses, at least in laminar regime. It is the geometry currently under research and development for aeroengines applications and the most promising

So, regenerators for aeronautical applications will be of the tubular type, in particular multi-pass cross-counterflow oval tube heat exchangers. This configuration yields good performances in terms of pressure losses and heat exchange, while being relatively easy to implement in the structure of a gas turbine engine. Also weight is minimized, while satisfying (thermo-)structural constraints.

Figure 5.1 reports the regenerator's matrix specific weight (for each unit of mass flow rate) as a function of the regeneration effectiveness R.

The band related to tubular geometries is not extremely accurate, since the actual regenerator's specific weight is affected by different other variables, such as temperatures, pressure, tube hydraulic diameter, wall thickness, material, flow configuration, etc. Furthermore, the band is built up starting from very few data, part of which comes from studies and not actual operating engines. So, the curves and band provided are to be used only to have and idea, a first estimation of the potential weight of the regenerator.

In addition, the figure reports only the specific weight of the matrix of the regenerator, without accounting for the weight of the manifolding, ducting and support structure.

However, for tubular heat exchangers the matrix represents the majority of its weight, and in any case the other heat exchanger components' weight is very case dependant and cannot be estimated without additional information.

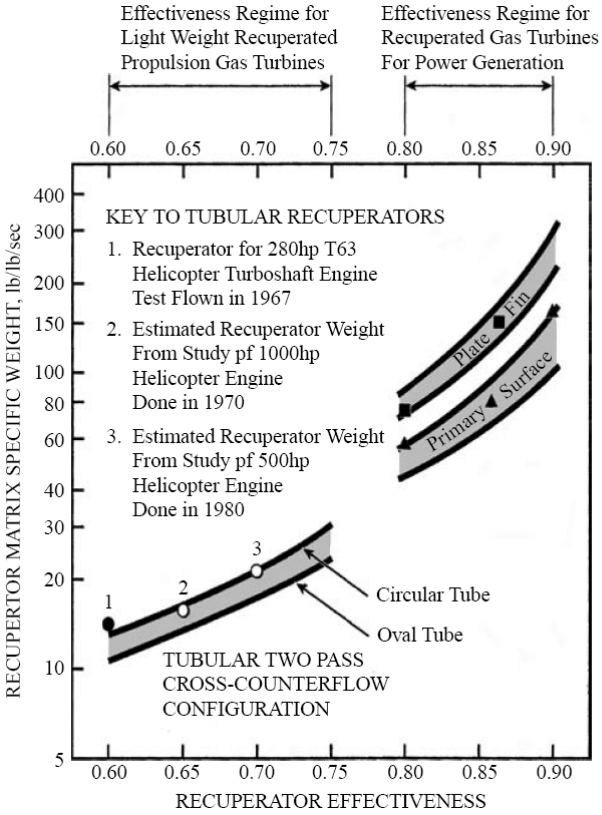

Figure 5.1: Regenerator specific weight as a function of its regeneration effectiveness [14]

Since the analysis conducted in section 5.1 considered R values beyond the ones present in figure 5.1, it is of interest to determine a curve that represents the regenerator's specific weight trend, in order to be able to estimate the regenerator's weight also for different R values.

To that end, several points are graphically taken from the tubular configuration band, and then a fitting curve is computed by means of the Matlab function *fit* [57].

The data distribution appears exponential in nature, so two different exponential fitting curves are considered: one composed by a single exponential, in the form of equation 5.3, and one composed by the sum of two exponentials, in the form of equation 5.4:

$$w_{reg} = a \cdot e^{b \cdot R} \tag{5.3}$$

$$w_{reg} = a \cdot e^{b \cdot R} + c \cdot e^{d \cdot R} \tag{5.4}$$

The two fitting curves, along with the points used for the fitting, are presented in figure 5.2. Both curves yield a specific weight ~ 0 for $R = 0$, which is consistent.

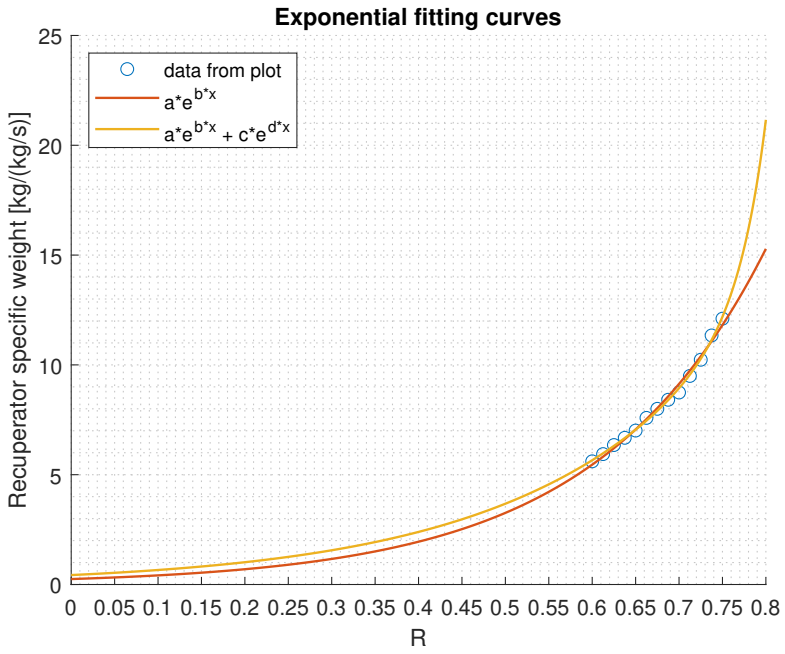

Figure 5.2: Regenerator specific weight as a function of regeneration effectiveness: comparison between two exponential fitting curves

The two-exponentials curve (yellow one) better fits the data, so its expression is used in the computations to estimate the regenerator's specific weight. Its expression is reported below:

$$w_{reg} = 0.4302 \cdot e^{4.292 \cdot R} + 1.274 * 10^{-11} \cdot e^{33.93 \cdot R} \tag{5.5}$$

It is true that the fitting is based on a small dataset, and thus it is not very accurate, but its accuracy is considered to be consistent with the one of the band presented in figure 5.1, from which the data for the interpolation is taken. Furthermore, scope of this study is just to have a preliminary estimation of the heat exchanger's weight.

5.2.1 Results

Here below are presented the results of the heat exchanger's weight estimation. The engine mass flow rate is provided by the code described in chapter 3, the regenerator's specific weight is provided by equation 5.5 and the intercooler weight is assumed to be half of that of the regenerator, since it operates at sensibly lower temperatures and thus lighter materials can be used.

Rigorously, the heat exchangers should be designed considering the maximum mass flow rate that they will operate with, that is the mass flow rate at take-off. But the computation of the aforementioned mass flow rate would require an off-design analysis, that is out of the scope of this study.

Also, the heat exchangers' weight reported in table 5.4 takes into account only the weight of the matrix without considering ducting, manifolding, etc. However, as already said before, the matrix takes up the majority of the heat exchanger weight and the estimation of the weight of the other components is impossible with the available information.

	R/E: 0.4	R/E: 0.5	R/E: 0.6	R/E: 0.7	R/E: 0.8
Engine mass flow rate [kg/s]	10.05	9.89	9.75	9.61	9.49
Sp. regenerator weight [kg/(kg/s)]	2.394	3.679	5.659	8.942	21.159
Regenerator weight [kg]	24.07	36.38	55.18	85.93	200.80
Intercooler weight [kg]	12.04	18.19	27.59	42.97	100.40
Total extra weight [kg]	36.10	54.57	82.77	128.90	301.20
Flight hrs for weight compensation [hr]	-	8.52	1.98	1.62	2.52

Table 5.4: Heat exchangers' weight estimation

It is also computed for how long the aircraft should fly in cruise conditions before the fuel saved by intercooling and regeneration compensates the extra weight of the heat exchangers. Graphs are provided below showing the fuel saved during cruise flight as a function of the flight time (red line), compared to the extra weight introduced by the heat exchangers (black line).

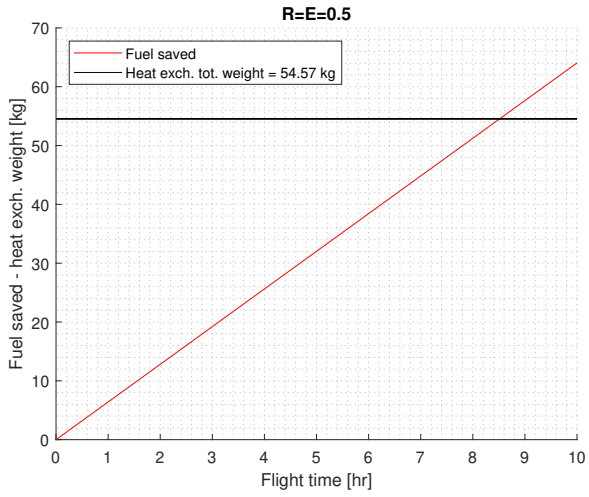

Figure 5.3: Saved fuel-time, $R = E = 0.5$

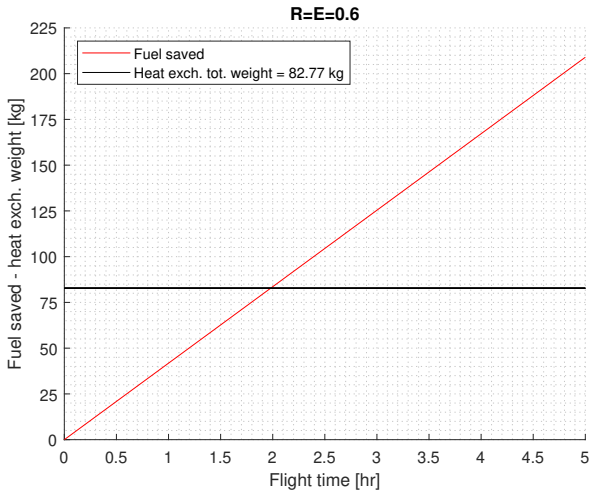

Figure 5.4: Saved fuel-time, $R = E = 0.6$

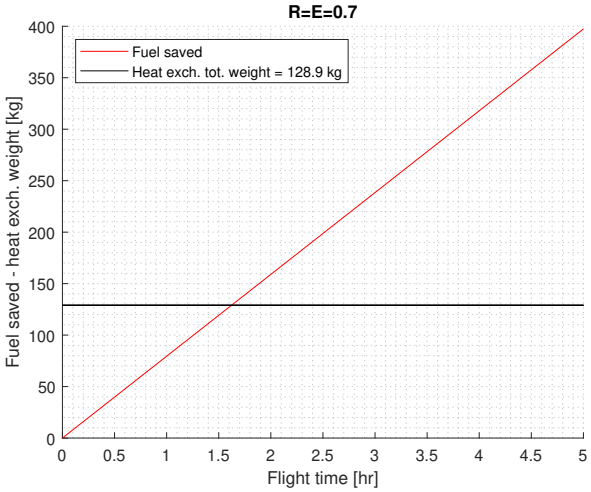

Figure 5.5: Saved fuel-time, $R = E = 0.7$

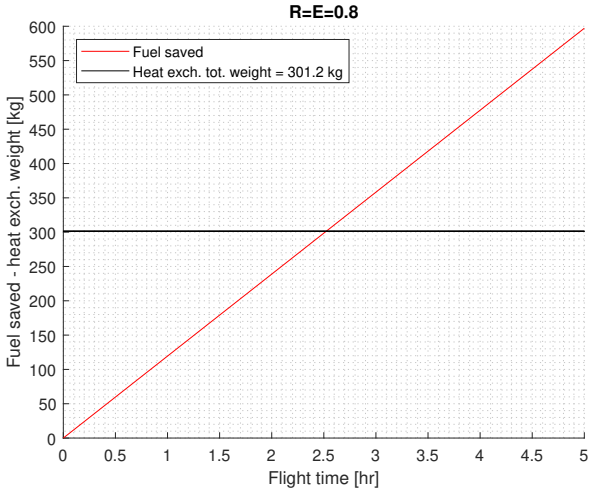

Figure 5.6: Saved fuel-time, $R = E = 0.8$

As the the intercooling and regeneration effectiveness increment, the time needed to compensate for the added weight can increase or decrease, due to the different mathematical nature of the relationships that link the fuel consumption and the heat exchangers' weight to R/E. The implementation of intercooling and regeneration could be "weight neutral" or "weight positive" even for relatively short routes if R/E values are between 0.6 and 0.8. Form this point of view, R/E values of 0.7 are a good trade-off between reduced fuel consumption and heat exchangers' weight and complexity.

5.3 Conclusions

In the past, recuperated propulsion engines were not deemed attractive due to very high engine weight, poor heat exchanger technology and the fact that at that time fuel prices were low and better simple-cycle performance were easily obtained by turbomachinery efficiency and turbine inlet temperature improvements.

Nowadays, on the other hand, the situation is quite different. Fuel price are high, heat exchanger technology has developed and legislations impose ever stringent limits on emission and noise. Furthermore, the simple-cycle gas turbine technology has been thoroughly developed and improvements are more and more difficult to achieve.

In this scenario, the interest in recuperated engines is on the rise. In fact, recuperated engines offer reduced fuel consumptions without completely revolutionize the technology of aeroengines. In this sense, if not a definitive solution to current problems, intercooling and regeneration might at least provide a "temporary/intermediate" and relatively cheap solution, until a new technology breakthrough provides all new next-gen aeroengines.

Scope of this thesis was to have an initial assessment of the potential and viability of the implementation of intercooling and regeneration on aeroengines, in particular on turbopropellers.

From this first assessment resulted that intercooling and regeneration show great potential in enhancing engine performances, in particular the specific fuel consumption, for a variety of operating conditions and engine configurations, and thus their implementation will give sensible benefits.

In addition, it was possible to identify optimal values for some of the engine parameters and how regeneration and intercooling effectiveness interact with them. In this regard,

the following considerations can be done:

- the optimal nozzle expansion ratio, in terms of minimum $EBSFC$, for an intercooled and regenerated engine is ~ 1.2 for most E/R values and for the usual operating conditions of turbopropellers. The value that gives the maximum specific power is instead lower, around 1.1
- the optimal overall compression ratio, in terms of minimum $EBSFC$, for an intercooled and regenerated engine is between 12 and 18, depending on E/R values and operating conditions. On the other hand, the values that give the maximum specific power are much higher. However, both $EBSFC$ and specific power curves are flatter than the ones that characterize traditional engines and therefore it is possible to find a trade-off between power and fuel consumption that does not penalize either of them too much
- intercooling and regeneration should be implemented together in order to obtain the best overall performances. In fact, their simultaneous implementation increases the heat that can be regenerated, the optimal overall compression ratio, the specific power of the engine and strongly reduces the equivalent fuel consumption
- regenerator and intercooler pneumatic efficiencies have a non negligible effect on the overall engine performances, resulting in more than a 1% performance gain for each 1% increment in both efficiencies. Thus this parameters are an additional tool available to obtain even better performances
- E/R must have values higher than ~ 0.4 in order to have a net performance enhancement, considering pneumatic efficiencies of 95% for the intercooler and regenerator, which are realistic and common values. Of course, higher efficiencies will make lower E/R values beneficial and the opposite for lower efficiencies
- E/R values greatly affect the improvement in engine performances, thus is crucial to be able to obtain high heat exchange effectiveness
- for high E/R values, intercooled and regenerated engines are expected to yield overall fuel consumption, and thus CO_2 and fuel costs, $\sim 13\%$ lower with respect to modern simple-cycle engines
- recuperated engines are more appealing for larger engines and longer routes. In fact, the overall emissions and fuel consumption depend on the engine's total power, and in longer routes the fuel saved due to the reduced fuel consumption can (over-) compensate the extra weight of the heat exchangers

Recuperated engines are promising, but their performances and benefits depend heavily on the heat exchangers used for regeneration and intercooling. In fact, is is imperative to have high heat exchange effectiveness, otherwise they will results detrimental or the benefits will be negligible. This usually is not a problem, since in industry heat exchangers have often effectiveness above 90%. But they are extremely heavy and bulky, while in aeronautic applications it is crucial to have low weight and compact components. So, obtaining high effectiveness while reducing weight and size is the most difficult challenge that this technology must overcome, considering that past data suggests an exponential

relationship between heat exchanger's weight and its effectiveness [14]. Furthermore, these performances must be obtained with low pressure losses.

To conclude, whether or not this kind of engines will be successfully manufactured depends on the successful realization of efficient, high performance, compact and lightweight heat exchangers. New surface geometries, close integration with the core engine and new materials, such as ceramics and carbon/carbon fiber composites [14], must be researched and tested, in order to develop heat exchangers that meet the requirements.

Acknowledgments

First of all, I would like to thank my advisor, Professor Roberto Andriani, who guided me in the development of this thesis.

I would also like to thank the professors of all my courses. Thanks to them I was able to discover the aerospace world and to expand my knowledge and competencies.

Then, I would like to thank my family, for giving me the opportunity to attend this university and for the support throughout the years.

I would also like to express my gratitude to the classmates with whom I shared my studies. Their help, support and presence made my time at university much more enjoyable and helped me overcome the toughest challenges during my studies.

Finally, I would like to thank all my friends, with whom I shared countless happy memories. During all these years they supported me, helped me, and where there for me when I was in need.

Bibliography

[1] Pratt & Whitney Canada. https://www.pwc.ca/en/.

[2] Rolls Royce. https://www.rolls-royce.com/.

[3] General Electric Aviation. https://www.geaviation.com/.

[4] JSC Kuznetsov. http://www.kuznetsov-motors.ru/.

[5] JSC "UEC-Klimov". http://www.klimov.ru/en/.

[6] Ivchenko-Progress ZMKB. http://ivchenko-progress.com/?lang=en.

[7] Honeywell Aerospace. https://aerospace.honeywell.com/en.

[8] PBS Aerospace. https://www.pbsaerospace.com/.

[9] C-130.net. http://www.c-130.net/g3/c-130-photos/C-130-Technical-Photos/rolls-royce-ae2100.

[10] Wikimedia Commons. https://commons.wikimedia.org/wiki/File:TV7-117S_International_salon_Engines-2010_02.jpg.

[11] Roberto Andriani. *Dispense del Corso di Motori per Aeromobili*. Politecnico di Milano, 2018/19.

[12] Francesco Nasuti; Diego Lentini; Fausto Gamma. *Dispense del Corso di Propulsione Aerospaziale*. Sapienza Università di Roma, 2011/12.

[13] Eclipse Foundation. https://www.eclipse.org/.

[14] C. Rodgers A. Stone C. F. McDonald, A. F. Massardo. Recuperated gas turbine aeroengines, part ii: engine design studies following early development testing. *Aircraft Engineering and Aerospace Technology: an International Journal, Vol. 80, No. 3, pp 280-294, Emerald Group Publishing Limited*, 2008.

[15] Airbus. https://www.airbus.com/.

[16] Piaggio Aerospace. http://www.piaggioaerospace.it/.

[17] Daher-SOCATA TBM. https://www.tbm.aero/.

[18] ATR Aircraft. http://www.atraircraft.com/.

[19] Pilatus Aircraft. https://www.pilatus-aircraft.com/en.

[20] H3 Grob Aircraft. https://grob-aircraft.com/en/.

[21] Diamond Aircraft Industries. https://www.diamondaircraft.com/en/.

[22] Antonov Airlines. https://www.antonov-airlines.com/.

[23] Ilyushin. http://www.ilyushin.org/en/.

[24] Lockeed Martin. https://www.lockheedmartin.com/en-us/index.html.

[25] Beechcraft. https://beechcraft.txtav.com/en.

[26] Piper Aircraft. https://www.piper.com/.

[27] Evolution Aircraft. https://www.evolutionaircraft.com/aircraft/.

[28] Epic Aircraft. https://epicaircraft.com/.

[29] Nextant Aerospace. https://www.nextantaerospace.com/.

[30] Bombardier. https://www.bombardier.com/en/aviation.html.

[31] Embraer. https://embraer.com/global/en.

[32] Nate Meyer's jet engine.net. http://www.jet-engine.net/.

[33] Federal Aviation Administration. *Airplane Flying Handbook*. United States Department of Transportation, Federal Aviation Administration, 2016.

[34] SKYbrary Aviation Safety. https://www.skybrary.aero/index.php/Turboprop_Engine.

[35] NASA Glenn Research Center. https://www.grc.nasa.gov/WWW/K-12/airplane/aturbp.html.

[36] NBAA National Business Aviation Association. https://nbaa.org/business-aviation/business-aircraft/turboprop-aircraft/.

[37] Motor Sich. http://www.motorsich.com/eng/products/aircraft/tr/.

[38] Carlo Osnaghi. *Teoria delle Turbomacchine*. Società Editrice ESCULAPIO, 2013.

[39] Claire Soares. *Gas Turbines: A Handbook of Air, Land and Sea Applications - 2^{nd}edition. Butterworth − Heinemann*, 2014.

[40] Dieter K. Huzel; David H. Huang. *Modern Engineering for Design of Liquid-Propellant Rocket Engines*. AIAA, 1992.

[41] S. Larry Dixon. *Fluid Mechanics,Thermodynamics of Turbomachinery - 4^{th}edition. Butterworth − Heinemann*, 1998.

[42] Valeri G. Nesterenko. *Thermal to Mechanical Energy Conversion: Engines and Requirements – Vol. III - Reduction Gears*. UNESCO - Encyclopedia of Life Support Systems (EOLSS), 2009.

[43] Barnes W. McCormick. *Aerodynamics, Aeronautics, and Flight Mechanics*. Wiley, 1979.

[44] Roberto Andriani; Fausto Gamma; Umberto Ghezzi. Thermodynamic analysis of a turboprop engine with intercooling and heat recovery. *Transactions of the Japan Society for Aeronautical and Space Sciences*, 2011.

[45] James T. Edwards. "kerosene" fuels for aerospace propulsion – composition and properties. *38th AIAA/ASME/SAE/ASEE Joint Propulsion Conference Exhibitg*, 2002.

[46] James T. Edwards. Reference jet fuels for combustion testing. *55th AIAA Aerospace Sciences Meeting*, 2017.

[47] Coordinating Research Council. *Handbook of Aviation Fuel Properties*. Defense Technical Information Center, 1983.

[48] T. Boulkeraa; A. Ghenaiet. Optimizations of turboprop engines using the non-dominated sorting genetic algorithm. *Proceedings of the Institution of Mechanical Engineers, Part G: Journal of Aerospace Engineering*, 2010.

[49] Bonnie J. McBride; Michael J. Zehe; Sanford Gordon. Nasa glenn coefficients for calculating thermodynamic properties of individual species. *NASA Technical Reports Server*, 2002.

[50] Sanford Gordon. Thermodynamic and transport combustion properties of hydrocarbons with air. part 1: Properties in si units. *NASA Technical Reports Server*, 1982.

[51] Pasquale M. Sforza. *Manned Spacecraft Design Principles*. Butterworth-Heinemann, 2016.

[52] MIT Open Courseware. `https://ocw.mit.edu/courses/aeronautics-and-astronautics/16-50-introduction-to-propulsion-systems-spring-2012/lecture-notes/MIT16_50S12_lec34.pdf`.

[53] MathWorks. `https://it.mathworks.com/products/matlab.html?s_tid=hp_products_matlab`.

[54] J.E. Sinor Consultants Inc. *Investigation of Byproduct Application to Jet Fuel*. NREL - National Renewable Energy Laboratory, U.S. Department of Energy, 2001.

[55] IATA Jet fuel price monitor. `https://www.iata.org/en/publications/economics/fuel-monitor/`.

[56] Morningstar. `https://www.morningstar.com/`.

[57] Matlab Exponential models. `https://it.mathworks.com/help/curvefit/exponential.html`.

[58] Aircraft Compare. `https://www.aircraftcompare.com/`.

[59] Biagio Raucci. Il linguaggio fortran 90/95 (pdf).

[60] Roberto Andriani; Umberto Ghezzi; Antonella Ingenito; Fausto Gamma. Fuel consumption reduction and weight estimate of an intercooled-recuperated turboprop engine. *International Journal of Turbo and Jet Engines*, 2012.